Final Report

Wellhead Protection Area and Vulnerability Assessment Update for the Freelton Water Supply City of Hamilton, Ontario

Prepared for:

The City of Hamilton
Public Works Department
Environment and Sustainable Infrastructure Division

Prepared by:

Earthfx Incorporated

3363 Yonge Street
Toronto, Ontario M4N 2M6

April 2021

Earth Science Information Systems

April 12, 2021

Mr. Mike Christie
Project Manager, Source Protection Planning
Hamilton Water | Public Works | City of Hamilton
77 James Street North, Suite 400
Hamilton, ON L84 2K3
905.546.2424 ext. 6194

RE: Wellhead Protection Area (WHPA) Delineation, Vulnerability Scoring, and Threats Assessment Update for the Freelton Supply Wells

Dear Mr. Christie:

We are pleased to provide the final report titled "Wellhead Protection Area Delineation, Vulnerability Scoring, and Threats Assessment for the Freelton Water Supply". The study described in this report was undertaken to provide updated wellhead protection areas (WHPA) and vulnerability and threats analysis for the Freelton supply wells under an amended permitted pumping rate. The current version of the report reflects changes to the permitted pumping rates.

The study began with a review previous work and a compilation of relevant hydrogeologic data. These data were used to update the "North Hamilton" hydrostratigraphic model, previously developed by Earthfx, and were incorporated into an updated three-dimensional groundwater flow model for the area. In addition, a detailed hydrologic model was developed and calibrated for the study area to provide improved estimates of long-term average groundwater recharge.

Once the updated models were recalibrated, reverse particle tracking techniques were applied to define WHPA zones based on time-of-travel from the new wells. Next, forward particle tracking techniques were applied to estimate water table to well advective travel times (WWAT). Unsaturated zone travel times (UZAT) were calculated and added to determine surface to well travel times (SWAT) and assign aquifer vulnerability scores. Results for the vulnerability analyses were then used to conduct a Drinking Water Threats Assessment and analyze uncertainty.

Should you have any questions regarding this report, the methods applied, or study results, please feel free to contact us.

Yours truly,
Earthfx Incorporated

Dirk Kassenaar, M.Sc., P.Eng.
President

E.J. Wexler, P.Eng., M.S.E., M.Sc.,
Director of Modelling Services

Wellhead Protection Area and Vulnerability Assessment Update for the Freelton Water Supply City of Hamilton, ON

Table of Contents

1 INTRODUCTION 8

1.1 STUDY OVERVIEW 8
1.2 PROJECT OBJECTIVE AND SCOPE 8
1.3 STUDY AREA 8

2 BACKGROUND WELLFIELD INFORMATION 10

2.1 PRODUCTION WELLS AND MONITORING WELLS 10
2.2 PERMIT TO TAKE WATER 10

3 PHYSICAL SETTING 13

3.1 STUDY AREA AND TOPOGRAPHY 13
3.2 PHYSIOGRAPHY 13
3.3 BEDROCK GEOLOGY 13
3.4 QUATERNARY GEOLOGY 19
3.5 CONCEPTUAL STRATIGRAPHIC MODEL 19
3.5.1 Updates to the Stratigraphic Model 19
3.6 HYDROGEOLOGY AND GROUNDWATER FLOW 24
3.6.1 Aquifers and Aquitards 24
3.6.2 Groundwater Flow Directions 26

4 HYDROLOGIC MODEL 30

4.1 SCOPE OF MODEL UPDATE 30
4.2 MODEL DESCRIPTION 30
4.3 CLIMATE DATA 33
4.3.1 Historic Precipitation and Temperature 33
4.3.2 Solar Radiation 34
4.4 MODEL PARAMETERIZATION 39
4.4.1 Topography 39
4.4.2 Land-use and Land Cover 39
4.4.1 Surficial Geology Mapping 45
4.4.1 Hydrological Process Parameters 47
4.5 STREAMFLOW CALIBRATION TARGETS 47
4.6 CALIBRATION AND VALIDATION 47
4.7 LONG-TERM SIMULATION AND DISCUSSION 52
4.8 LIMITATIONS OF THE PRMS GROUNDWATER RECHARGE ESTIMATES 55

5 GROUNDWATER FLOW MODEL 58

5.1 SCOPE OF MODEL UPDATE 58
5.2 MODEL DESCRIPTION 58
5.3 BOUNDARY CONDITIONS 58
5.3.1 Streamflow 61
5.3.1 Hydrostratigraphy 61
5.3.1 Recharge and Surface Leakage 63
5.4 SIMULATED GROUNDWATER TAKINGS 65
5.5 GROUNDWATER FLOW MODEL CALIBRATION 65

5.5.1 Calibration Targets for the Steady-State Groundwater Model 65
5.5.2 Model Hydraulic Conductivity Values 68
5.5.3 Groundwater Level Comparisons and Calibration Statistics 79
5.5.4 Transient Validation 84

6 AQUIFER VULNERABILITY ASSESSMENT 86

6.1 WELLHEAD PROTECTION AREAS (WHPAS) 86
6.1.1 WHPA Delineation Methodology 86
6.1.2 WHPA Delineation 89
6.1.3 WHPA-E and WHPA-F Delineations 89
6.2 HIGH, MEDIUM, AND LOW VULNERABILITY ZONES 94
6.2.1 Vulnerability Assessment Methodology 94
6.2.1 Unsaturated Zone Advective Times 95
6.2.1 Water Table to Well Advective Times 98
6.2.2 High, Medium, and Low Vulnerability Zone Delineation 98
6.3 PREFERENTIAL PATHWAYS ANALYSIS 98
6.3.1 Transport Pathways 98
6.3.2 Private Water Wells 103
6.3.3 Adjustment of Vulnerability Zone Ratings 104
6.4 VULNERABILITY SCORES 107
6.5 UNCERTAINTY ASSESSMENT 110
6.5.1 Overview 110
6.5.2 Uncertainty related to Data Distribution Variability, Quality, and Relevance 111
6.5.3 Groundwater Model Uncertainty 111
6.5.4 Recharge Model Uncertainty 112
6.5.5 Time of Travel Analysis Uncertainty 112
6.5.6 Vulnerability Mapping Uncertainty 113

7 SUMMARY 114

8 LIMITATIONS 115

9 REFERENCES 116

LIST OF TABLES

Table 2.1: Well completion details for the Freelton municipal wells. 10
Table 2.2: Table A from PTTW 4650-BB2HXG for the Freelton Municipal wells. 12
Table 2.3: Pumping configurations for WHPA delineation. 12
Table 3.1: Summary of hydrogeologic properties of the Gasport/Amabel Formation 24
Table 4.1: List of solar radiation stations used to compile solar radiation estimates. 34
Table 4.2: Distribution of land classes within the Freelton area (SOLRIS and LANDSAT coverages). 42
Table 4.3: Summary of land use/land cover properties. 43
Table 4.4: List of surficial geology types and properties used in the PRMS model. 45
Table 4.5: Streamflow statistics for the Bronte Creek at Carlisle (02HB022) stream gauge. 47
Table 4.6: Summary of calibration statistics for PRMS model subbasins. 51
Table 4.7: PRMS statistics at the Bronte Creek near Carlisle gauge during the simulation period. 52
Table 5.1: Description of the numerical model layers. 63
Table 5.2: Aquifer and aquitard properties for the hydrostratigraphic units. 68
Table 5.3: Summary of calibration statistics. 79
Table 6.1: Porosity values assigned to geologic units. 86
Table 6.2: Framework for risk level assignments to other wells. 103
Table 6.3: Number of wells assigned to each risk level within the WHPA zones. 104
Table 6.4: Vulnerability scoring matrix. 107
Table 6.5: Summary of uncertainty analysis for WHPA delineation. 110
Table 6.6: Summary of uncertainty analysis for vulnerability scoring. 111

LIST OF FIGURES

Figure 1.1: Study area and North Hamilton (NH) model extents. 9
Figure 2.1: Freelton municipal wells. 11
Figure 3.1: Land surface topography in the study area. 14
Figure 3.2: Physiographic regions of the study area (physiography modified from Chapman and Putnam, 1984). 15
Figure 3.3: Paleozoic bedrock geology of the study area. 16
Figure 3.4: Bedrock surface topography. 17
Figure 3.5: Bedrock stratigraphic nomenclature across the study area (from Earthfx, 2014). 18
Figure 3.6: Surficial geology of the study area (data from OGS, 2010). 20
Figure 3.7: Overburden thickness, in m (white areas indicate bedrock at surface). 21
Figure 3.8: North-South cross section showing hydrostratigraphic layers (section location shown in inset map). 22
Figure 3.9: Change in top of bedrock elevation. 23
Figure 3.10: Theis drawdown curve match to Wood (2018a) pump test at FM-01-17d. 25
Figure 3.11: Theis drawdown curve match to Wood (2018a) pump test at FDF01-02. 25
Figure 3.12: Location of water wells within the model area. 27
Figure 3.13: Interpolated overburden water levels for boreholes less than 20 m deep. 28
Figure 3.14: Interpolated water levels for boreholes greater than 20 m deep. 29
Figure 4.1: Updated hydrologic model (PRMS) area. 31
Figure 4.2: PRMS hydrological process flow chart. 32
Figure 4.3: Influence of soil zone moisture on recharge, interflow, and runoff processes. 33
Figure 4.4: Location of climate stations. 35
Figure 4.5: Annual average precipitation in the study area (AES Stations, WY1951 – WY2018). 36
Figure 4.6: Annual average temperature in the study area (AES Stations, WY1951 – WY2018). 36
Figure 4.7: Long-term average annual water year precipitation WY1951 – WY2018. 37
Figure 4.8: Long-term average daily temperature WY1951 – WY2018. 38
Figure 4.9: Subset of the cascade network for the study area. 40
Figure 4.10: Distribution of dominant land use types (based on SOLRIS and LANDSAT coverages). 41
Figure 4.11: Distribution of maximum daily percolation rates. 46
Figure 4.12: Topographic catchment boundary for the PRMS model. 48
Figure 4.13: Observed daily streamflow at Bronte Creek near Carlisle (WSD ID: 02HB022). 49
Figure 4.14: Simulated (red) versus observed mean daily stream flow (blue) at Bronte Creek near Carlisle during the calibration period. Precipitation and snowmelt shown on secondary axis. 50
Figure 4.15: Simulated (red) versus observed mean daily log stream flow (blue) at Bronte Creek near Carlisle during the calibration period. 50
Figure 4.16: Simulated (red) versus observed mean monthly stream flow (blue) at Bronte Creek near Carlisle during the calibration period. 51
Figure 4.17: 25-year comparison between daily mean simulated (red) and observed (blue) streamflow at Bronte Creek near Carlisle. 53
Figure 4.18: 25-year comparison between daily mean log simulated (red) and observed (blue) streamflow at Bronte Creek near Carlisle. 53
Figure 4.19: 25-year comparison between monthly mean simulated (red) and observed (blue) streamflow at Bronte Creek near Carlisle. 53
Figure 4.20: Long-term average annual Hortonian generated runoff. 54
Figure 4.21: Long-term average annual actual ET. 56
Figure 4.22: PRMS groundwater recharge estimate. 57
Figure 5.1: Finite difference grid with higher resolution in the wellfield areas. 59
Figure 5.2: Model boundary conditions. 60
Figure 5.3: North-south cross section showing hydrostratigraphic numerical model layers. 62
Figure 5.4: Composite recharge map. 64
Figure 5.5: Static water levels in Boreholes less than 20 m deep. 66
Figure 5.6: Static water levels in boreholes greater than 20 m deep. 67

Figure 5.7: Hydraulic conductivity distribution in model Layer 1. 69
Figure 5.8: Hydraulic conductivity distribution in model Layer 2. 70
Figure 5.9: Hydraulic conductivity distribution in model Layer 3. 71
Figure 5.10: Hydraulic conductivity distribution in model Layer 4. 72
Figure 5.11: Hydraulic conductivity distribution in model Layer 5. 73
Figure 5.12: Hydraulic conductivity distribution in model Layer 6. 74
Figure 5.13: Hydraulic conductivity distribution in model Layer 7. 75
Figure 5.14: Hydraulic conductivity distribution in model Layer 8. 76
Figure 5.15: Hydraulic conductivity distribution in model Layer 9. 77
Figure 5.16: Hydraulic conductivity distribution in model Layer 10. 78
Figure 5.17: Comparison between interpolated WWIS water levels and simulated heads in model Layer 3. 80
Figure 5.18: Comparison between interpolated WWIS water levels and simulated heads in model Layer 7. 81
Figure 5.19: Distribution of overburden groundwater calibration residuals. 82
Figure 5.20: Scatterplots of calibration residuals in the (a) shallow wells (less than 20 m deep) and (b) deep wells (greater than 20 m deep). 83
Figure 5.21: Observed and simulated heads during Wood (2018a) pump test at FM-01-17-d. 85
Figure 5.22: Observed and simulated heads during Wood (2018a) pump test at FM-01-17-sb. 85
Figure 5.23 Observed and simulated heads during Wood (2018a) pump test at FDF01-02 85
Figure 6.1: Simulated water levels in numerical model Layer 7 – Pumping scenario 1. 87
Figure 6.2: Simulated water levels in numerical model Layer 7 – Pumping scenario 2. 88
Figure 6.3: Backward particle tracks from Freelton supply wells under Scenarios 1 and 2 and the composite 25-year Time of Travel zone. 90
Figure 6.4: Comparison of backward particle tracks for all scenarios to interpolated water levels. 91
Figure 6.5: Composite WHPA delineation for Freelton Well FDF01 and FDF03. 92
Figure 6.6: Comparison between the 25-year time-of-travel zone from Earthfx (2010) and that for the current study. 93
Figure 6.7: Schematic section showing definitions of time-of-travel terms for SWAT analysis. 94
Figure 6.8: Depth to the water table, based on subtracting the simulated heads in Layer 1 from land surface topography. 96
Figure 6.9: Unsaturated zone advective times (UZAT), in years, in the Freelton area. 97
Figure 6.10: Forward particle tracking from the water table for pumping Scenario 4. 99
Figure 6.11: Simulated minimum time of travel from the water table to the Freelton supply wells (WWAT), in years, for all scenarios. 100
Figure 6.12: Composite time of travel from the surface to the Freelton supply wells (SWAT), in years, for all scenarios. 101
Figure 6.13: Vulnerability Index (H, M, L) for the Freelton supply wells based on surface to well advection time (SWAT). 102
Figure 6.14: Identified non-municipal wells within the Freelton WHPAs. 105
Figure 6.15: Vulnerability Index (H, M, L) for the Freelton supply wells after adjusting for potential transport pathways. 106
Figure 6.16: Final composite vulnerability scores (2 – 10) for the Freelton supply wells. 109

1 Introduction

1.1 *Study Overview*

The rural settlement area (RSA) of Freelton recently completed a new permit to take water (PTTW) application to increase the maximum daily withdrawal rate at one of their two production wells, FDF01. The new pumping rate will change the groundwater flow patterns in the wellfield areas and, as a result, an update to the previously-defined wellhead protection areas (WHPA) and vulnerability scoring is required, as per The Clean Water Act (2006). The permit was granted by the Ontario Ministry of the Environment and Parks (MECP) but with additional restrictions on water use.

Earthfx Incorporated was retained by The City of Hamilton, herein referred to as "The City" to conduct this groundwater study to update the delineation of the wellhead protection areas and assign new vulnerability scores for the Freelton municipal wells. Earthfx completed the previous WHPA delineation and vulnerability scoring for Freelton, Carlisle, Lynden and Greensville using a regional-scale MODFLOW model referred to as the "North Hamilton" model (NH Model) as described in Earthfx (2010). The NH Model provided the foundation for this study.

1.2 *Project Objective and Scope*

The principal objective of this study was to update the delineation of the WHPAs and assign vulnerability scores for the Freelton supply wells. Specifically, the study involved completion of the following key tasks:

- review previous work and compile relevant hydrologic and hydrogeologic data;
- update the previously developed "North Hamilton" hydrostratigraphic model (described in Earthfx, 2010) and groundwater flow model with recent data;
- update the previously-developed hydrologic model to refine estimates of long-term average groundwater recharge in the study area;
- conduct steady-state groundwater simulations using the new permitted pumping rates
- apply reverse particle tracking techniques to define WHPA zones based on time-of-travel from the municipal wells;
- use forward particle tracking from the water table to the municipal well intakes to estimate water table to well advective travel times (WWAT) and assign aquifer vulnerability scores;
- analyze uncertainty related to the WHPA delineation and vulnerability scoring.

1.3 *Study Area*

The NH Model covers 1141 square kilometres (km^2) encompassing the North Hamilton and surrounding area. The study area surrounds Freelton, which falls in the northeast portion of the NH Model (Figure 1.1). For brevity, this report focuses only on the study area. For background and modelling information outside of the study area, the reader is referred to Earthfx (2010).

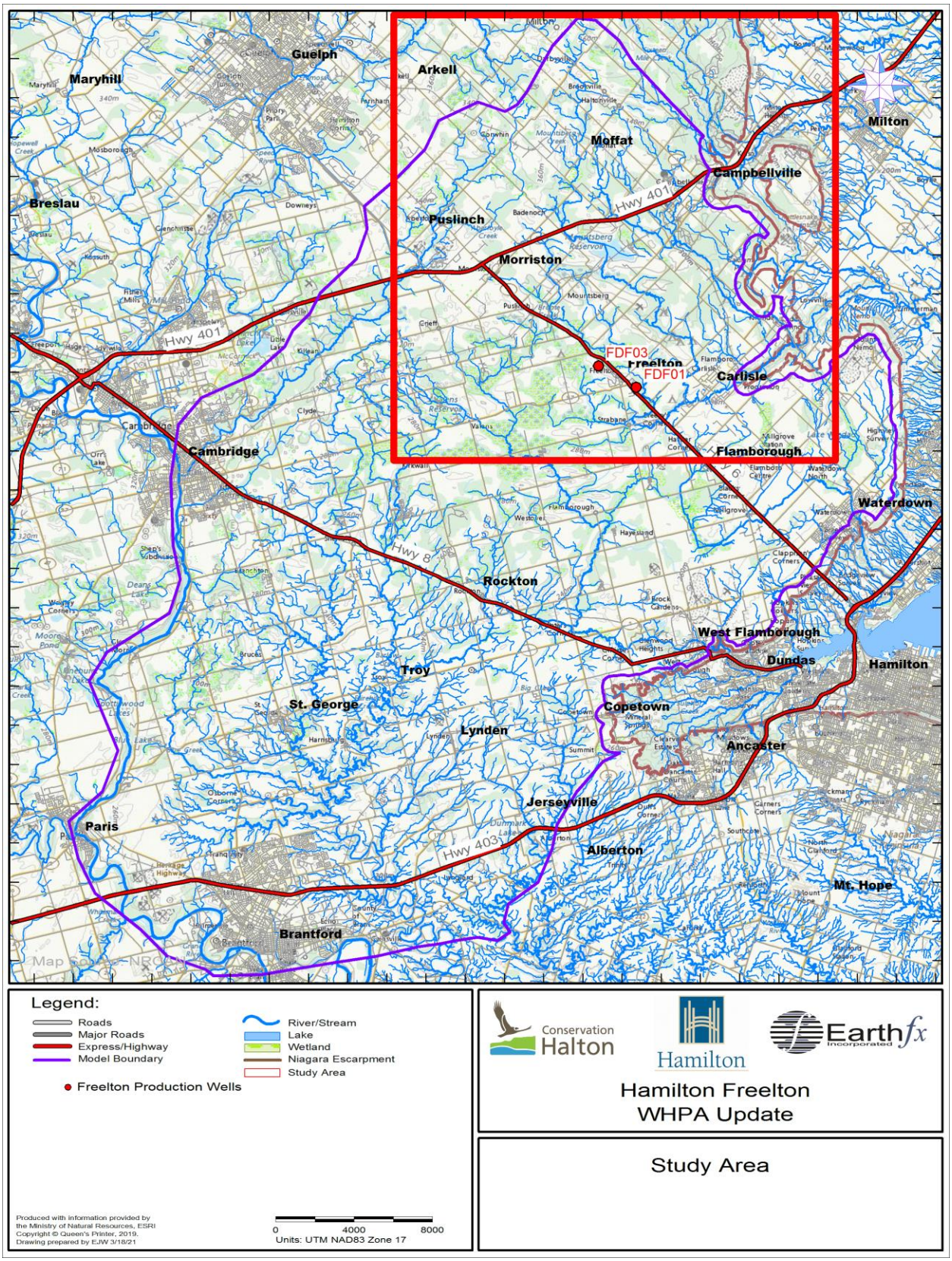

Figure 1.1: Study area and North Hamilton (NH) model extents.

2 Background Wellfield Information

2.1 *Production Wells and Monitoring Wells*

The majority of Freelton residents obtain their drinking water from two municipal pumping wells: FDF01 and FDF03. Both wells are completed in a confined or semi-confined bedrock aquifer. FDF01, the shallower of the two wells, is located in a residential neighbourhood at 15 Fireside Drive. It is completed to a depth of 21.13 metres below ground surface (mbgs), and in 2011, a stainless-steel liner was extended through the bedrock to a depth of 19.13 mbgs, isolating a productive aquifer zone at the base of the well. Only about a metre of till overburden overlies the bedrock at FDF01. FDF03 is located north of the main settlement area at 369-413 Freelton Road. A steel casing was completed through the overburden to the top of bedrock located at 22.56 mbgs and the well was extended as an open hole down to 50.3 mbgs (Dillon, 2008).

The Freelton municipal monitoring network consists of nine wells, all completed in bedrock. Each screen/open hole is monitored by a pressure transducer recording at 1- to 30-minute intervals. The location of the production wells and monitoring wells are shown in Figure 2.1. Well completion details for all wells are summarized in Table 2.1.

Table 2.1: Well completion details for the Freelton municipal wells.

Well Name	Date Completed	Well Depth (mbgs)	Interval Top (mbgs)	Interval Bottom (mbgs)
FDF01	21/07/2011	21.13	19.13	21.13
FDF03	30/11/2005	50.3	22.6	50.3
FDF-01-02	23/10/2002	11.90	8.60	11.90
FM-01-03	31/01/2003	21.64	6.10	21.64
FM-03	25/10/1982	21.34	2.13	21.34
FM-04	30/10/1982	30.48	12.80	30.48
FM-06-05	11/11/2005	48.77	21.64	48.77
FM-01-10-D	11/12/2010	54.86	9.14	54.86
FM-02-10-D	16/11/2010	54.86	6.10	54.86
FM-01-17-SB	25/09/2017	11.85	8.80	11.85
FM-01-17-D		20.74	19.22	20.74
FM-01-18-SB	9/4/2018	12.19	na	na
FM-01-18-D		19.18	13.41	16.46

2.2 *Permit to Take Water*

An amended permit to take water (PTTW) was issued to the City of Hamilton in for the Freelton wells (see Table 2.2 below) in April 2019. While granting the request to increase the maximum daily pumping rate for FDF01 from 10.2 L/s to 18.3 L/s, the permit introduced (1) a restriction for the combined maximum daily taking from the two wells of 1,607,040 L/day (18.6 L/s), and (2) the amended permit further restricted the annual daily average taking from the two wells to 648,000 L/day (7.5 L/s). Given these new restrictions on the maximum and average takings, the WHPA delineation provided in the previous draft of this report was felt to be overly conservative because it used a combined pumping rate of 28.8 L/s.

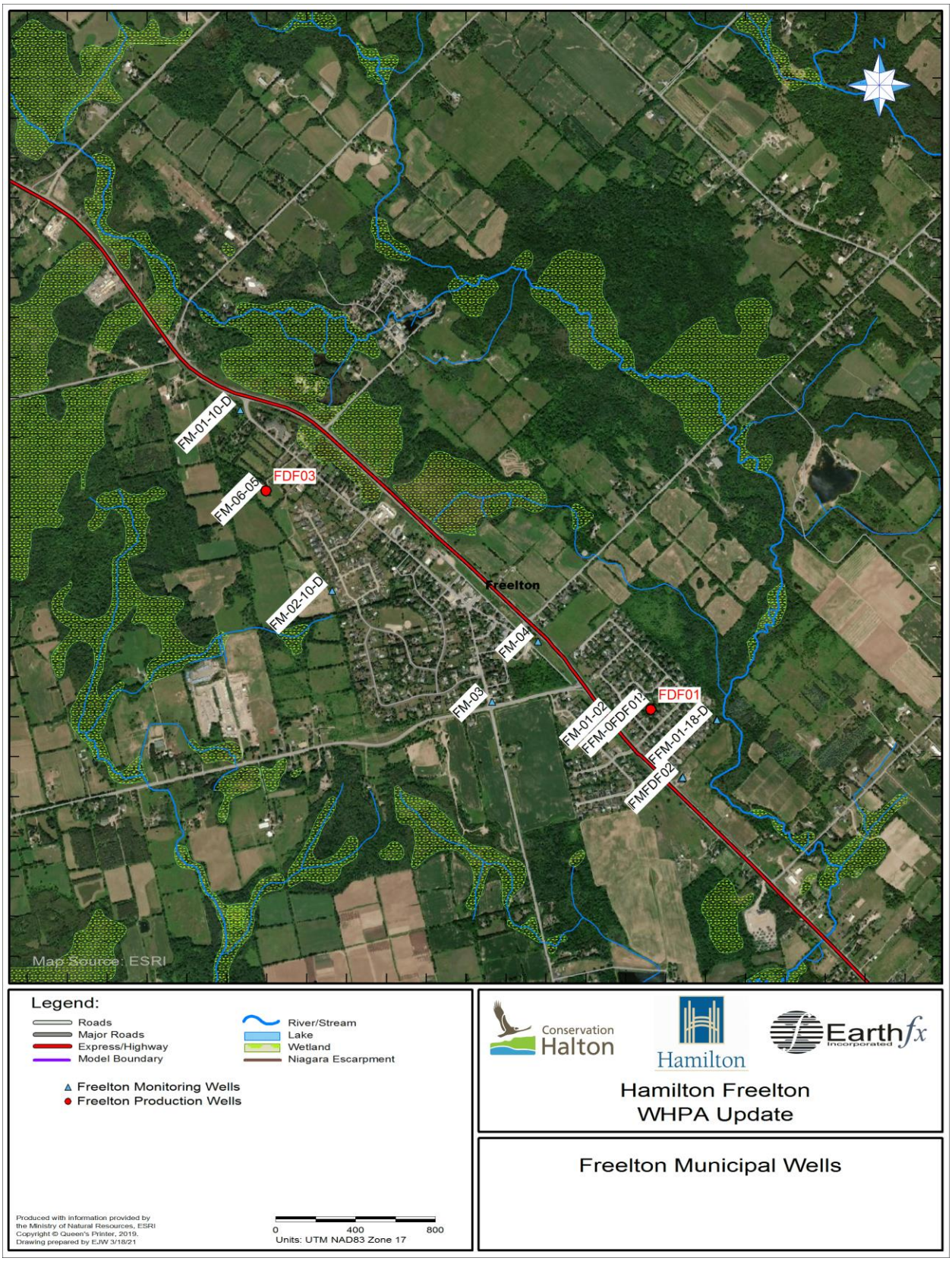

Figure 2.1: Freelton municipal wells.

Based on discussions with the City of Hamilton, it is likely that one or the other of the municipal wells will be operated at their maximum permitted rates (18.3 L/s for FDF01 or 18.6 L/s for FDF03) during the summer months. Much lower rates will be used during the rest of the year to keep the average annual usage below the permitted maximum rate of 7.5 L/s.

Several pumping scenarios were considered in this analysis, including having maximum pumping from FDF01 (18.3 L/s), maximum pumping from FDF03 (18.6 L/s), and various combinations of combined pumping from the two well totalling 18.6 L/s. This was done to ensure that the composite WHPAs from the scenarios would cover all likely combinations of sustained pumping. The five pumping rate configurations used in the analysis are shown in Table 2.3. WHPAs were delineated for the first two scenarios which represent the extreme cases and then adjusted slightly to delineate a composite WHPA that covered differences arising out of the various combined pumping scenarios.

Table 2.2: Table A from PTTW 4650-BB2HXG for the Freelton Municipal wells.

	Source Name / Description:	Source: Type:	Taking Specific Purpose:	Taking Major Category:	Max. Taken per Minute (litres):	Max. Num. of Hrs Taken per Day:	Max. Taken per Day (litres):	Max. Num. of Days Taken per Year:	Zone/ Easting/ Northing:
1	FDF01	Well Drilled	Municipal	Water Supply	1,100	24	1,584,000	365	17 578726 4805236
2	FDF03	Well Drilled	Municipal	Water Supply	1,116	24	1,607,040	365	17 576792 4806337
						Total Taking:	1,607,040		

3.3 Notwithstanding the Total Taking specified in Table A of Condition 3.2, the taking from the wellfield (individual wells or combination) shall not exceed 648,000 Litres Per Day (LPd) on an annual daily average basis.

Table 2.3: Pumping configurations for WHPA delineation.

Pumping Configuration	FDF01 (L/s)	FDF03 (L/s)
Scenario 1	18.3	0
Scenario 2	0	18.6
Scenario 3	9.3	9.3
Scenario 4	4.7	13.9
Scenario 5	13.9	4.7

3 Physical Setting

3.1 *Study Area and Topography*

The study focuses on the RSA of Freelton and the portion of the Bronte Creek watershed located above the Niagara Escarpment. Topography slopes from north to south and from west to east and ranges between 200 metres above sea level (masl) to 350 masl (Figure 3.1). Areas of highest relief correspond to the Galt Moraines along the northern edge of the study area whereas low areas correspond to areas close to the Niagara Escarpment. Below the escarpment, topography slopes gently towards Lake Ontario. Several drumlins, oriented west-east and northwest-southeast, are found in the study area and represent local topographic highs.

3.2 *Physiography*

The physiography of the study area is very diverse, with portions of several physiographic regions, as defined in Chapman and Putnam (1984), present in the area. These include the Horseshoe Moraines, Flamborough Plain, Norfolk Sand Plain, and the Niagara Escarpment (Figure 3.2).

The Horseshoe Moraines make up a long northeast-southwest oriented moraine system that flanks the northern edge of the study area. The deposits are mixed till, kame, and sand and gravel terraces. Portions of the moraines, particularly to the south of Cambridge (at the western edge of the model area), contain hummocky topography with significant local depressions and ponds; however, this does not appear to be prevalent in the study area.

South of the Horseshoe Moraines lies the Flamborough Plain. This feature is largely made up of thin drift overlying dolostone bedrock. It is bounded to the northwest by the Galt Moraine and to the east by the Waterdown Moraine and Niagara Escarpment. Swamps are plentiful in this plain and a few drumlins are found, including one that runs parallel to Highway 6 through Freelton. The dolostone has been washed bare in places, particularly near the edge of the Niagara Escarpment. What little overburden there is, apart from the drumlins, is either bouldery glacial till or sand and gravel. The shallow dolostone bedrock of the Flamborough Plain forms the Freelton municipal supply aquifer.

The Niagara Escarpment is essentially an extension of the Flamborough Plain that is truncated in the east where the bedrock outcrops and forms steep cliffs. Extending back from the edge of the escarpment, the surficial deposits overlying the dolostone bedrock are generally thin to non-existent.

Further south lies the Norfolk Sand Plain, which is one of two major deltas of glacial Lake Whittlesey and Lake Warren. Typical of deltaic deposits, the soil within the Norfolk Sand Plain is composed predominantly of medium to coarse sand.

3.3 *Bedrock Geology*

The study area is underlain by clastic and carbonate sedimentary rocks of Late Ordovician to Middle Silurian age (Figure 3.3). The bedrock surface in the study area regionally slopes gently to the south and southwest in areas above the Niagara Escarpment (Figure 3.4). The strata dip gently to the southwest and the shallower bedrock units subcrop in that direction. In Freelton, the bedrock surface is quite undulating but generally slopes towards the southeast between approximately 285 masl and 260 masl. More dramatic changes in bedrock topography can be seen at the edge of the escarpment and in the bedrock valleys (e.g., Bajc et al., 2009). The most prominent bedrock surface feature in the study area is a tributary valley directed to the southwest toward the larger Dundas bedrock valley and a deep re-entrant valley east of Carlisle.

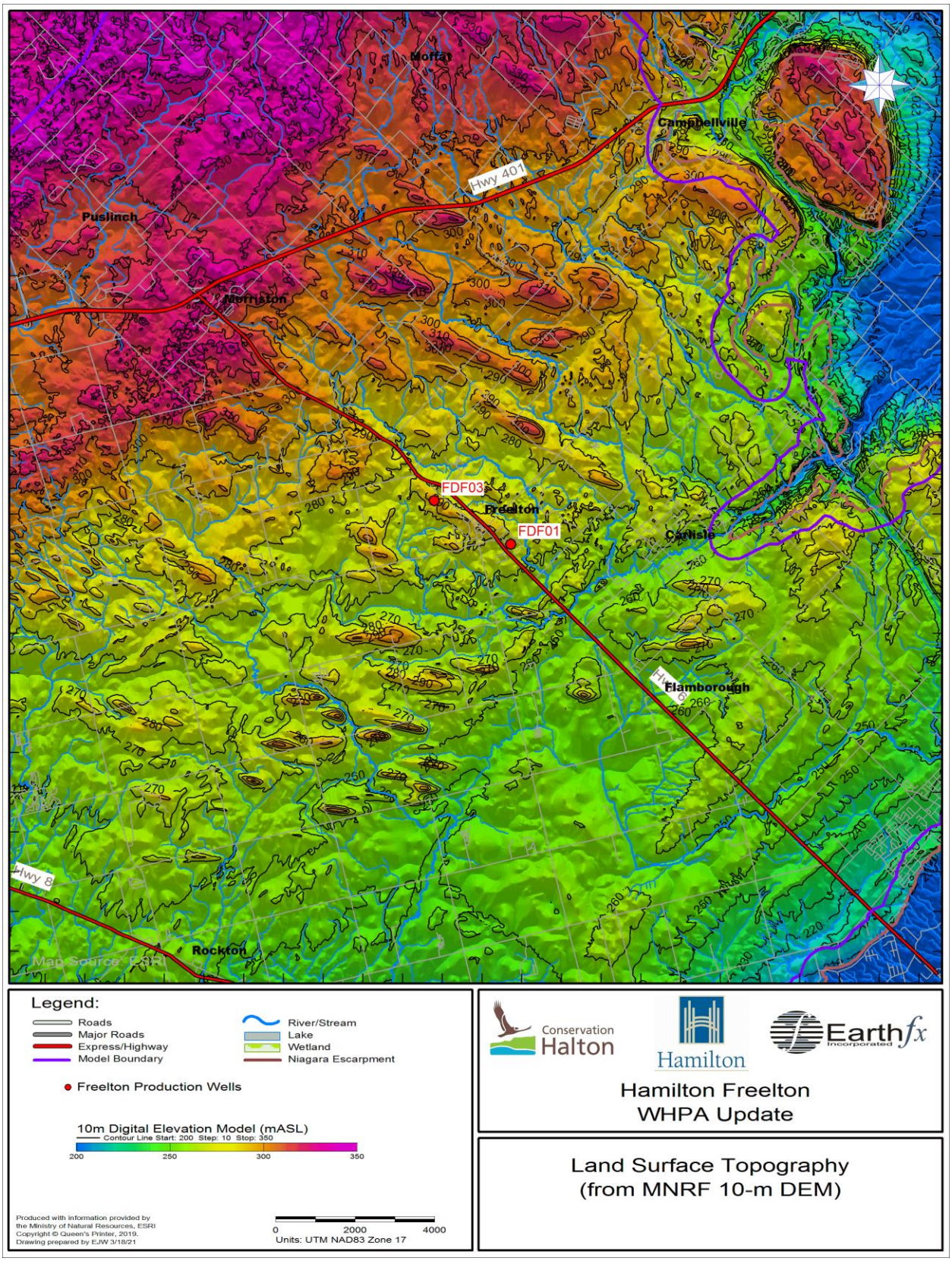

Figure 3.1: Land surface topography in the study area.

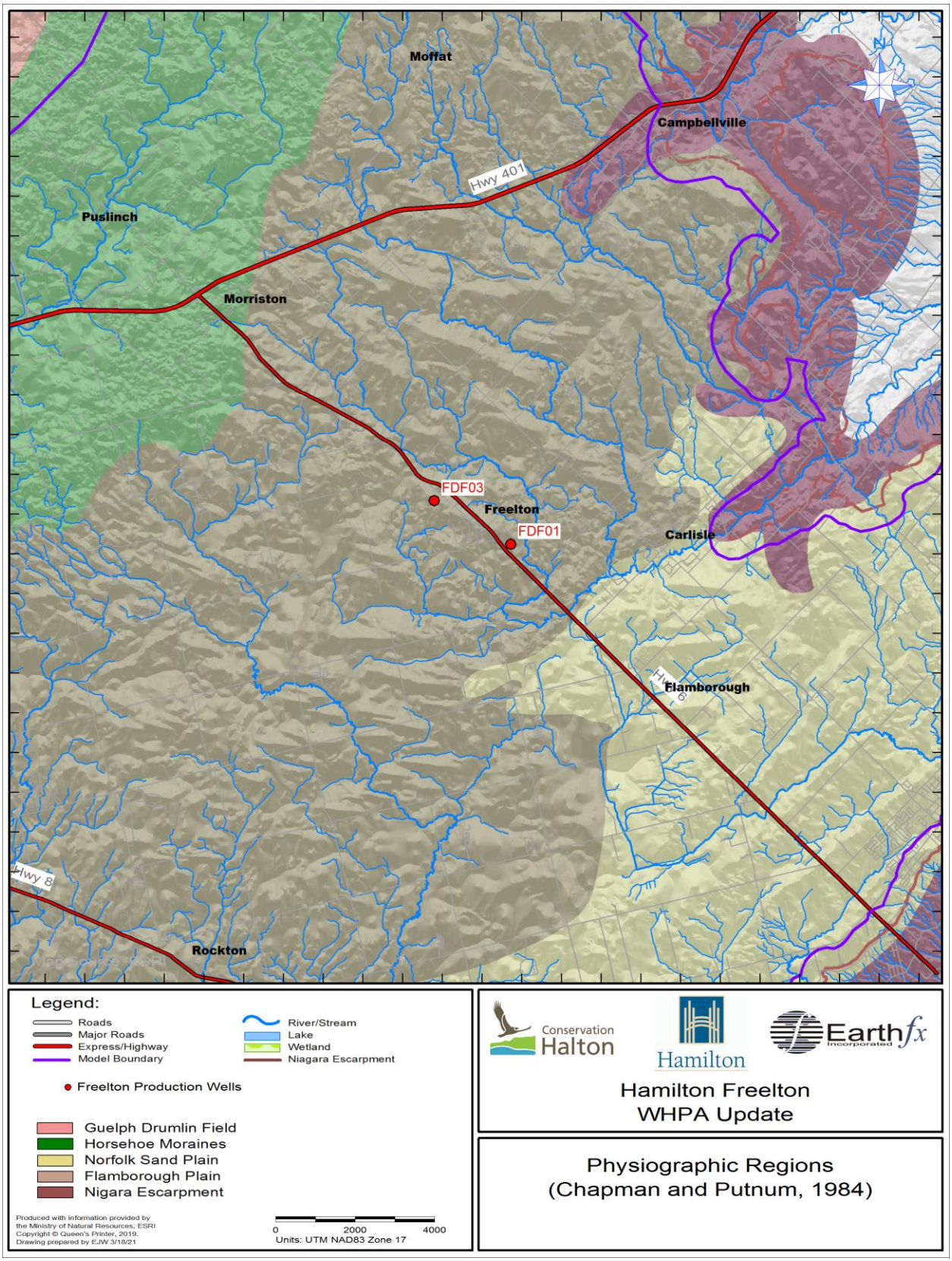

Figure 3.2: Physiographic regions of the study area (physiography modified from Chapman and Putnam, 1984).

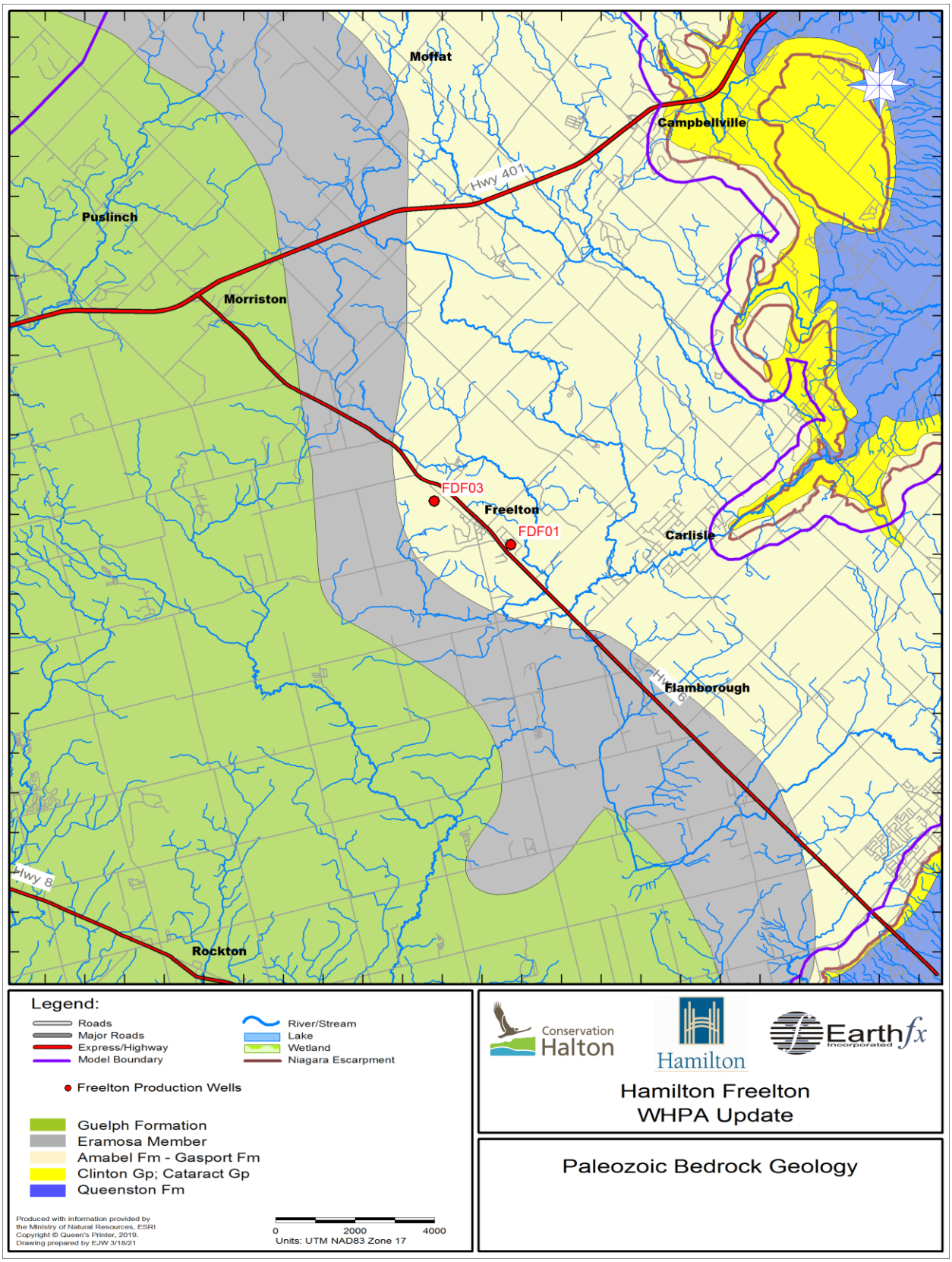

Figure 3.3: Paleozoic bedrock geology of the study area.

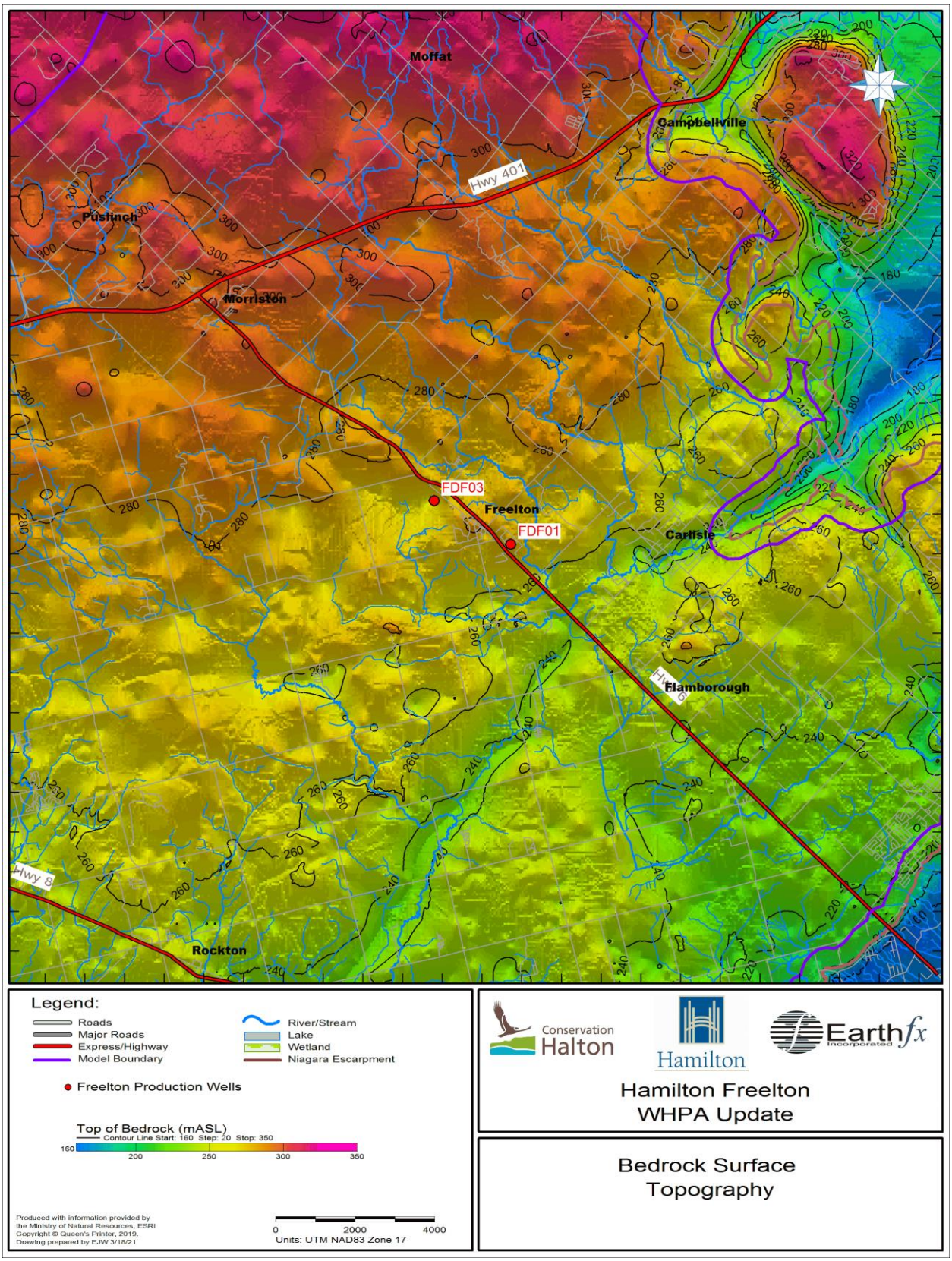

Figure 3.4: Bedrock surface topography.

The bedrock nomenclature in the study area is made complicated because it falls between two different naming conventions historically used for North Hamilton and for the area east of Hamilton along the Niagara Peninsula. The most recent interpretation of the stratigraphic sequence between Tobermory and Guelph was proposed by Brunton (2009). A schematic reconciliation of the naming conventions is presented below in Figure 3.5.

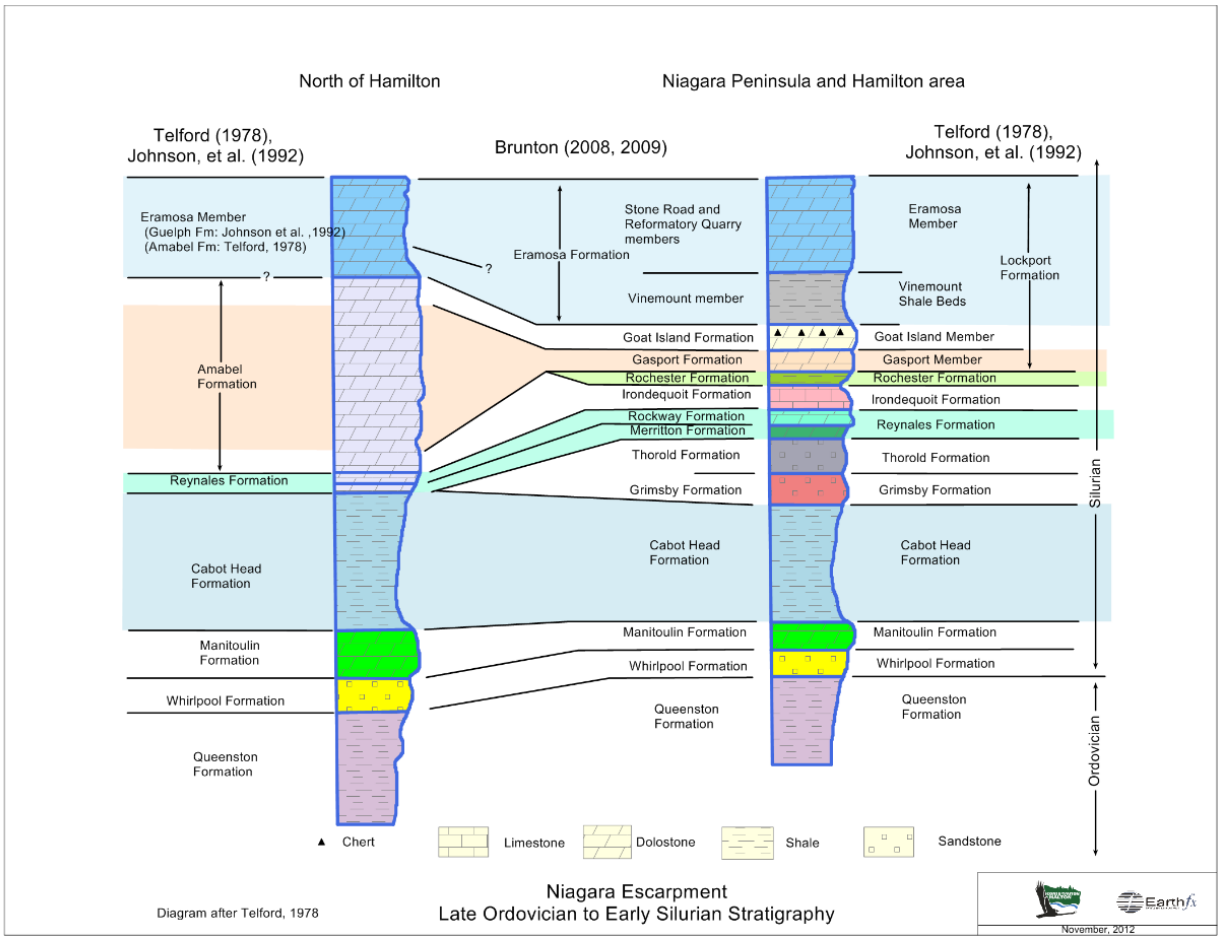

Figure 3.5: Bedrock stratigraphic nomenclature across the study area (from Earthfx, 2014).

The youngest geologic unit that subcrops in the western portion of the study area is the Guelph Formation, which comprises thinly-to thickly-bedded fossiliferous dolostones, typically fine- to medium-crystalline in texture, deposited in both open marine and lagoonal environments (Brunton, 2009). The Guelph Formation is generally considered a good water-supply aquifer. Underlying the Guelph Formation is the Eramosa Formation. The lower part of the Eramosa Formation includes the Vinemount shale beds (Vinemount Member), which act as a regional aquitard restricting the downward movement of groundwater. The Vinemount is mostly eroded away in Freelton although a small number of boreholes report shallow deposits of shale that may indicate some isolated patches of Vinemount may still remain in the area.

Most of the study area, including the town of Freelton is underlain by the Goat Island and Gasport Formations, or what was previously referred to as the Amabel Formation. While the new integrated nomenclature promoted by Brunton (2009) is becoming more widely adopted, the older term “Amabel” is still widely used in the area to refer to the Goat Island and Gasport, along with the deeper Rochester and Irondequoit Formations.

3.4 *Quaternary Geology*

A map of surficial geology is presented in Figure 3.6. The tills in the study area are generally associated with the Port Bruce and Mackinaw phase of the Late Wisconsinan, during which a number of ice advances out of the Lake Ontario basin resulted in the deposition of till sheets as well as several end moraines.

The Wentworth Till outcrops in the western part of the study area, making up the Paris and Galt Moraines. The Wentworth Till is generally a sandy-silt to silty-sand till and locally can be very stony. The surface of the Wentworth Till is drumlinized and, at locations such as north of Flamborough, the tops of Wentworth drumlins 'poke through' the thin cover of younger sediments.

There are significant glaciofluvial deposits at surface near Flamborough, Carlisle, and Freelton. There is an extensive body of gravelly ice-contact stratified material between Carlisle and Freelton that includes two eskers. Around Flamborough, the deposits are flat-lying outwash gravel and gravelly sand. These deposits are younger than the Wentworth Till and may be equivalent in time to the post-Wentworth outwash deposits studied by Costello and Walker (1972) in the Georgetown area, which Karrow (2005) later referred to as the Maple Formation.

Overburden thickness is highly variable, with extensive areas of thinly-covered bedrock in the northeastern part of the study area (Figure 3.7). Overburden thickness exceeds 80 m under the moraines along the western portion of the study area. Overburden is up to 20 m thick through much of Freelton and thins to less than 2 m toward Bronte Creek at the southern extent of the settlement.

3.5 *Conceptual Stratigraphic Model*

A critical step in the construction of a groundwater flow model is the interpretation and representation of the physical system as three-dimensional numerical model layers. Development of the model layers first involved the development of three-dimensional geologic (stratigraphic) model. This study employed the previously developed conceptual geologic model of North Hamilton by Earthfx (2010). The model consists of 16 bedrock layers and 8 overburden layers and spans across North Hamilton and Halton Region.

A geologic cross section through the study area and the Freelton municipal wells is shown in Figure 3.8. For a full description of how the model was developed, the reader is referred to the original report (Earthfx, 2010).

3.5.1 **Updates to the Stratigraphic Model**

Additional borehole data in Freelton have become available since the previous study. New borehole data were added to the project database and reviewed through visual comparison with the geologic model. Discrepancies in the elevation of the bedrock surface of up to several metres were identified at a cluster of private wells in Freelton, west of Highway 6. Upon closer inspection, many of the wells locations had been revised since the previous study, resulting in discrepancies between the borehole logs and the model surface elevations. The bedrock contacts in the problematic wells were re-picked and the bedrock surface was re-interpolated in a local "patch" around Freelton. All elevations outside the local patch were preserved. The change in the top of the bedrock surface is shown in Figure 3.9. In most cases, the bedrock surface was pushed up and, as a result, the top of the Amabel/Gasport Formation also had to be re-interpolated within the same patch area. Any remaining difference between the updated bedrock surface and the updated top of the Amabel/Gasport was infilled with either Eramosa, or Guelph Formation. The Goat Island was not used to infill because it is not interpreted to be present in significant thickness within the patch area.

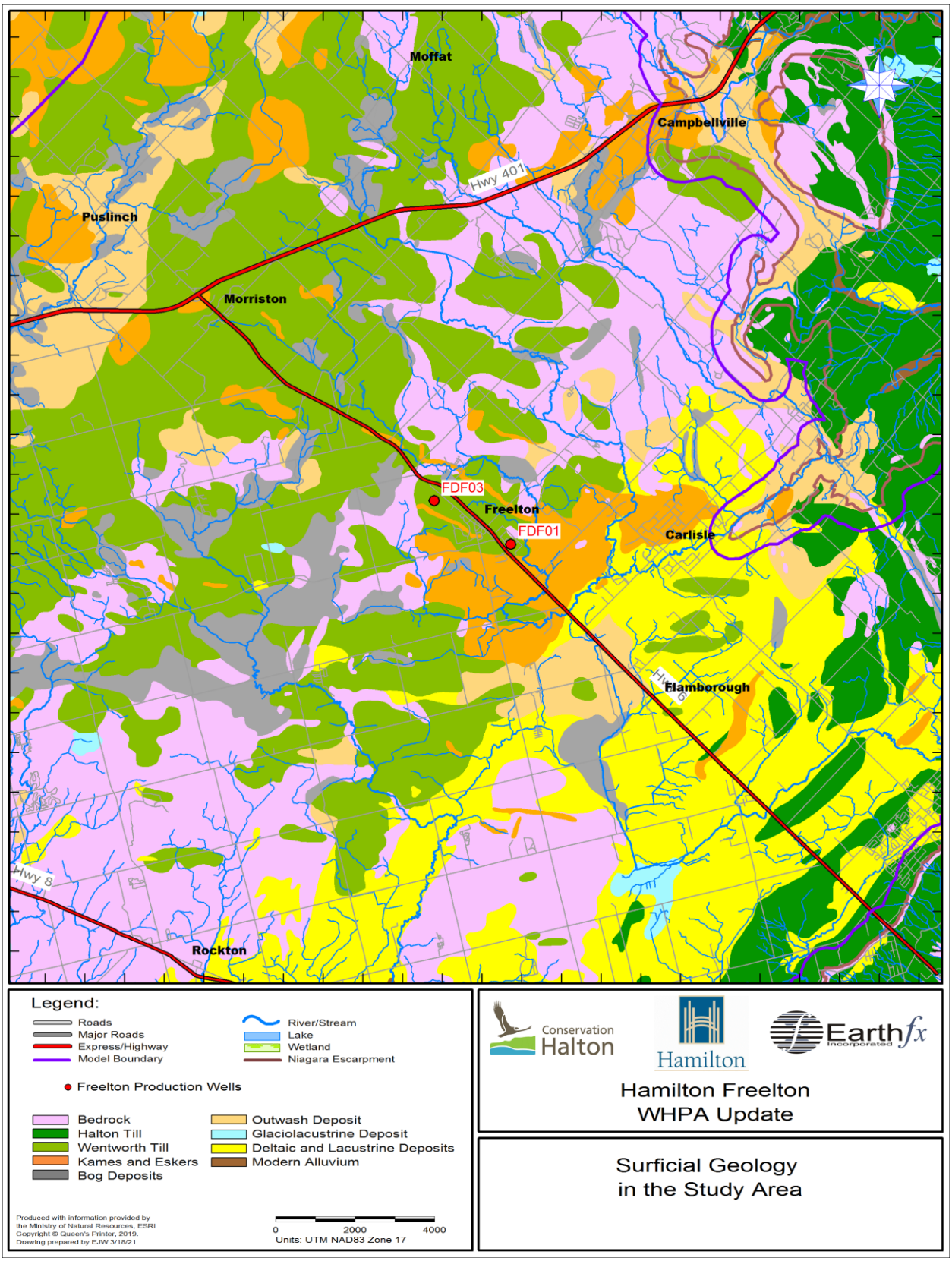

Figure 3.6: Surficial geology of the study area (data from OGS, 2010).

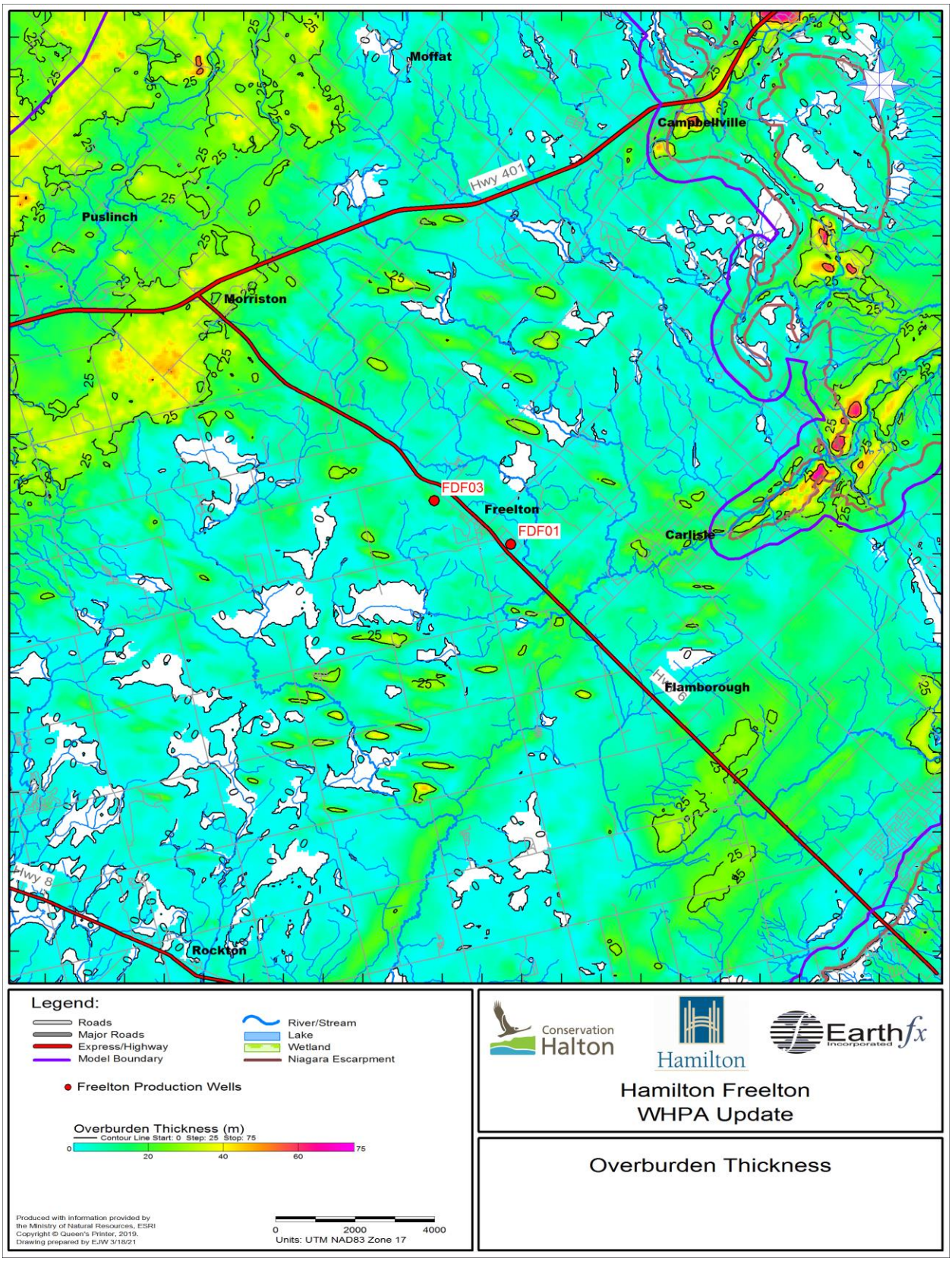

Figure 3.7: Overburden thickness, in m (white areas indicate bedrock at surface).

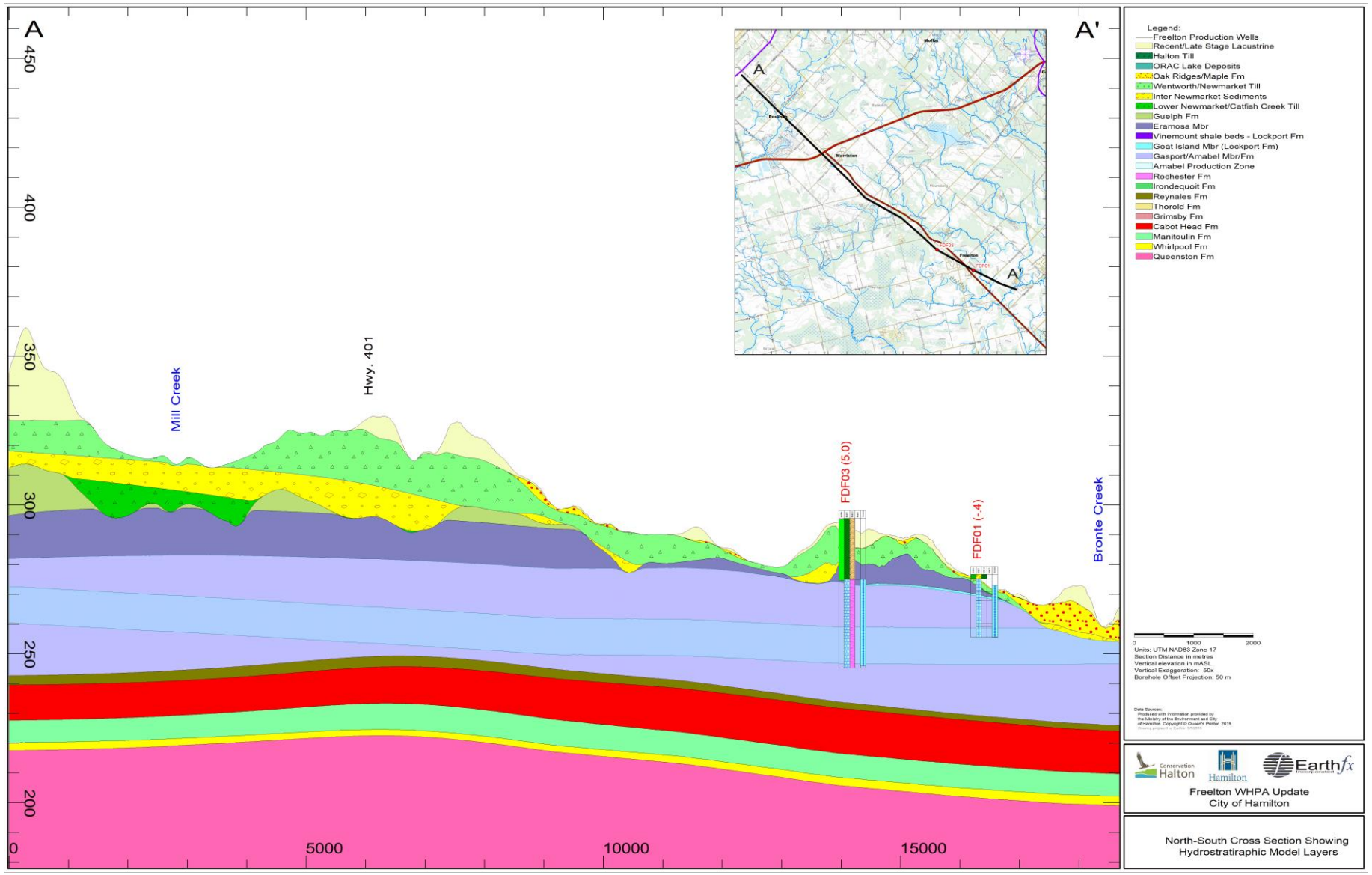

Figure 3.8: North-South cross section showing hydrostratigraphic layers (section location shown in inset map).

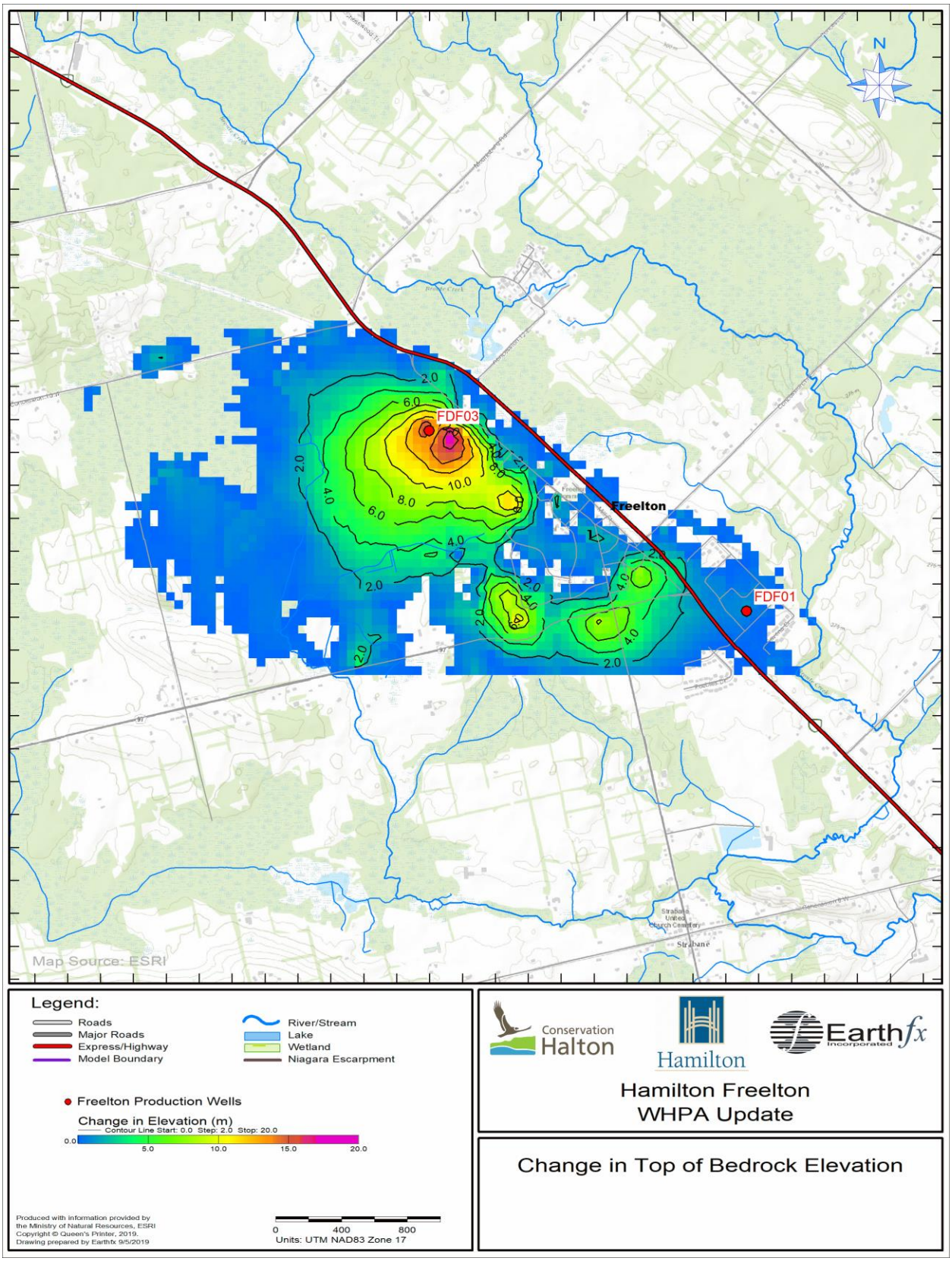

Figure 3.9: Change in top of bedrock elevation.

3.6 *Hydrogeology and Groundwater Flow*

Several hydrogeological investigations were conducted previously in the Freelton area in support of the continued development of the water supply system. Relevant studies, including Jagger Hims (2002, 2003), SNC Lavalin & Charlesworth and Associates (2006), and Dillon (2008) were incorporated into the NH Model development described in Earthfx (2010). While we consulted the past reports again for this study, we focused on incorporating new information, not available at the time of the previous study, into our conceptual understanding of the Freelton area. Two recent studies associated with the increased permitted taking at FDF01 (Wood, 2018a, 2018b) were the primary source of new information considered in this study.

3.6.1 **Aquifers and Aquitards**

The Freelton municipal supply wells are screened in a dolostone bedrock aquifer within the Gasport Formation. As noted above, the “Amabel” is another commonly used name to describe this unit. The Gasport Formation contains the main bedrock aquifer for the region and it is interpreted to contain a middle zone capable for producing high yields. Both FDF01 and FDF03 have been interpreted to intersect the highly permeable fractured zone within the Gasport. The lateral extent of the production zone is unknown. For instance, Brunton (2007) identifies a production zone within the Gasport Formation in the Guelph area; however, packer test data for a proposed quarry located 5 km northeast of Freelton characterizes the formation as having no distinct production zone (AECOM, 2009). Table 3.1 summarizes previous estimates of the hydraulic properties of the Gasport Formation. It should be noted that transmissivity vary with the effective thickness of the aquifer, which may account for some of the variability.

Table 3.1: Summary of hydrogeologic properties of the Gasport/Amabel Formation

Study	Transmissivity (m^2/d)	Storativity	Method
Jagger Himms (2003)	400 - 770	$1.0x10^{-4}$ - $5.0x10^{-4}$	Cooper-Jacob (C-J)
Charlesworth & Assoc. (2006)	155 - 668	$8.8x10^{-5}$ - $3.7x10^{-4}$	Theis, Moench, Walton
Dillon (2008)	69 - 270	$1.2x10^{-2}$ – $6.0x10^{-2}$	C-J, Hantush
GLL (2005)/AECOM (2009)	95 - 1520	N/A	C-J, Hantush, Walton
OGS (2010)	1824 - 4905	N/A	FLUTe
Wood (2018a)	680	$1.0x10^{-5}$	Theis
Earth*fx* Analysis of Wood (2018a)	560	$1x10^{-4}$	Theis

Wood (2018a) recently concluded that the aquifer supplying FDF01 was very productive and highly confined with an estimated transmissivity of 680 m²/d and a storativity of $1x10^{-5}$ based on an analysis of the drawdown response at the nearby monitoring well FM-01-17-d. Earthfx completed an independent review of the Wood (2018a) pump test data at FM-01-17d and FDF-01-02. A Theis analysis, similar to that of Wood (2018a) was used to estimate the aquifer properties and is presented in Figure 3.10. We reach a similar conclusion to Wood (2018a) at FM-01-17-d with an estimated transmissivity of 560 m²/d and a slightly higher storativity of $1x10^{-4}$. Water levels at FDF-01-02 responded in a less confined manner with an estimated transmissivity of about 300 m²/d and a storativity of 0.04 (Figure 3.11).

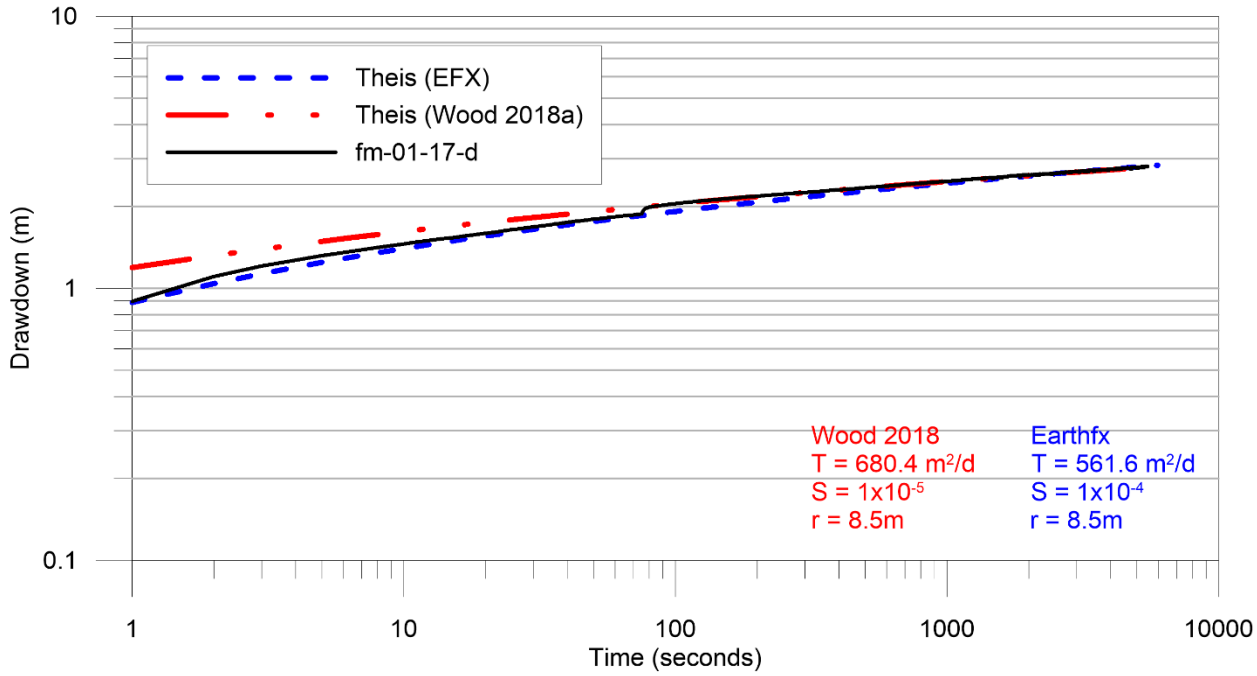

Figure 3.10: Theis drawdown curve match to Wood (2018a) pump test at FM-01-17d.

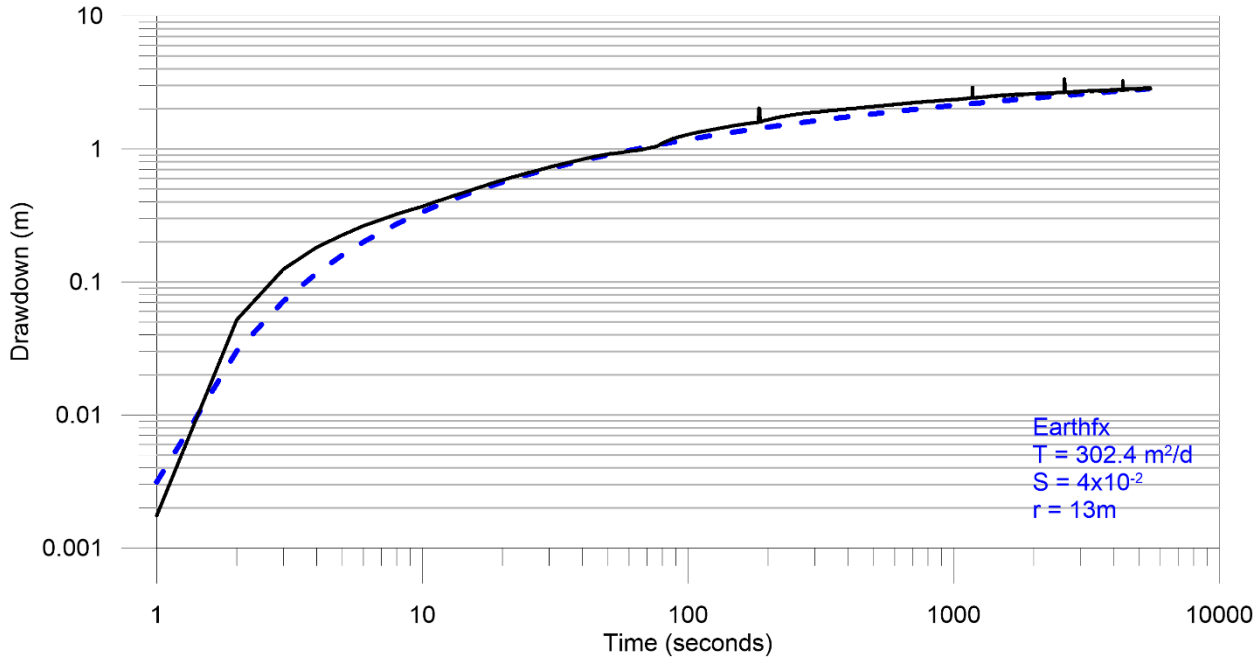

Figure 3.11: Theis drawdown curve match to Wood (2018a) pump test at FDF01-02.

The Wentworth Till acts as the primary aquitard in the study area; however due to its sandy composition, its competency as a confining unit is likely limited. The shallow bedrock may also locally act as an aquitard in places where it is less fractured. Several pump tests related to PTTW applications and groundwater under direct influence of surface water (GUDI) studies indicated that FDF03 is completed in a "leaky aquifer" (Dillon, 2008) while FDF01 was believed to be highly confined (Wood, 2018a). It is therefore not unreasonable to assume that the shallow bedrock behaves has both an aquifer and aquitard in places depending on the degree of weathering and on local connectivity of fractures. Without knowing the precise extents and connectivity of the fracture network, the NH 2019 Model assumes the productive zone can generally be represented as a regionally-extensive high-permeability layer within the Gasport/Amabel Formation.

3.6.2 Groundwater Flow Directions

Static water level data were obtained from the wells in the Ministry of the Environment Conservation and Parks (MECP) Water Well Information System (WWIS) database and from The City. The WWIS water level data represent one-time measurements taken upon construction of the wells. Numerous biases and errors are known to exist in the water well record data including the time of year drilled, the accuracy of the location, and the measurement methods to name a few. The reader is referred to Kassenaar and Wexler (2006) for a detailed description of the intrinsic error and variation in the WWIS dataset. Despite these limitations, the WWIS data have good regional coverage and provide important insight into regional trends in aquifer levels and flow patterns. MECP wells were filtered to remove poor quality data using the location accuracy code and through visual detection of outliers.

Static water level measurements in 12,572 shallow wells (less than 20 m deep) and 12,378 deep wells, which included wells outside the model boundary, were used in groundwater flow characterization, model development, and model calibration. Locations of the shallow and deep water wells in the study area are shown in Figure 3.12. Water-level data were interpolated using a geostatistical technique known as "kriging" to determine general patterns of groundwater flow. Figure 3.13 and Figure 3.14 present the interpolated water levels for the shallow and deep wells, respectively. Groundwater flow is generally perpendicular to the contours of equal groundwater elevation.

The density of shallower wells is higher across in the Freelton area, however both datasets show similar trends in the groundwater flow directions. High water levels occur along the axis of the Galt Moraine and direct flow in a southerly and southeasterly direction. Groundwater flow from the northwest and the north converges toward Freelton and the bending of contours around Bronte creek to the north suggests that this portion of the stream may be a groundwater discharge area.

A recent study in September 2017 by Wood (2018a) surmised that flow in the vicinity of FDF01 is actually from the north or even the northeast. Interpolated water levels generally support incoming flow from the north but do not support incoming flow from the northeast. This discrepancy may be the result of 2017 being a very wet year and higher-than-average recharge in the sand and gravel deposits to the east of the wellfield may have contributed to this change in flow pattern. In contrast, the inter-annual variability in static water levels tends to become lost when interpolating the MECP water levels, which may explain the discrepancy between the interpolated surface and the snapshot water level map from Wood (2018a).

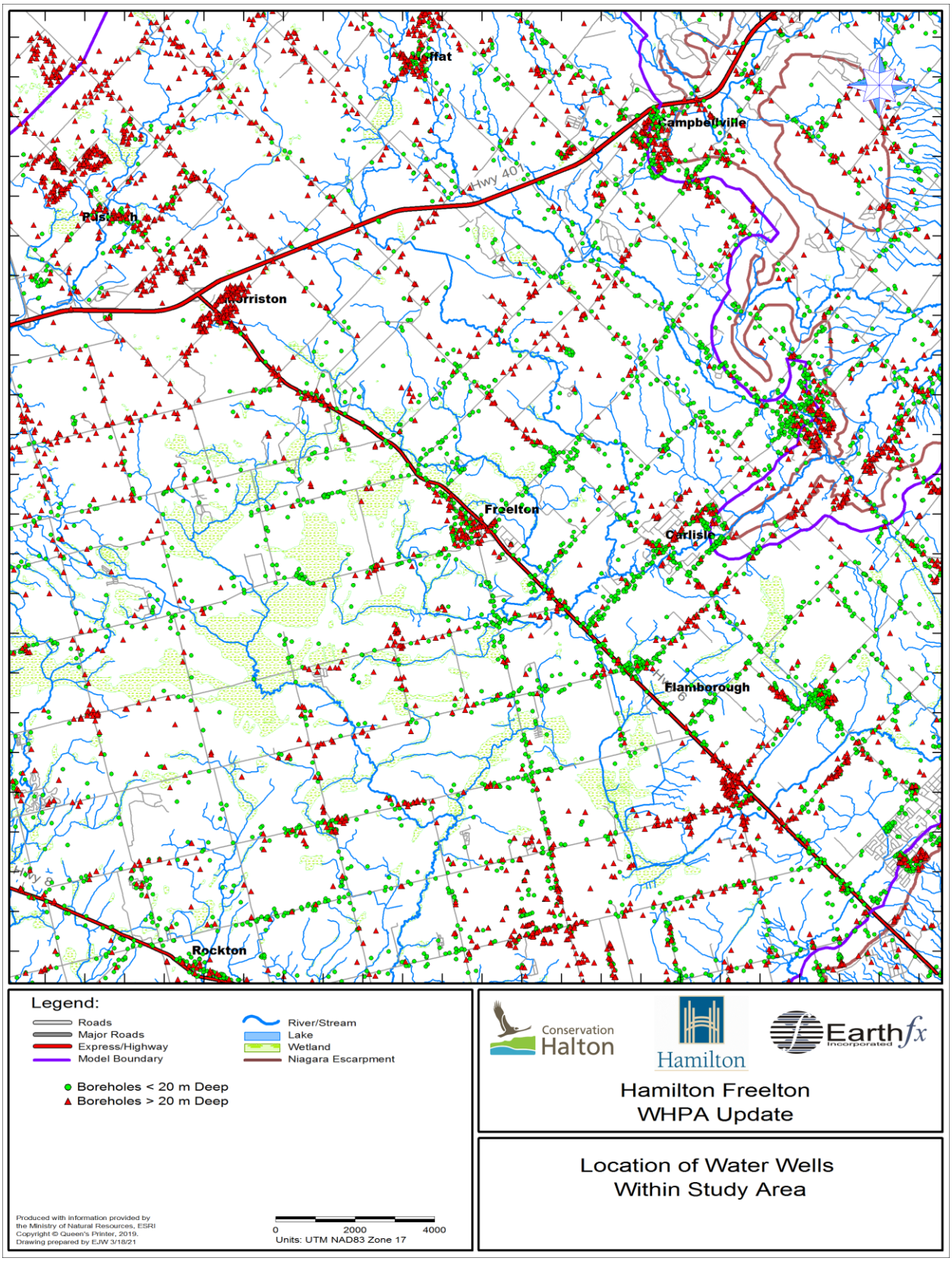

Figure 3.12: Location of water wells within the model area.

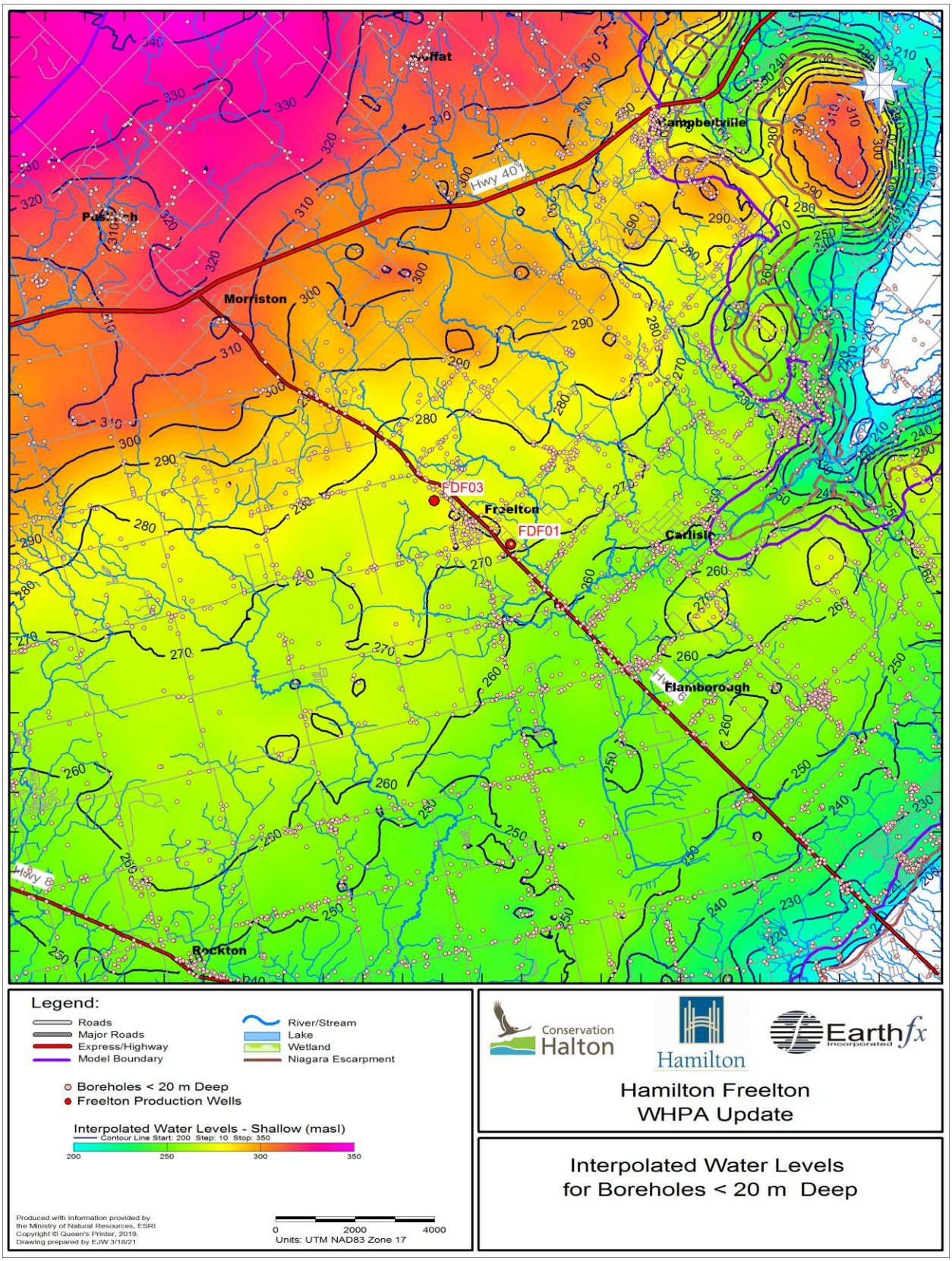

Figure 3.13: Interpolated overburden water levels for boreholes less than 20 m deep.

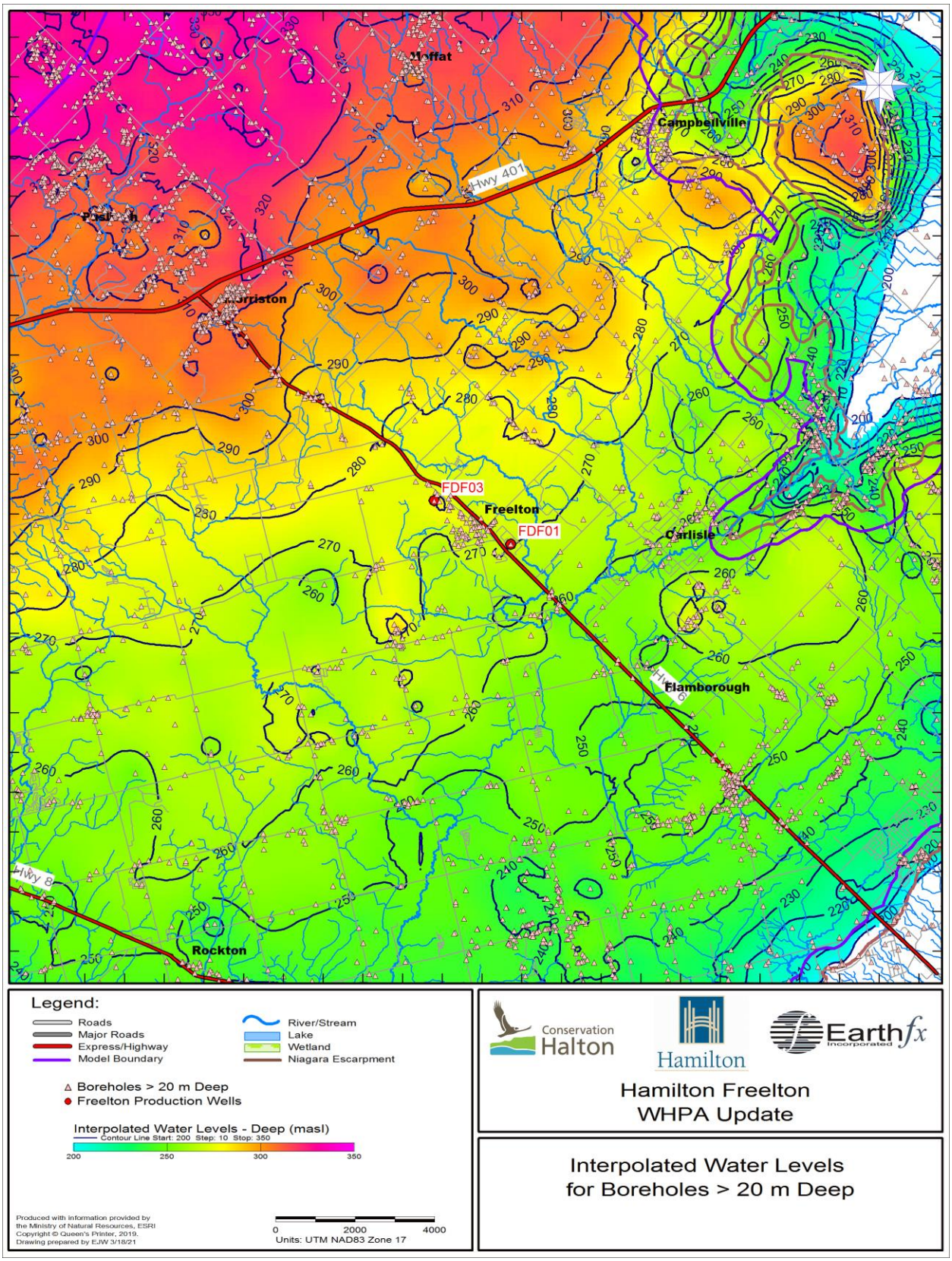

Figure 3.14: Interpolated water levels for boreholes greater than 20 m deep.

4 Hydrologic Model

4.1 *Scope of Model Update*

The NH model study (Earthfx, 2010) employed the U.S. Geological Survey (USGS) Precipitation-Runoff Modelling System (PRMS) to estimate the distribution of long-term average recharge applied to the steady-state groundwater model, described in Section 5. The model was calibrated by matching long-term average streamflow at 23 gauges across the Halton-Hamilton study area. The calibration period spanned from Water Year (WY) 1990 to WY1997.

At the time of the previous study, PRMS was a catchment-based model and Earthfx modified the code to be able to calculate a water balance on a distributed cell-by-cell basis. The study area was represented using 100 m by 100 m cells (also referred to as hydrologic response units) which enabled Earthfx to produce recharge estimates compatible with the MODFLOW grid. Since that time, several versions of PRMS have been released with various improvements, including the ability to natively function as a distributed cell-based model. Another key advancement has been the addition of the cascade overland flow routing module, which allows overland runoff and interflow to move from cell-to-cell down a topographically-driven cascade flow network. The version of PRMS employed in this study was V3.0.5.

A local PRMS model update was completed in the northeast portion of the original model above the Niagara Escarpment to obtain an updated recharge estimate for the Freelton area. Figure 4.1 shows the extent of the PRMS update and gauged catchment area within the Bronte Creek watershed used for calibration. Recharge values from the previous model were used everywhere outside the updated area. The following sections detail the scoped model construction and calibration and present model results including the updated recharge estimate.

4.2 *Model Description*

PRMS is an open-source code for calculating all components of the hydrologic cycle at a watershed, subwatershed, or cell-based scale. PRMS is a modular, deterministic, physically-based, fully-distributed model developed to evaluate the impacts of various combinations of climate (daily precipitation, temperature, and solar radiation), topography, soil type, and land use on streamflow and groundwater recharge. The PRMS code is well documented in Leavesley *et al.* (1983) and Markstrom *et al.* (2008).

The study area was first discretized into a grid of cell-based hydrologic response units (HRUs). Each cell-based HRU, herein referred to as “model cell”, was assigned representative values to characterize slope, slope aspect, elevation, vegetation type, soil type, land use, and surficial geology; such that every cell within the model area had a unique set of properties. Square cells, 100 m on a side, were used to discretize the model area, resulting in 54,604 active model cells covering 546 km². Daily climate data (i.e., rainfall, snowfall, and minimum and maximum temperature) were assigned to each cell by interpolating observations from nearby stations using an inverse-distance-squared weighting scheme. Daily solar radiation values were also assigned to each cell after the model adjusted for cell slope and aspect. Water and energy balances were computed on a daily time step for every cell. Excess water (i.e., overland flow and interflow) was routed between cells along a topographically-driven cascade flow network. The cascade directed outflows from upslope cell as run-on to downslope cells or as discharge to a stream segment.

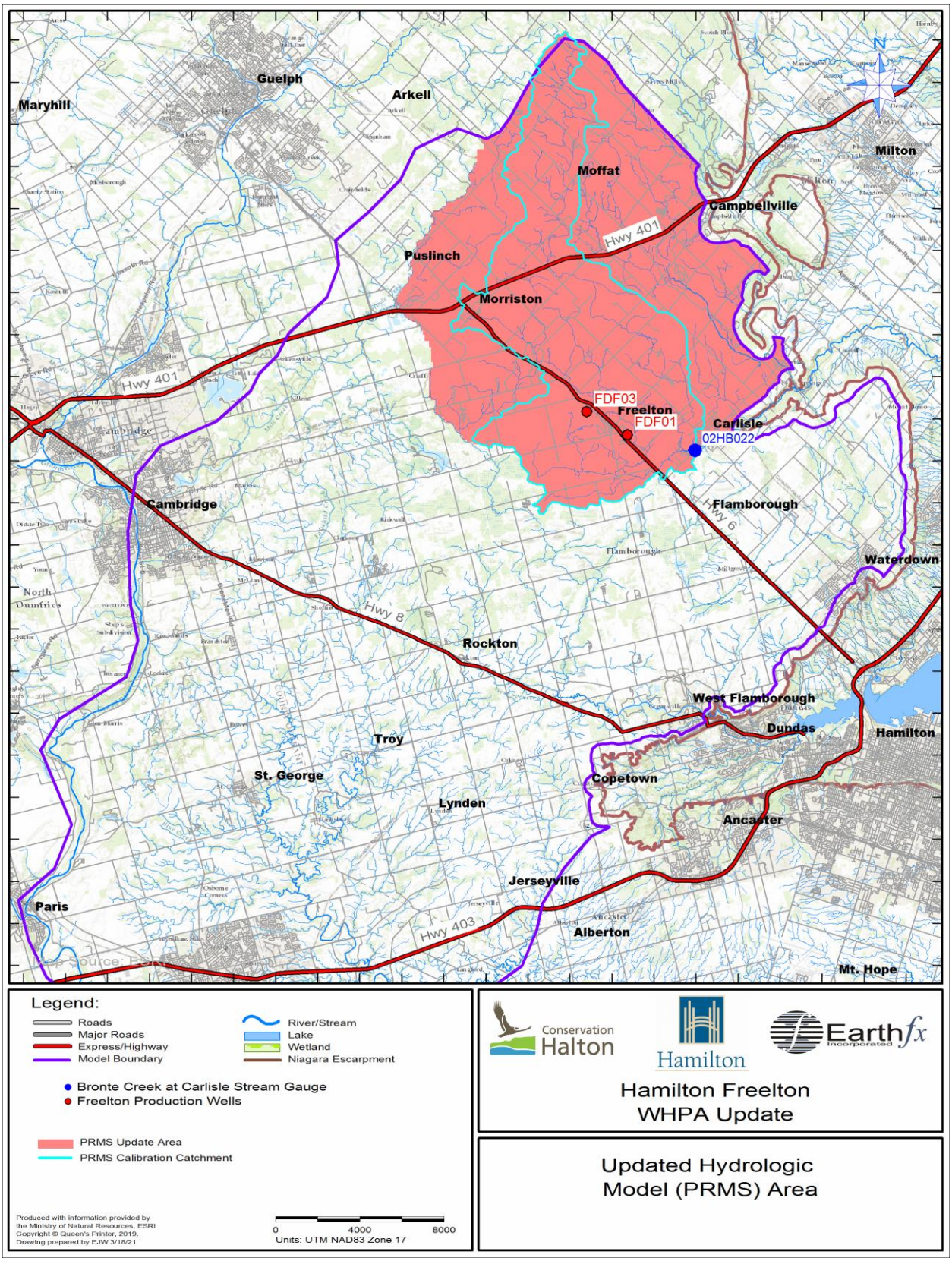

Figure 4.1: Updated hydrologic model (PRMS) area.

A flow chart describing the operation of the PRMS code is shown in Figure 4.2. In brief, the model tracks volumes of water for each cell in a number of storage reservoirs. These include interception storage, depression storage, snowpack storage, capillary zone storage (soil water above wilting point and below field capacity), gravity zone storage (soil water above field capacity and below saturation), and groundwater storage. A two-layer, energy-balance model for the snowpack computes snowpack depth, density, albedo, temperature, sublimation, and snowmelt on a daily basis using maximum and minimum air temperature, solar radiation, and precipitation data.

Each cell can contain both pervious and impervious surfaces; a daily water balance is computed independently for each subarea. The model first computes canopy interception by vegetation for both area types. The amount intercepted depends on vegetation type, precipitation type (rain or snow mixed), and winter/summer vegetation cover density. When interception storage capacity is exceeded, the surplus is allowed to fall though onto the snowpack, if present, or directly onto the ground surface (referred to as throughfall). For impervious areas, the model computes the capture of precipitation and snowmelt by depression storage. When depression storage capacity is exceeded, the surplus runs off. Water is removed from the depression storage reservoir in each cell by evaporation.

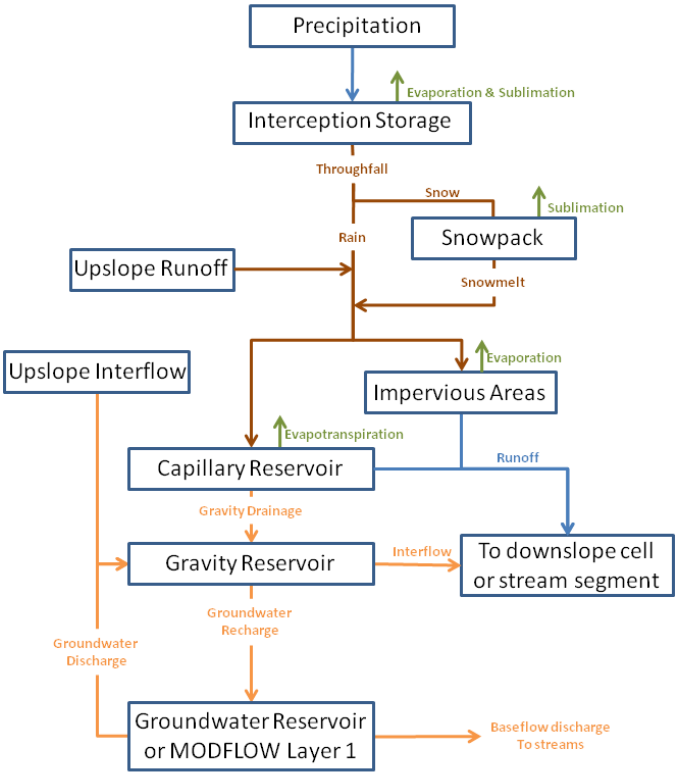

Figure 4.2: PRMS hydrological process flow chart.

During precipitation events, the model first determines whether a snowpack exists. If the temperature is below a user-defined base temperature (T_b), all throughfall is added to the snowpack as new snow. If the temperature is higher than T_b, the throughfall is added to the snowpack as rain which can raise the temperature of the snowpack through sensible and latent heat exchange. If the energy input is high enough and the snowpack becomes isothermal, all or part of the snowpack can melt. The snowpack can also melt or refreeze based on air temperature change and is subject to sublimation. Snowmelt is allowed to infiltrate the soil up to a maximum daily amount and any excess will run off down the cascade network.

Throughfall in the absence of a snowpack is partitioned between infiltration and runoff. The original PRMS code included a “contributing area” method to partition flows (Dickinson and Whiteley, 1970). Earthfx added the Natural Resources Conservation Service (NRCS) Curve Number (CN) method for calculating infiltration to the PRMS code. In this module, runoff is computed based on the characteristics of different combinations of soils, cover type, and antecedent moisture conditions. Overland runoff is routed down the cascade flow network. Any remaining water is assumed to infiltrate the soil.

Soil zone processes are controlled by the amount of moisture in the soil zone as shown schematically in Figure 4.3. Evapotranspiration can remove water from the capillary zone only when the moisture content is above the wilting point. Water is retained against gravity drainage when the moisture content is between field capacity and wilting point. ET rates increase in proportion to the

ratio of the available moisture content (i.e., moisture content minus the wilting point) to the maximum available moisture (field capacity minus the wilting point).

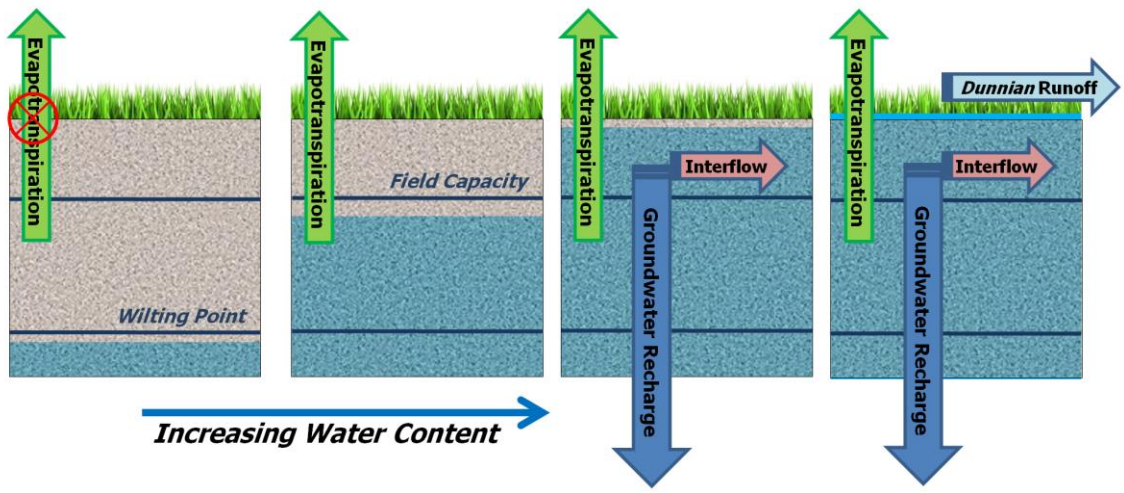

Figure 4.3: Influence of soil zone moisture on recharge, interflow, and runoff processes.

Gravity drainage is the principle process driving groundwater recharge. Gravity drainage occurs when infiltration raises the moisture content in the soil zone above field capacity. The PRMS model assumes that excess soil moisture (i.e., water above field capacity) leaves the cell as either interflow at a rate proportional to the volume in storage (first-order rate) or as gravity drainage. Water in excess of the amount that can be passed as interflow and gravity drainage is retained in the soil zone for the next day. Moisture content may build up in a single event or over successive events to reach saturation. Once the capillary reservoir is filled, additional rain or upslope runoff entering the cell will run off as saturation-excess Dunnian flow.

The maximum daily seepage rate controls the volume of water that is allowed to percolate from the soil zone to the groundwater system. Rates were assigned based on the estimated saturated vertical hydraulic conductivity of the surficial soils. In PRMS, percolating water enters a groundwater reservoir associated with the cell. Discharge to streams from the groundwater reservoir (baseflow) occurs at a rate dependent on the volume of water stored in the groundwater reservoir and a linear decay coefficient. The coefficient was selected to best match recession rates observed in gauge discharge records.

4.3 *Climate Data*

There are three main climate time-series required for the PRMS model: 1) daily precipitation (as separate rainfall and snowfall amounts); 2) daily minimum and maximum temperature (required for calculation of evaporation/ET and snowmelt); and 3) daily net solar irradiation (also required for calculation of evaporation/ET and snowmelt). Periods of records vary among the available climate data sources. A historical analysis of climate data in the study area was completed and is presented in subsequent sections. Information obtained was used to construct a complete climate dataset for WY1951 through WY2018 (note: a water year begins on October 1st of the preceding calendar year).

4.3.1 Historic Precipitation and Temperature

Characterization of the climate of the study area began with an assessment of precipitation and temperature data collected at 126 Environment Canada Atmospheric Environment Stations (AES) proximal to the study area (Figure 4.4). Figure 4.5 presents the annual average precipitation

observed in the study area for a 68-year period showing long-term trends and the number of available stations. The estimated average annual precipitation between WY1951 and WY2018 was 870 millimetres per year (mm/yr) with a range in values between 680 and 1200 mm/yr. Average annual temperature was 7.7 C (Figure 4.6). Figure 4.7 and Figure 4.8 show the long-term average daily precipitation and temperature, respectively, as interpolated over the study area.

4.3.2 Solar Radiation

Incoming solar radiation, used in computing potential ET and snowmelt, is controlled primarily by the number of possible hours of sunshine per day and the percent cloud cover. Solar radiation data are collected at very few stations in Ontario; therefore, data had to be compiled from a variety of sources. Through linear regression analysis, it was shown (Earthfx, 2010b) that the widely-separated southern Ontario solar radiation stations exhibited good inter-station correlation. A continuous data set was created by averaging and infilling daily solar radiation data from 10 stations.

The incoming solar radiation dataset was based primarily on the average of measurements from four climate stations maintained by EC after 1985. These stations include: 611KBE0 (Egbert CARE); 6142285 (Elora Research Station); 6158350 (Toronto); and 6158740 (Toronto MET Research Station). Unfortunately, the period of record of these four sites does not extend beyond August 31, 2003; therefore, the remaining data up to 2016 had to be infilled using measurements from the University of Waterloo, York University, the Burford Tree Farm, and the University of Toronto Mississauga campus. The properties of the climate stations used to create the composite solar radiation dataset are summarized in Table 4.1. Where direct observations were unavailable, solar radiation was estimated by the Hargreaves and Samani (1982) method using daily minimum and maximum temperatures to correct incidental extraterrestrial radiation to match local conditions.

Table 4.1: List of solar radiation stations used to compile solar radiation estimates.

Station	Location	Coordinates (°or UTM(m))	Data Interval	Period of Record
University of Waterloo Weather Station	North Campus	43.4739° N 80.5578° W	15 min	1998-2014
University of Toronto Weather Station	U of T at Mississauga Meteorological Station (UTMMS)	43.5500° N 79.6667° W	hourly	1999- *Present*
York University ESSE Meteorological Observation Station (EMOS)	York University (northwest gate)	43.7753° N 79.510 0° W	5 min	2006-2015
GRCA Burford	Burford Tree Farm	556199 E 4777329 N	5 min	2012-2015
Environment Canada	611KBE0 Egbert Care	597434 E 4898143 N	daily	1988-2003
Environment Canada	6142285 Elora Research Station	546774 E, 4833164 N	daily	1970-2003
Environment Canada	6143083 Guelph OAC	562230 E, 4818850 N	daily	1962-1970
Environment Canada	6158350 Toronto	628988 E, 4836465 N	daily	1956-2000
Environment Canada	6158740 Toronto Met Res Station	616643 E, 4850681 N	daily	1967-1988
Environment Canada	6158776 Toronto Scarborough	642575 E 842297 N	daily	1959-1973

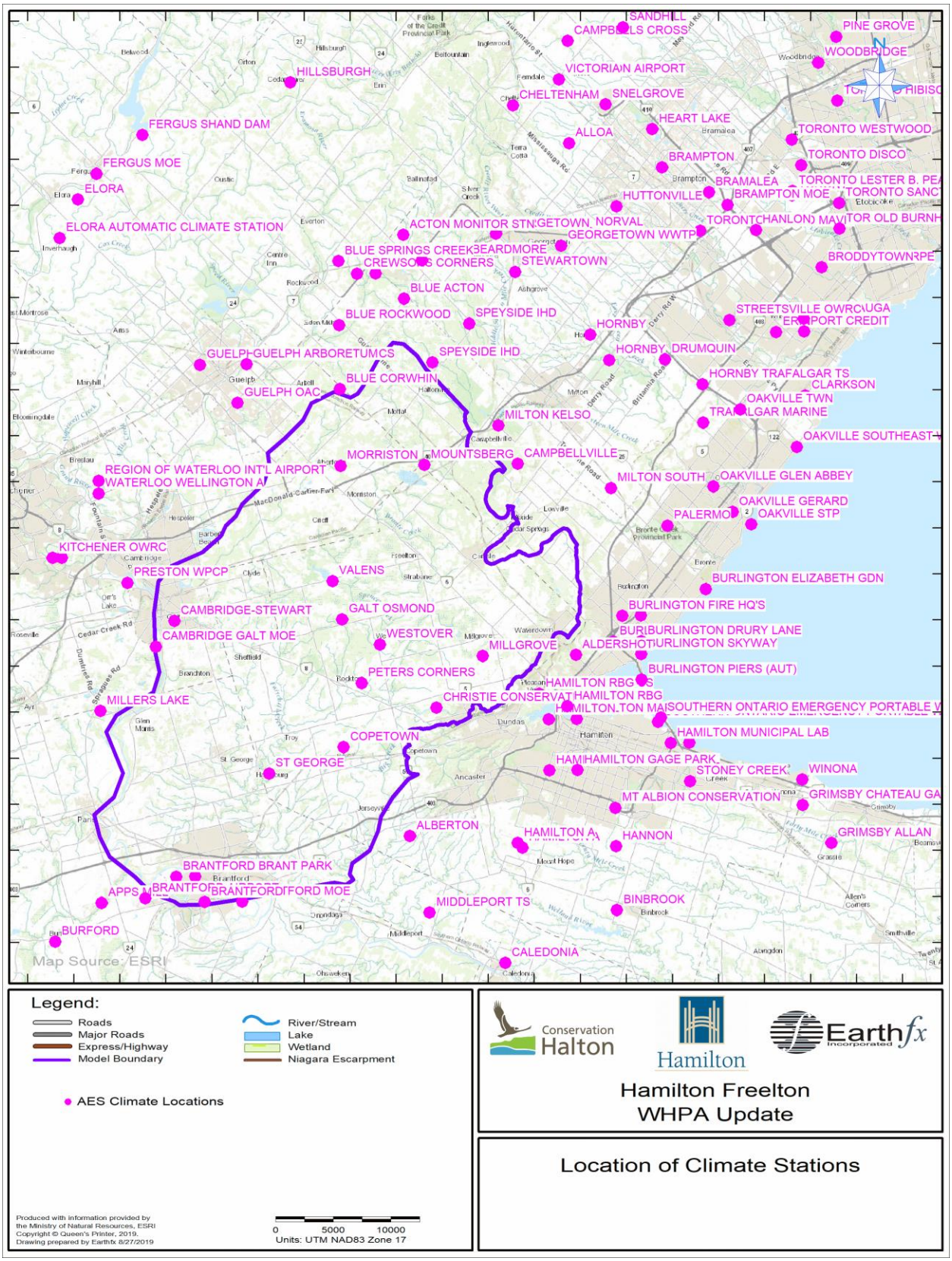

Figure 4.4: Location of climate stations.

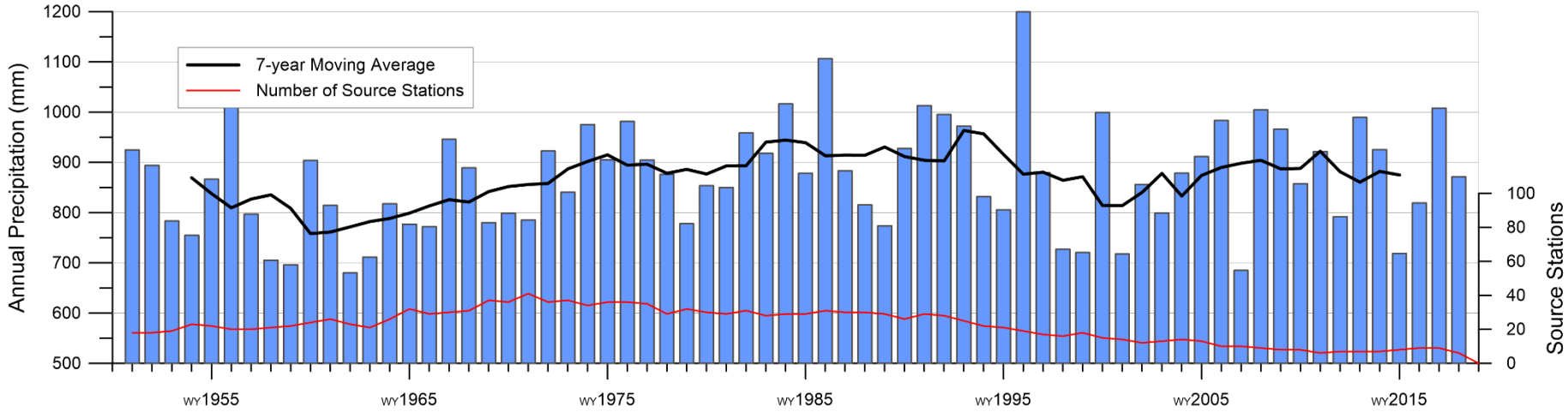

Figure 4.5: Annual average precipitation in the study area (AES Stations, WY1951 – WY2018).

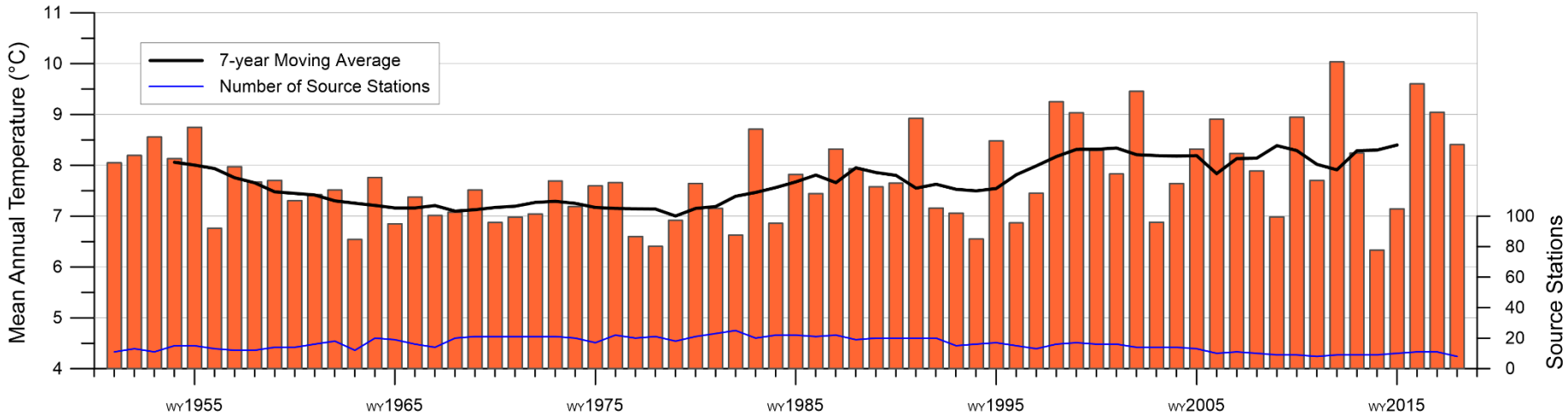

Figure 4.6: Annual average temperature in the study area (AES Stations, WY1951 – WY2018).

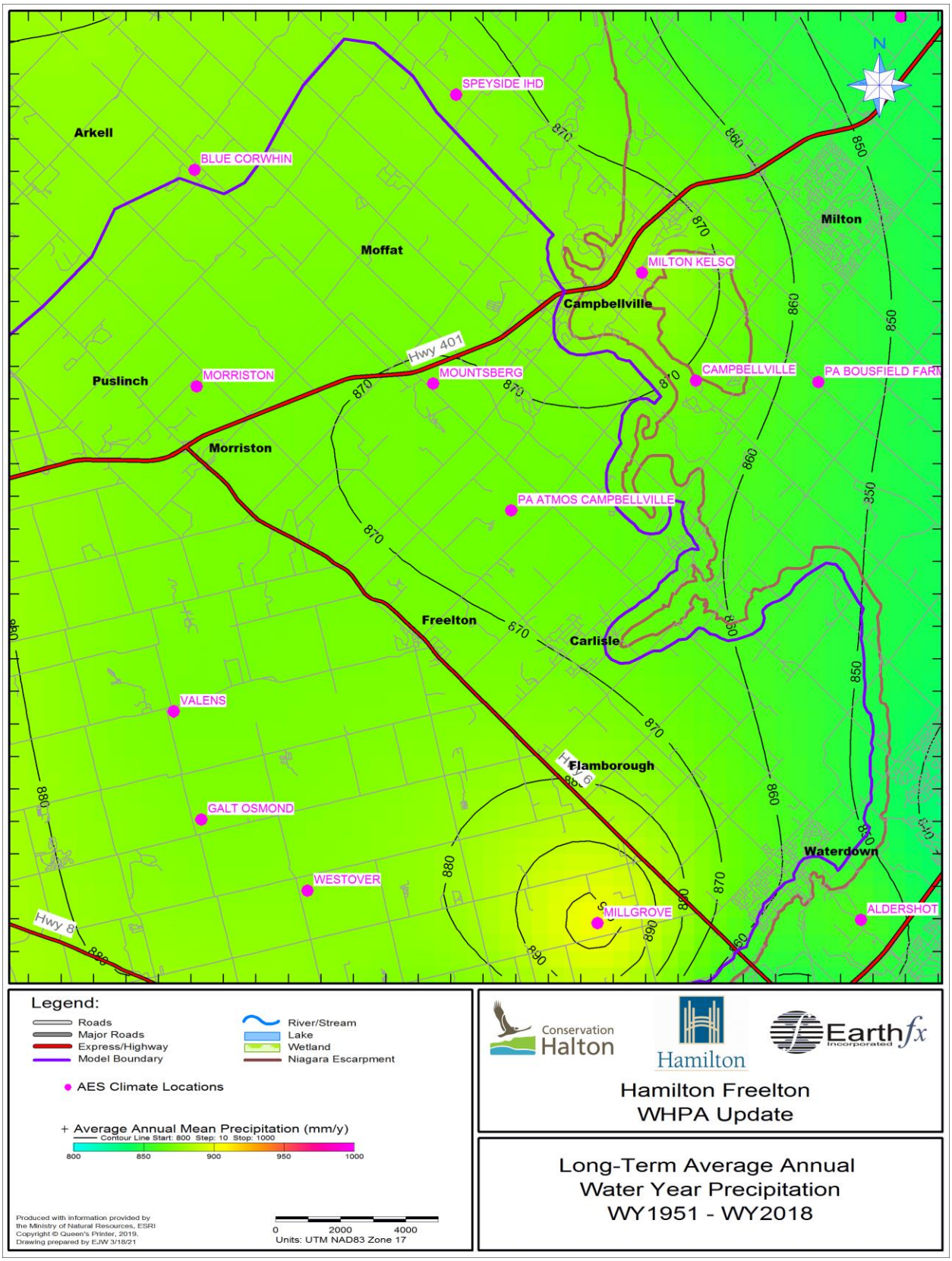

Figure 4.7: Long-term average annual water year precipitation WY1951 – WY2018.

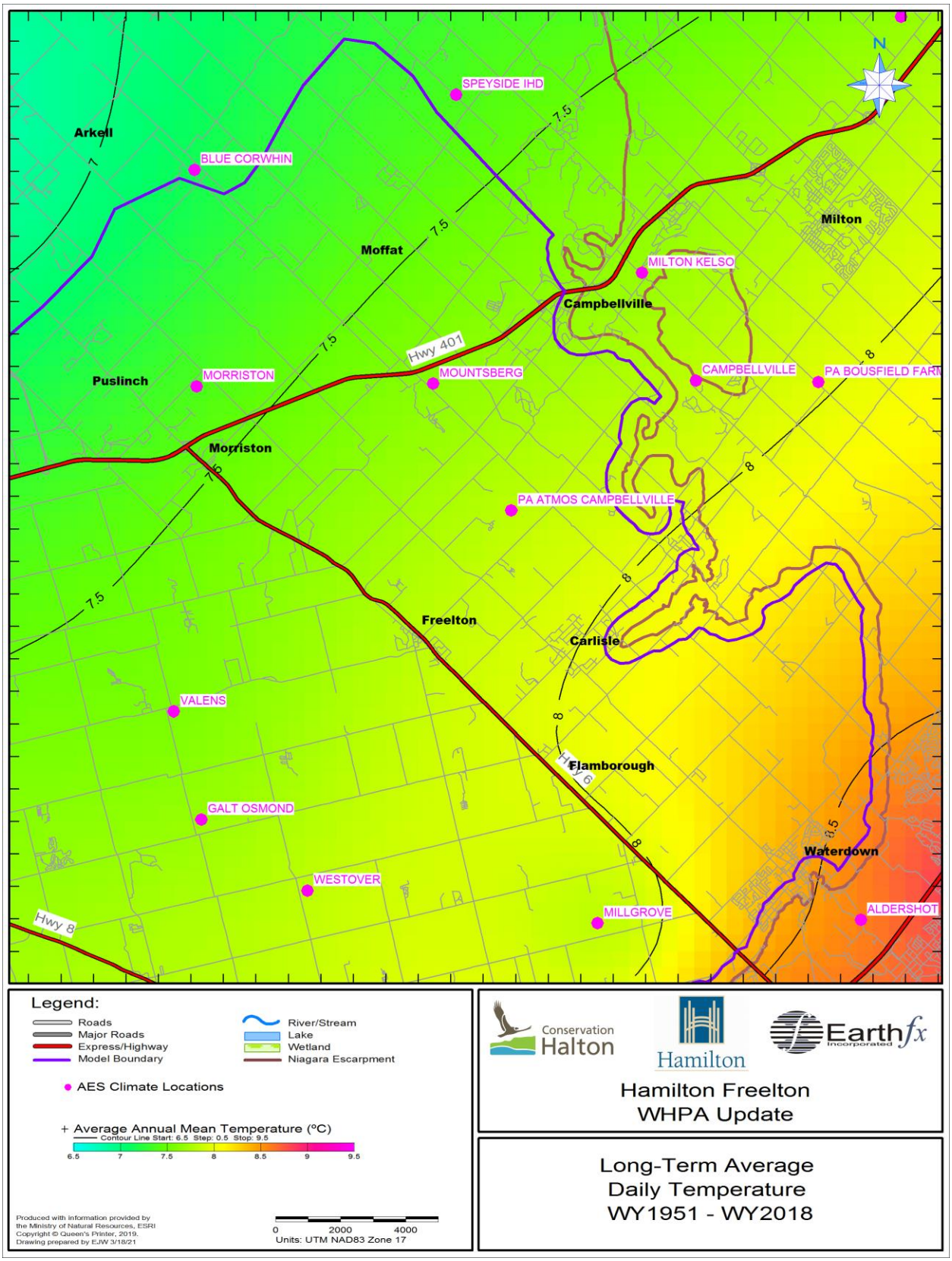

Figure 4.8: Long-term average daily temperature WY1951 – WY2018.

4.4 *Model Parameterization*

The calibrated model parameters used in Earthfx (2010) served as a starting point for this study. It was expected that a minor re-calibration exercise would be required for the model update. Broadly, the PRMS model parameters can be grouped into four data types, including:

1. topography-related properties (e.g., slope, slope aspect, and the cascade network);
2. vegetation and land-cover related properties (e.g., cover density and percent imperviousness);
3. soil-type and surficial geology properties (e.g., field capacity and wilting point);
4. other parameters related to hydrological processes such as snowmelt and ET.

The software package VIEWLOG-GIS (Kassenaar, 2013) was used to create gridded data (such as topography and land cover) and to assign parameters using lookups for tabulated values and cell-based indices. The four data types are discussed below.

4.4.1 **Topography**

Topography for the model area is based on a 10-m DEM (Figure 3.1) produced by the Ontario Ministry of Natural Resources and Forestry (MNRF) which was re-sampled to the 100 m PRMS cells. Re-sampling was done by averaging the values located within every 100 m cell. Slope and slope aspect values were calculated from the re-sampled DEM.

The cascading flow algorithm that routes overland flow and interflow from one cell to adjacent cells (Markstrom *et al.*, 2008) in PRMS allows the possibility of infiltration along the cascade pathway. Runoff from one cell is added as run-on to the adjacent cell, and the total volume of water is available for infiltration and/or runoff to a downslope cell. Interflow is also routed down the cascade network; upslope interflow directly enters the capillary reservoir of the downslope cell. Accumulation of flows from upstream cells and the convergence of the cascade network typically results in a dendritic pattern for runoff to streams with enhanced infiltration in the downslope areas. Actual ET (AET) is also enhanced because more water is available in these cells during summer months.

Topographic data and terrain analysis techniques were used to generate the cascade overland flow routing network. An 8-direction steepest-descent method was selected because it generates an efficient many-to-one cascade network. A small portion of the cascade flow network around Freelton along with the resampled land surface topography is presented in Figure 4.9. A cascade pathline goes from cell to cell until a stream reach, lake, or a closed depression (referred to in PRMS as a “swale”) is encountered.

4.4.2 **Land-use and Land Cover**

Land use and land cover are important inputs to the PRMS models because they strongly influence hydrologic response. The primary sources for land use/land cover data was the Southern Ontario Land Resource Information System (SOLRIS v1) and LANDSAT. While newer SOLRIS datasets are available (e.g., v2 and v3), comparing them indicates that only 0.1% of the PRMS update area has undergone change since the original study in the year 2000. Accordingly, updating to a newer land use dataset was not expected to offer any significant model improvement and was not done. A land use map and the distribution of land use types are shown in Figure 4.10. The per-cent coverage for land use types within the study area is presented in Table 4.2.

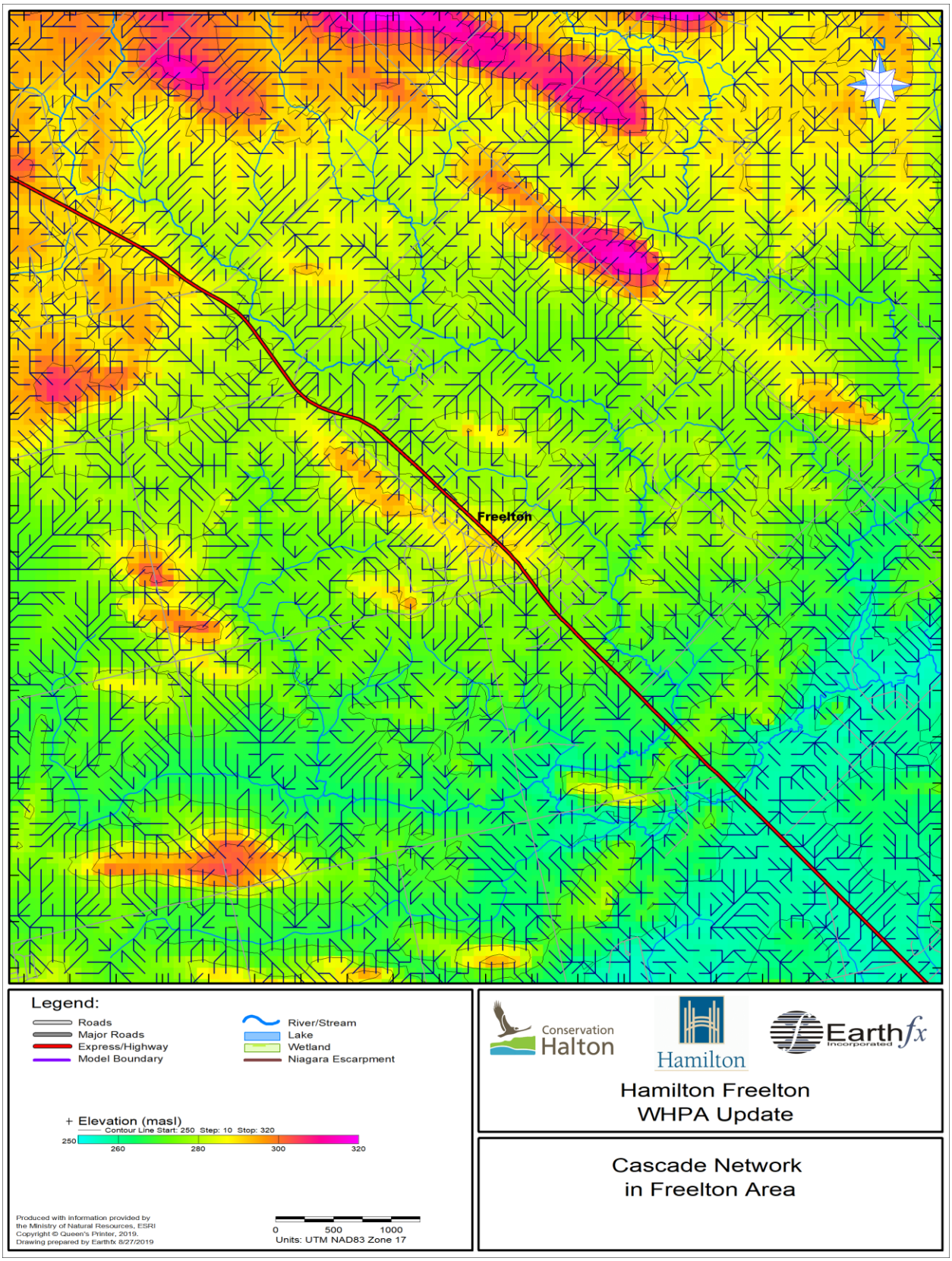

Figure 4.9: Subset of the cascade network for the study area.

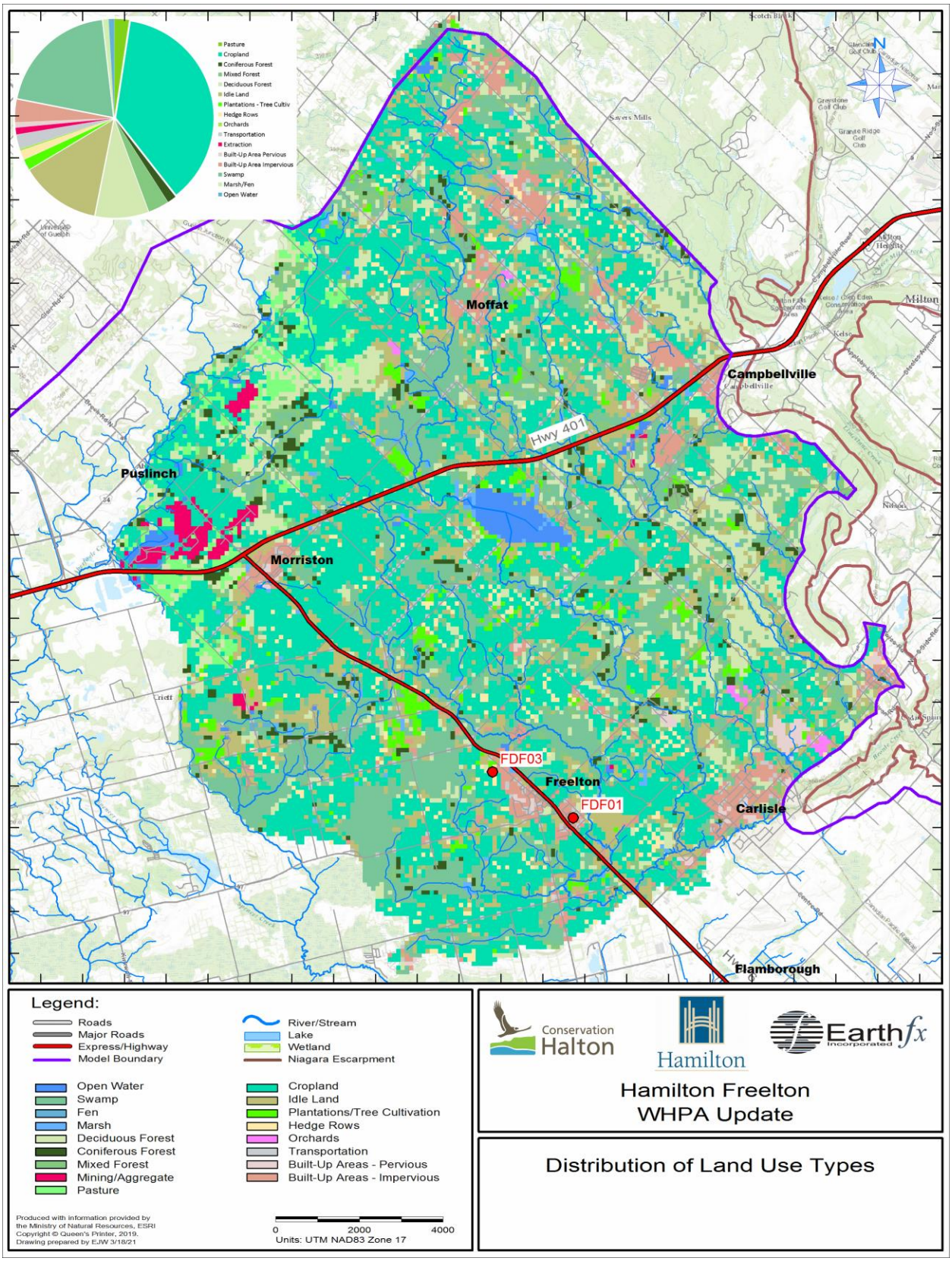

Figure 4.10: Distribution of dominant land use types (based on SOLRIS and LANDSAT coverages).

Table 4.2: Distribution of land classes within the Freelton area (SOLRIS and LANDSAT coverages).

Land Use Class	Index[1]	%of Area
Pasture	25	2.40
Cropland	26	37.0
Coniferous Forest	58	1.48
Mixed Forest	59	3.45
Deciduous Forest	60	8.80
Idle Land	65	13.3
Plantations - Tree Cultivation	66	1.77
Hedge Rows	67	1.55
Orchards	68	0.27
Transportation	72	2.39
Extraction	73	1.11
Built-Up Area Pervious	74	0.82
Built-Up Area Impervious	75	3.76
Swamp	80	20.1
Marsh/Fen	93	0.91
Open Water	96	0.91

[1] See Table 4.3 for more information on index numbers. Similar land use types were assigned similar properties and have been combined for this table.

A large number of land-use categories are found in the study area and several of hydrologic properties used in the PRMS model could be reasonably correlated with the different categories. These were assigned to model cells using a look-up table with parameter values for each land-use class. An underlying assumption was that properties for a particular class (e.g., “built-up area - pervious”) were the same in one part of the model area as another. Hydrologic properties included:

- percent imperviousness - the proportion of the cell area assumed to be impervious;
- depression storage - the amount of water retained over impervious areas;
- vegetation index – dominant vegetation type (bare, grass, shrub, or trees) in the cell;
- vegetative cover density - the fraction of pervious area covered by vegetation and/or tree canopy. Two values are provided: one for the growing season and one for winter;
- interception storage - the amount of precipitation retained on vegetative surfaces and/or tree canopy. Three values are provided: interception storage for summer rain, winter rain, and winter snow. Effective interception capacity is the product of vegetative cover density and interception storage;
- soil zone and extinction depth thickness – used to calculate the size of the capillary and gravity reservoirs when combined with soil properties (porosity, field capacity, and wilting point), as described in the next section.

The land use lookup table for the study area is provided in Table 4.3. The assumption of consistent property values across the study area was felt to be reasonable for most land use classes. While the breakdown of urban areas into “built-up area pervious” and “built-up area impervious” may be overly simplified, the portion of the study area with these classifications is small.

Table 4.3: Summary of land use/land cover properties.

Description	Index	Source	Impervious Fraction	Depression Storage (mm)	Vegetation Index [1]	Winter Cover Density	Summer Cover Density	Winter Radiation Transmission Fraction	Snow Interception Storage (mm)	Summer Rain Interception Storage (mm)	Winter Rain Interception (mm)	Soil Zone Depth (mm)	Extinction Depth (mm)
Water	1	LANDSAT	0	0	0	0	0	1	0.00	0.00	0.00	1828.80	1828.80
Coastal Mudflats	2	LANDSAT	0	0	1	0.1	0.2	0.95	2.03	1.78	0.76	1219.20	304.80
Intertidal Marsh	3	LANDSAT	0.4	7.62	2	0.2	0.55	0.65	2.03	1.78	0.76	1219.20	304.80
Supertidal Marsh	4	LANDSAT	0.4	7.62	2	0.2	0.55	0.65	2.03	1.78	0.76	1219.20	304.80
Freshwater.	5	LANDSAT	1	50.8	0	0	0	1	0.00	0.00	0.00	1219.20	304.80
Deciduous Swamp	6	LANDSAT	0	25.4	2	0.4	0.8	0.55	5.08	1.78	0.76	1524.00	914.40
Conifer Swamp	7	LANDSAT	0	25.4	2	0.4	0.8	0.55	5.08	2.29	1.02	1524.00	914.40
Open Fen	8	LANDSAT	0	25.4	2	0.4	0.8	0.65	2.03	2.03	0.76	1524.00	914.40
Treed Fen	9	LANDSAT	0	25.4	2	0.5	0.9	0.65	2.54	2.54	1.02	1524.00	914.40
Open Bog	10	LANDSAT	0	25.4	2	0.4	0.8	0.65	2.03	1.78	0.76	1524.00	914.40
Treed Bog	11	LANDSAT	0	25.4	2	0.5	0.9	0.65	2.54	2.29	1.02	1524.00	914.40
Tundra Heath	12	LANDSAT	0	12.7	2	0.3	0.55	0.65	2.03	1.78	0.76	1524.00	609.60
Dense Deciduous	13	LANDSAT	0	0	3	0.45	0.9	0.25	3.05	3.56	1.27	1524.00	304.80
Dense Coniferous	14	LANDSAT	0	0	3	0.5	0.8	0.15	3.81	3.05	1.27	1524.00	304.80
Coniferous Plantation	15	LANDSAT	0	0	3	0.4	0.7	0.25	3.81	2.79	1.27	1524.00	304.80
Mixed - Deciduous	16	LANDSAT	0	0	3	0.5	0.85	0.25	3.05	3.30	1.27	1524.00	304.80
Mixed - Coniferous	17	LANDSAT	0	0	3	0.45	0.85	0.15	3.81	3.05	1.27	1524.00	304.80
Sparse Coniferous	18	LANDSAT	0	0	3	0.5	0.7	0.15	3.81	2.79	1.27	1524.00	304.80
Sparse Deciduous	19	LANDSAT	0	0	3	0.4	0.75	0.25	3.05	3.05	1.27	1524.00	304.80
Recent Cutovers	20	LANDSAT	0	0	1	0.4	0.7	0.95	2.03	2.03	1.02	1524.00	304.80
Recent Burns	21	LANDSAT	0	0	1	0.1	0.2	0.95	2.03	1.78	0.76	609.60	304.80
Old Cuts and Burns	22	LANDSAT	0	0	1	0.1	0.2	0.95	2.03	1.78	0.76	1219.20	304.80
Mine Tailings, …	23	LANDSAT	0.4	12.7	1	0.1	0.2	1	1.27	2.03	1.02	609.60	304.80
Settlement …	24	LANDSAT	0.3	1.27	2	0.4	0.7	0.95	2.03	2.03	1.02	304.80	152.40
Pasture …	25	LANDSAT	0	0	2	0.5	0.9	0.4	3.05	2.54	1.27	1219.20	304.80
Cropland	26	LANDSAT	0	0	2	0.3	0.9	0.7	2.03	2.54	0.76	1219.20	304.80
Alvar	27	LANDSAT	0.3	1.27	2	0.3	0.5	0.95	1.78	1.78	0.76	609.60	304.80
Unclassified …	28	LANDSAT	0	0	2	0.3	0.5	0.95	2.03	2.03	1.02	1219.20	304.80
Open Cliff and Talus	32	SOLRIS	0	0	1	0.1	0.2	0.95	2.03	1.78	0.76	609.60	304.80
Shoreline	35	SOLRIS	0	0	1	0.1	0.2	0.95	2.03	1.78	0.76	609.60	304.80
Open Shoreline	36	SOLRIS	0	0	1	0.1	0.2	0.95	2.03	1.78	0.76	609.60	304.80
Open Bluff	38	SOLRIS	0	0	1	0.1	0.2	0.95	2.03	1.78	0.76	609.60	304.80
Open Sand Barren and Dune	40	SOLRIS	0	0	1	0.1	0.2	0.95	2.03	1.78	0.76	609.60	304.80
Open Tallgrass Prairie	50	SOLRIS	0	0	2	0.4	0.8	0.65	2.03	2.03	1.02	1219.20	304.80

Description	Index	Source	Impervious Fraction	Depression Storage (mm)	Vegetation Index [1]	Winter Cover Density	Summer Cover Density	Winter Radiation Transmission Fraction	Snow Interception Storage (mm)	Summer Rain Interception Storage (mm)	Winter Rain Interception (mm)	Soil Zone Depth (mm)	Extinction Depth (mm)
Tallgrass Savannah	51	SOLRIS	0	0	3	0.3	0.8	0.5	2.03	2.29	1.27	1219.20	304.80
Tallgrass Woodland	52	SOLRIS	0	0	3	0.4	0.8	0.3	2.03	2.54	1.27	1219.20	304.80
Coniferous Forest	58	SOLRIS	0	0	3	0.5	0.8	0.15	3.30	3.30	1.52	1219.20	304.80
Mixed Forest	59	SOLRIS	0	0	3	0.45	0.8	0.2	3.81	3.05	1.27	1219.20	304.80
Deciduous Forest	60	SOLRIS	0	0	3	0.4	0.9	0.25	3.30	3.30	1.52	1219.20	304.80
unknown	61	SOLRIS	0	0	2	0.3	0.6	0.7	3.05	3.56	1.27	1219.20	304.80
Annual Crop	62	SOLRIS	0	0	2	0.2	0.9	0.95	2.03	2.03	0.76	1219.20	304.80
Mixed Crop	63	SOLRIS	0	0	2	0.3	0.9	0.7	0.25	2.03	0.25	1219.20	304.80
Perennial Crop	64	SOLRIS	0	0	2	0.5	0.85	0.4	0.25	2.03	0.25	1219.20	304.80
Idle Land	65	SOLRIS	0	0	2	0.3	0.4	0.8	0.25	2.03	0.25	1219.20	304.80
Plantations - Tree Cultivation	66	SOLRIS	0	0	3	0.5	0.8	0.25	2.03	2.03	1.02	1219.20	304.80
Hedge Rows	67	SOLRIS	0	0	3	0.5	0.8	0.25	2.54	2.54	1.27	1219.20	304.80
Orchards	68	SOLRIS	0	0	3	0.5	0.8	0.25	2.54	2.54	1.27	1219.20	304.80
Vineyards	69	SOLRIS	0	0	2	0.4	0.7	0.3	2.54	2.54	1.27	1219.20	304.80
Transportation	72	SOLRIS	0.35	0	2	0.25	0.55	0.95	2.29	2.29	1.02	1219.20	304.80
Extraction	73	SOLRIS	0.4	1.27	1	0.1	0.2	1	2.03	2.03	1.02	1219.20	304.80
Built-Up Area Pervious	74	SOLRIS	0	12.7	2	0.3	0.55	0.95	1.27	2.03	1.02	25.40	25.40
Built-Up Area Impervious	75	SOLRIS	0.33	0	2	0.3	0.55	0.95	2.03	2.03	1.02	914.40	304.80
Swamp	80	SOLRIS	0	1.27	2	0.3	0.6	0.55	2.03	2.03	1.02	304.80	152.40
Fen	85	SOLRIS	0	25.4	2	0.4	0.8	0.65	5.08	2.03	0.76	1524.00	609.60
Bog	89	SOLRIS	0	25.4	2	0.4	0.8	0.65	2.03	2.03	0.76	1524.00	609.60
Marsh	93	SOLRIS	0	25.4	2	0.4	0.8	0.65	2.03	2.03	0.76	1524.00	609.60
Open Water	96	SOLRIS	0	25.4	0	0	0	1	2.03	2.29	1.02	1524.00	914.40
Shallow Water	98	SOLRIS	0	0	0	0	0	1	0.00	0.00	0.00	1828.80	1828.80
Undefined	100	SOLRIS	0	0	2	0.3	0.9	0.7	0.00	0.00	0.00	1219.20	1219.20

[1] Vegetation Index: 0 – Bare, 1 – Grass, 2-Shrub, 3-Trees

4.4.1 Surficial Geology Mapping

Soil properties have a significant influence on hydrological processes because they control the amount of water that can infiltrate and be transmitted to the water table as well as the amount of water lost to evaporation and transpiration by plants (i.e., actual ET). Soil water-holding capacity in the capillary and gravity reservoirs (see Markstrom *et al.*, 2008) were model parameters calculated as functions of soil zone thickness (from land cover), porosity (*n)*, field capacity (*fc*), and wilting point (*wp*). Parameters that controlled the partitioning of flow between interflow and percolation to the water table were also specified as soil-type properties.

OGS (2010) surficial geology maps (see Figure 3.6) were used to assign soil-type related parameters. The surficial geology classes and associated parameter values used by the model are listed in Table 4.4. Initial values were derived from Earthfx (2010) and were refined during the calibration process. As an example, a map of groundwater seepage rates is shown in Figure 4.11.

PRMS v3.0.5 has limited capabilities for representing lakes and ponds; however, areas of open water were added to the surficial geology mapping and given special treatment. It was assumed that these areas contained large amounts of water available for ET and act mostly as groundwater sinks (i.e., contribute minimal recharge to the groundwater system). This was represented in the model by assigning a negligible gravity reservoir and a very large capillary reservoir. This compensating measure could be eliminated through use of an integrated model that provides feedback between surface and subsurface flow regimes; however, this was beyond the scope of the present study.

Table 4.4: List of surficial geology types and properties used in the PRMS model.

Geologic Description	Index	Soil Type	Porosity	Field Capacity	Wilting Point	Percolation Rate (m/s)	Snowmelt Infiltration (mm/d)
Bedrock	1	Clay	0.05	0.02	0.01	8.0×10^{-6}	103.68
Older Clay-Silt Till	2	Clay	0.40	0.28	0.17	1.0×10^{-8}	0.13
Sandy Silt Till	3	Loam	0.35	0.17	0.08	1.0×10^{-6}	12.96
Clay Till	4	Clay	0.40	0.27	0.15	1.0×10^{-8}	0.13
Ice Contact Sand and Gravel	5	Clay	0.30	0.05	0.03	1.0×10^{-5}	129.60
Outwash Sand and Gravel	6	Sand	0.30	0.06	0.03	1.0×10^{-5}	129.60
Outwash Sand	7	Sand	0.32	0.08	0.03	1.0×10^{-5}	129.60
Outwash Gravel	8	Sand	0.30	0.06	0.03	1.0×10^{-5}	129.60
Glaciolacustrine Clay and Silt	9	Clay	0.40	0.27	0.15	1.0×10^{-8}	0.13
Glaciolacustrine Sand	10	Sand	0.32	0.07	0.03	1.0×10^{-6}	12.96
Older Alluvium - Sand and Gravel	11	Sand	0.30	0.07	0.04	1.0×10^{-5}	129.60
Modern Alluvial Sand	12	Sand	0.35	0.07	0.03	1.0×10^{-6}	12.96
Modern Alluvium	13	Loam	0.35	0.07	0.03	1.0×10^{-6}	12.96
Organic Deposits	14	Clay	0.45	0.28	0.17	1.0×10^{-8}	0.13
Ice Contact Sand	15	Sand	0.35	0.08	0.03	1.0×10^{-5}	129.60
Undefined	16	Loam	0.40	0.21	0.11	1.0×10^{-7}	1.30
Open Water	17	Sand	1.00	0.99	0.01	1.0×10^{-7}	1.30

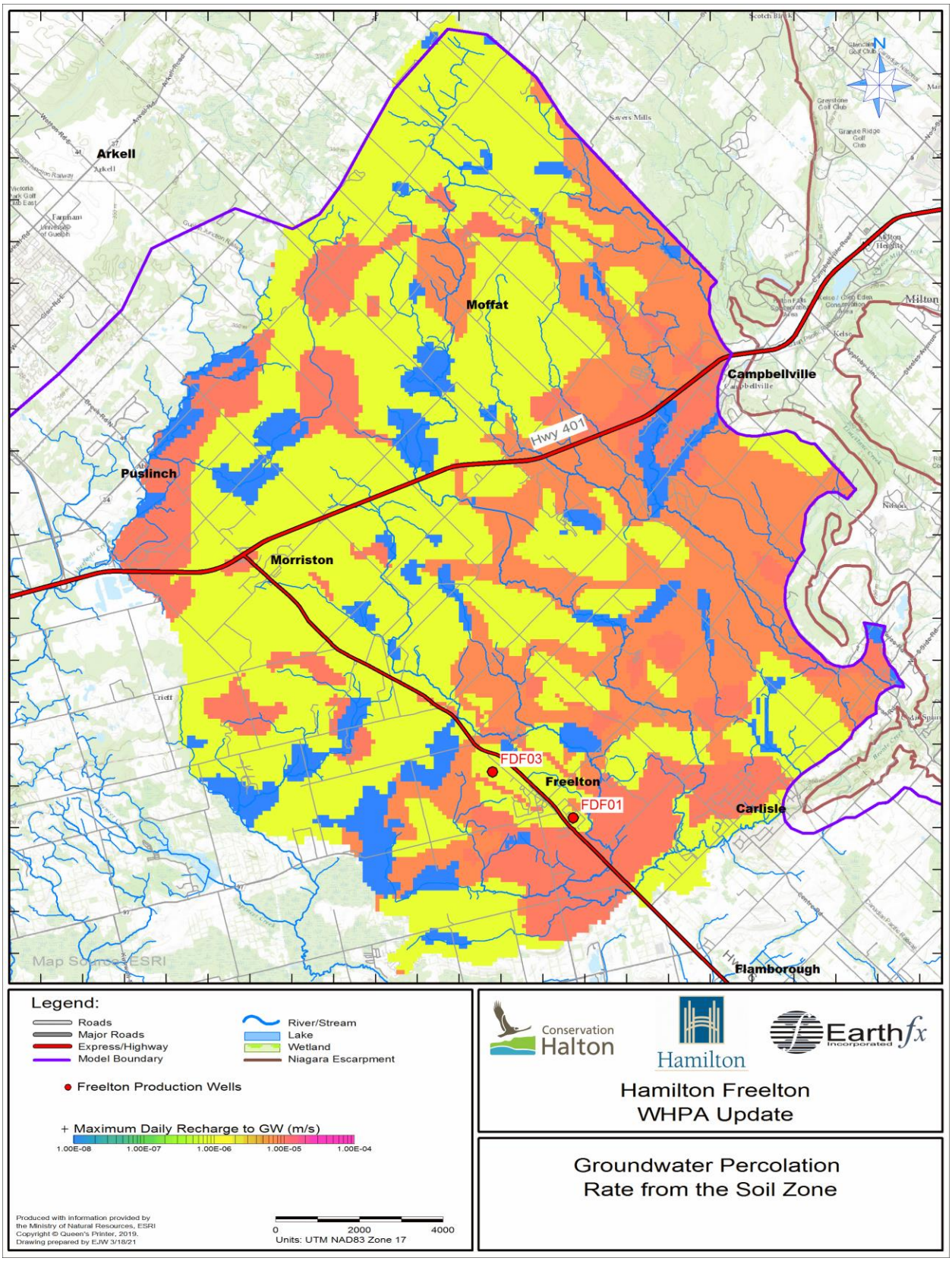

Figure 4.11: Distribution of maximum daily percolation rates.

4.4.1 Hydrological Process Parameters

The PRMS model contains a number of sub-models, such as the NRS CN model, the energy balance snowmelt model, and various ET models (e.g., Jensen Haise method). These sub-models have numerous parameters, of which many can be assigned on a cell-by-cell basis. For simplicity and consistency, regional values were used where appropriate. Independent testing of the sub-models was done to determine optimal values for these parameters, where possible.

4.5 *Streamflow Calibration Targets*

The Earthfx (2010) model was calibrated to 23 gauged catchments. Model parameters were adjusted regionally, rather than optimizing parameter values within each catchment. As noted earlier, the recharge rates computed by the 2010 model were preserved over most of the model area. The PRMS model update focussed on the northeast portion of the 2010 model area.

One of the 23 catchments, Bronte Creek at Carlisle (02HB022), falls completely within the current study area and gauged flows served as calibration targets for the PRMS model update. The gauged catchment area was delineated topographically as shown in Figure 4.12.

The gauge is operated by the Water Survey of Canada (WSC is a division of Meteorological Service of Canada, Environment Canada). The location of the gauge is shown on Figure 4.12. Table 4.5 provides a summary of the gauge properties and streamflow characteristics. The period of record is reasonably good, with uninterrupted data going back to 1989. The daily mean discharge observed at the stream gauge is presented in Figure 4.13.

Table 4.5: Streamflow statistics for the Bronte Creek at Carlisle (02HB022) stream gauge.

ID	Name	Water-shed Area (km^2)	Easting (m)	Northing (m)	Q_{Avg} (m^3/s)	Q_{50} (m^3/s)	Estimated Average Baseflow (m^3/s)	Years of Record	Start of Record
02HB022	Bronte Creek at Carlisle	123	581,956	4,804,500	1.30	0.87	0.82	30	1989

The uncertainly with the individual measurements in the available streamflow data was difficult to quantify. An awareness of the inherent uncertainty, such as the difficulties of accurately measuring low flows, and the ability to estimate flow during ice cover, is critical when setting model calibration targets and evaluating the quality of the model calibration, particularly on a daily basis. Given that the outcome of the PRMS modelling work is to produce a long-term average recharge map, monthly average and long-term volumetric discrepancy between simulated and observed flows were also considered as calibration targets.

4.6 *Calibration and Validation*

The PRMS model was calibrated for the five-year period spanning WY1998 and WY2002. Once an acceptable calibration was achieved, the model then validated against a different five-year period spanning WY2011-WY2015. The calibration-validation approach ensured that the model was not biased towards one particular time period.

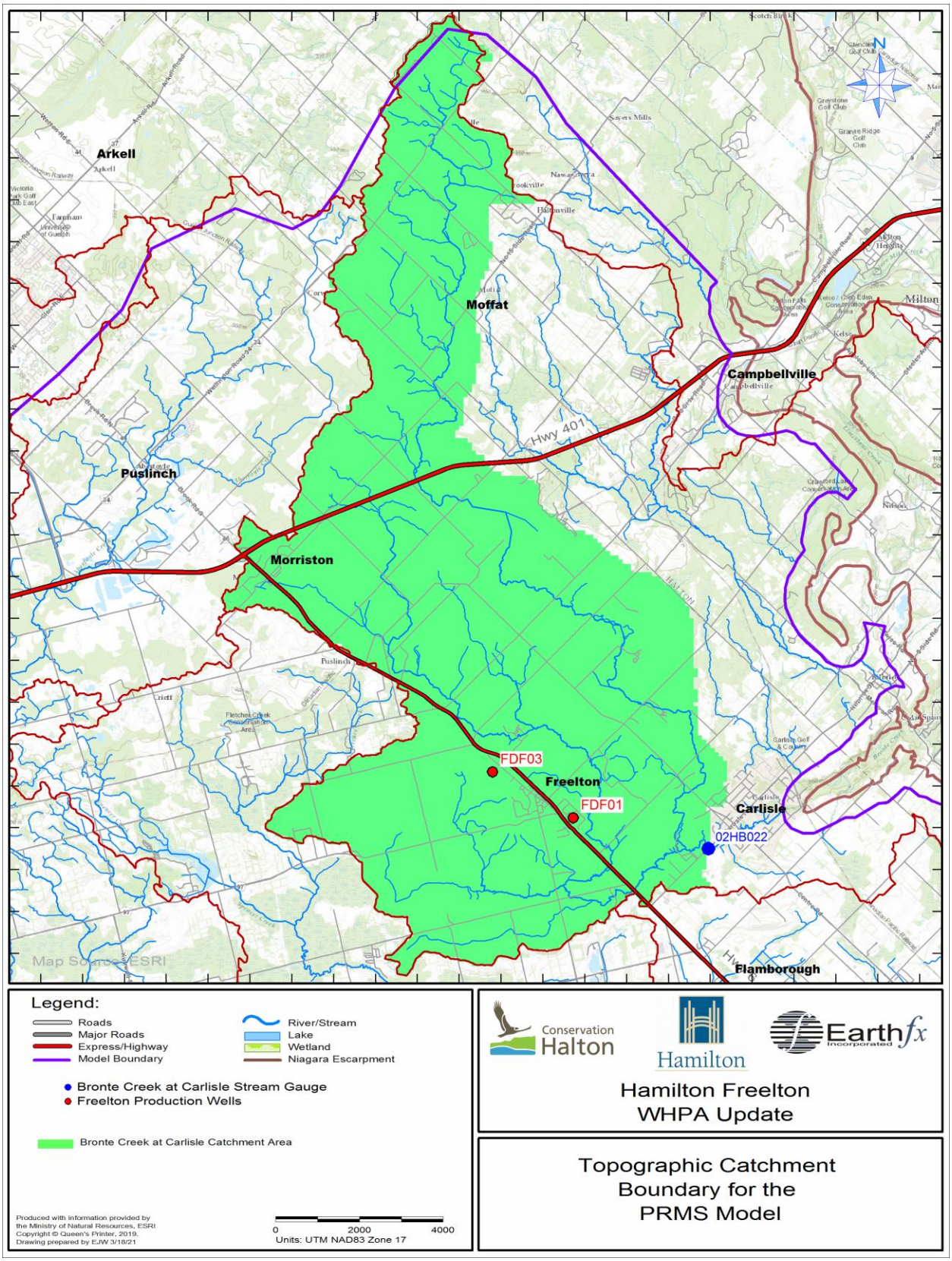

Figure 4.12: Topographic catchment boundary for the PRMS model.

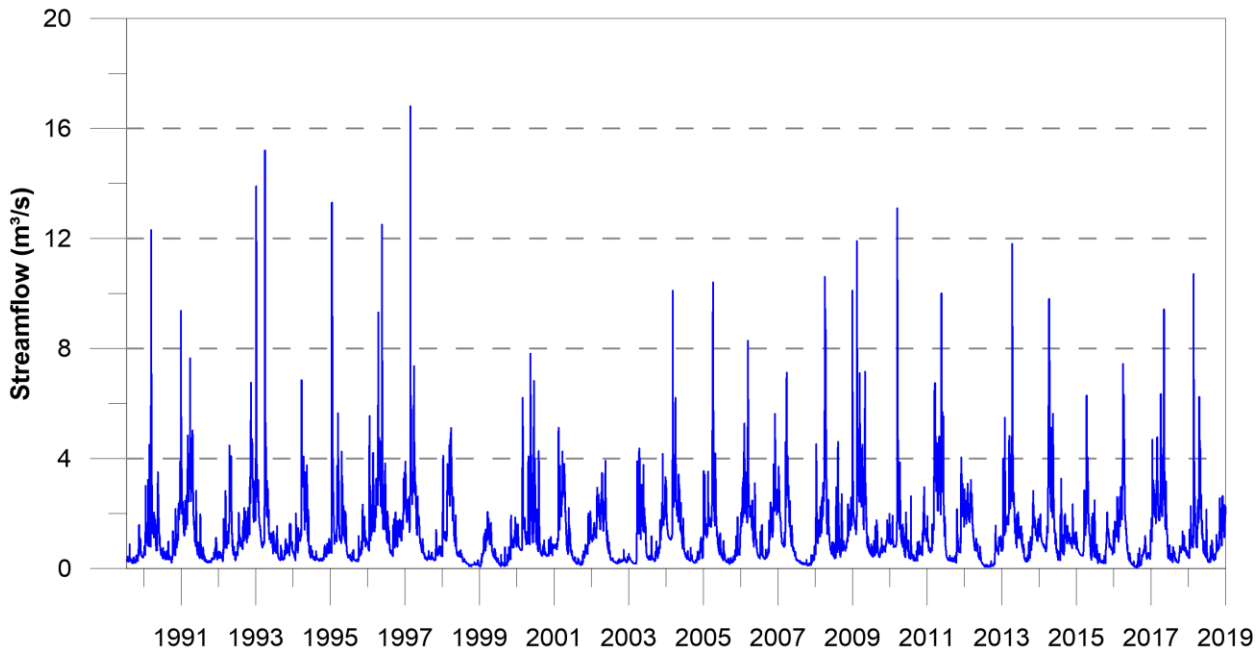

Figure 4.13: Observed daily streamflow at Bronte Creek near Carlisle (WSD ID: 02HB022).

All model parameter values were regionalized by the land use, soils mapping, or surficial geology mapping as described in Section 4.4. A sensitivity approach was undertaken by testing a range of values for multiple parameters to identify near-optimal values as it related to the simulated match to streamflow. Groundwater seepage rates, interflow, soil zone storage, ET, and snowmelt parameters were varied during calibration to improve the match between observed and simulated stream flows.

Three objective functions were used to evaluate the quality of the calibration: Nash-Sutcliffe efficiency (NSE) (Nash and Sutcliffe, 1970), Log Nash-Sutcliffe efficiency, and the percent volume difference between the observed and simulated streamflow. It must be recognized that the model simulates flow operates on a daily time step and differences with the observed flow may occur when rainfall or snowmelt events occur near the end of the day. Because the purpose of the PRMS model was to predict the long-term average recharge, emphasis was given to the Log Nash-Sutcliffe efficiency and volumetric efficiency, which are better measure of the model calibration to lower volume flows.

Figure 4.14 and Figure 4.15 show the observed mean daily discharge hydrograph compared with the simulated PRMS flows during the calibration period on regular and log-scales. Comparisons of monthly mean discharge hydrographs are shown in Figure 4.16. Calibration statistics for the gauged catchments are provided in Table 4.6. The model achieved a reasonable NSE of 0.50 and a log-NSE of 0.69 at the Bronte Creek gauge for daily flows. Monthly NSE and log-NSE were good at 0.68 and 0.75, respectively. Percent volume discrepancy over the 5-year period is very low at only 0.56%. The model did, however, miss the spring freshet in 2001, which may be related to simulated snowpack dynamics or erroneous climate inputs. The model also tended to miss the magnitude of the summer baseflow recession. In reality, baseflow recession occurs rapidly but is still maintained during summer months. It is believed that the Mountsberg reservoir, which is not represented in the PRMS model, plays a role in this behaviour. Once again, given that the objective of the PRMS model is to provide long-term average groundwater recharge, the timing of the baseflow recession as an indicator of model performance is of less importance than the total streamflow volume. Overall, the model does an excellent job at matching the total stream flow volume.

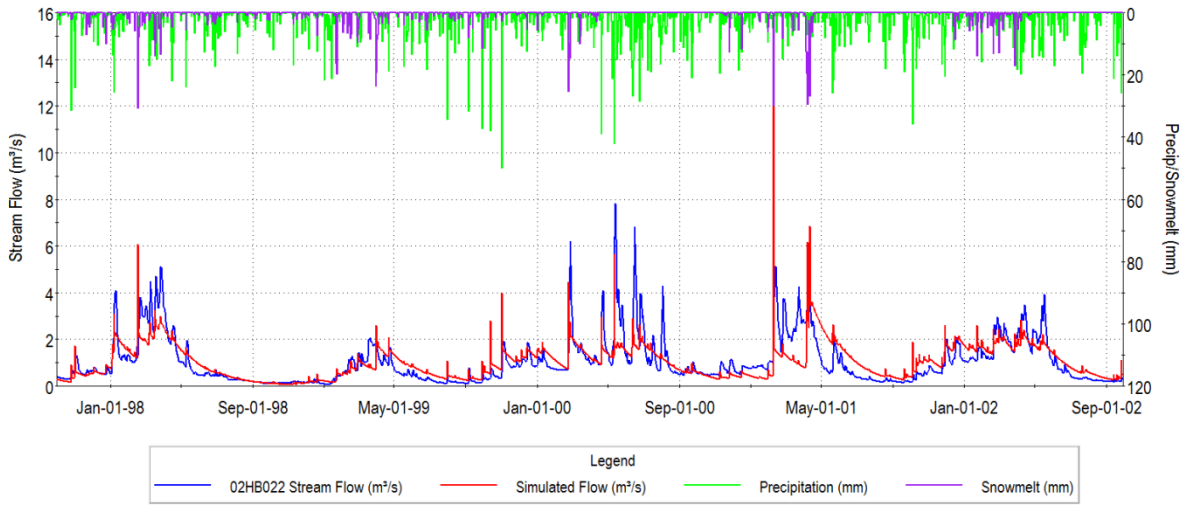

Figure 4.14: Simulated (red) versus observed mean daily stream flow (blue) at Bronte Creek near Carlisle during the calibration period. Precipitation and snowmelt shown on secondary axis.

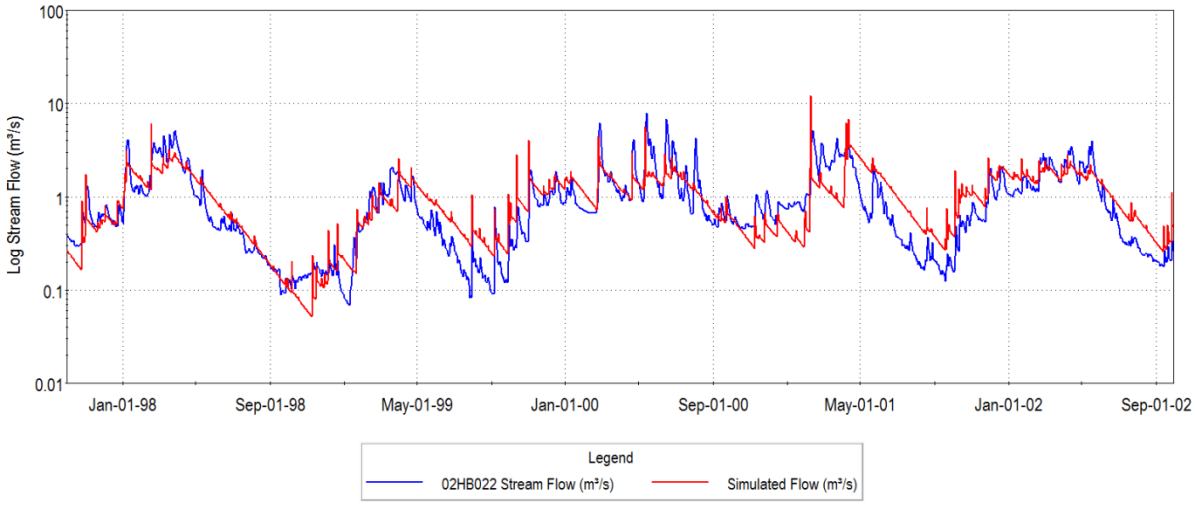

Figure 4.15: Simulated (red) versus observed mean daily log stream flow (blue) at Bronte Creek near Carlisle during the calibration period.

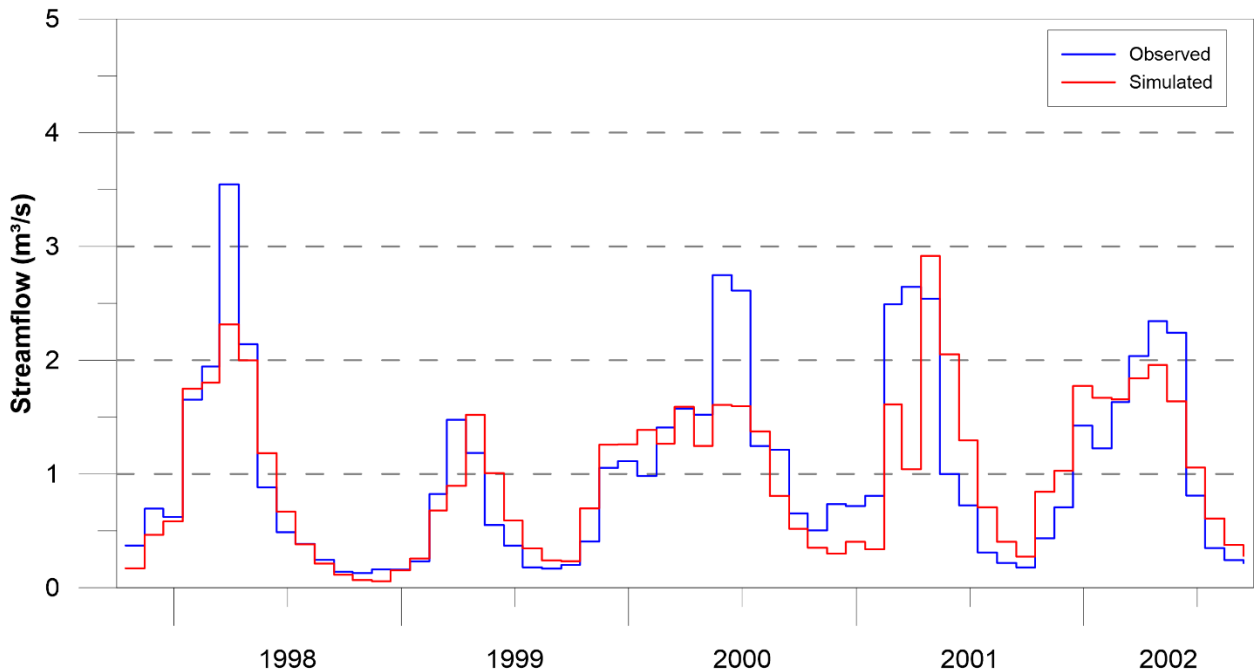

Figure 4.16: Simulated (red) versus observed mean monthly stream flow (blue) at Bronte Creek near Carlisle during the calibration period.

The model was checked against the validation period and achieved very similar statistics as shown in Table 4.6. The model performed slightly worse during the validation period. One possible factor is that the number of climate stations has declined in recent years and there were fewer stations available for interpolation of the climate dataset during the validation period. Consequently, there is more uncertainty in the climate inputs and it is not unreasonable to expect a reduction in model performance as a result. Regardless, the long-term average percent difference in volume remained very low at only 1.1%.

Table 4.6: Summary of calibration statistics for PRMS model subbasins.

Period	**Nash-Sutcliffe Efficiency**		**Log-Nash Sutcliffe Efficiency**		**Percent Volume Difference**
	Daily	***Monthly***	***Daily***	***Monthly***	
Calibration (WY1998 – WY2002)	0.50	0.69	0.68	0.75	+0.56%
Validation (WY2011 – WY2015)	0.56	0.65	0.59	0.66	+1.1%

4.7 *Long-term Simulation and Discussion*

After calibration, the PRMS model was run from WY1986 to WY2010 (inclusive) to further assess the adequacy of the model and to quantify the long-term average water budget within the study area. The time period chosen represents a reasonable compromise between representing a more recent period and the amount and quality of the available climate data.

The primary goal of the 25-year run was to provide an estimate of long-term average groundwater recharge to be used as input to the MODFLOW model. Simulated mean daily and mean monthly streamflow hydrographs at the Bronte Creek gauge for the 25-year simulation period are shown in Figure 4.17 through Figure 4.19. Table 4.7 presents the calibration statistics (similar to the calibration and validation exercise discussed above). The calibration improved in every category with the exception of the daily NSE. The percent volume difference improved further and was only -0.13% (model low). The performance of the model is essentially the same as for the 5-year calibration period, exhibiting the same bias related to the timing of the summer baseflow recession.

Table 4.7: PRMS statistics at the Bronte Creek near Carlisle gauge during the simulation period.

Period	**Nash-Sutcliffe Efficiency**		**Log-Nash Sutcliffe Efficiency**		**Percent Volume Difference**
	Daily	***Monthly***	***Daily***	***Monthly***	
Long-Term (WY1986 -WY2010)	0.54	0.75	0.71	0.79	-0.13%

Average annual generated overland runoff is shown in Figure 4.20. Areas of high runoff are mainly associated with poorly draining soils overlying geological units with low hydraulic conductivity. Low runoff is associated with surficial sands and gravels in rural settings which contribute a significant volume of recharge to the groundwater system.

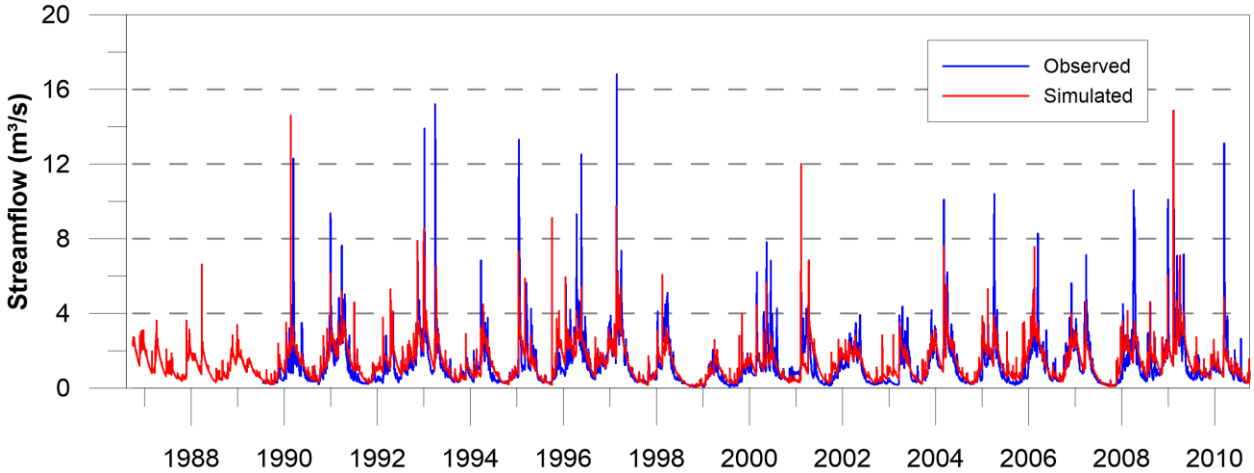

Figure 4.17: 25-year comparison between daily mean simulated (red) and observed (blue) streamflow at Bronte Creek near Carlisle.

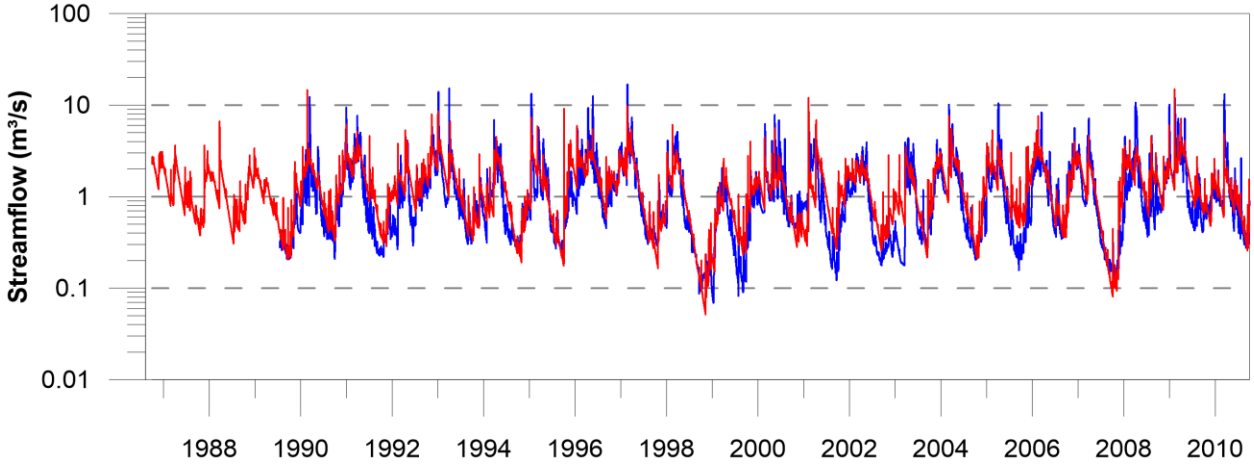

Figure 4.18: 25-year comparison between daily mean log simulated (red) and observed (blue) streamflow at Bronte Creek near Carlisle.

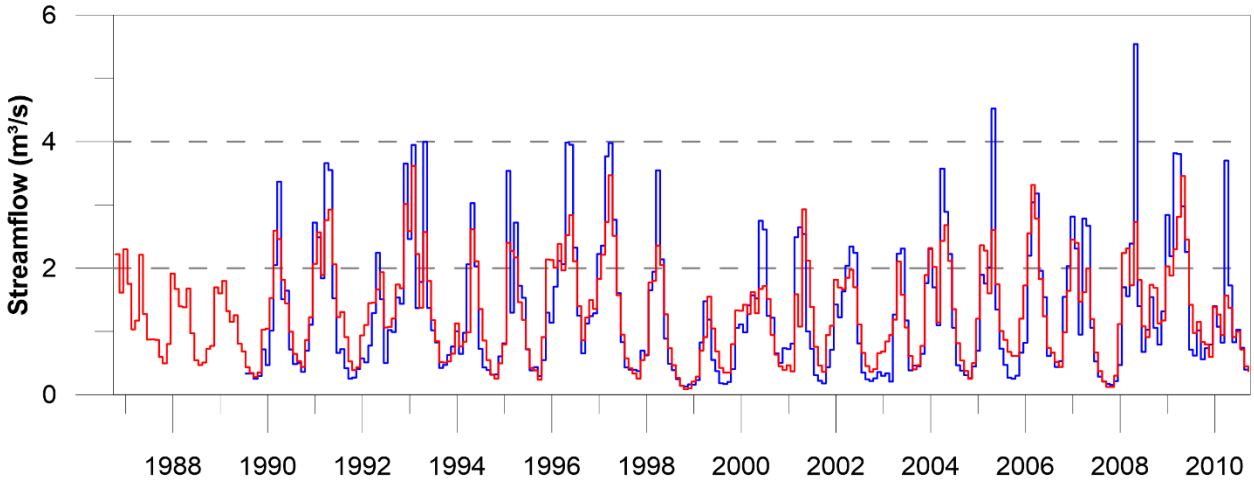

Figure 4.19: 25-year comparison between monthly mean simulated (red) and observed (blue) streamflow at Bronte Creek near Carlisle.

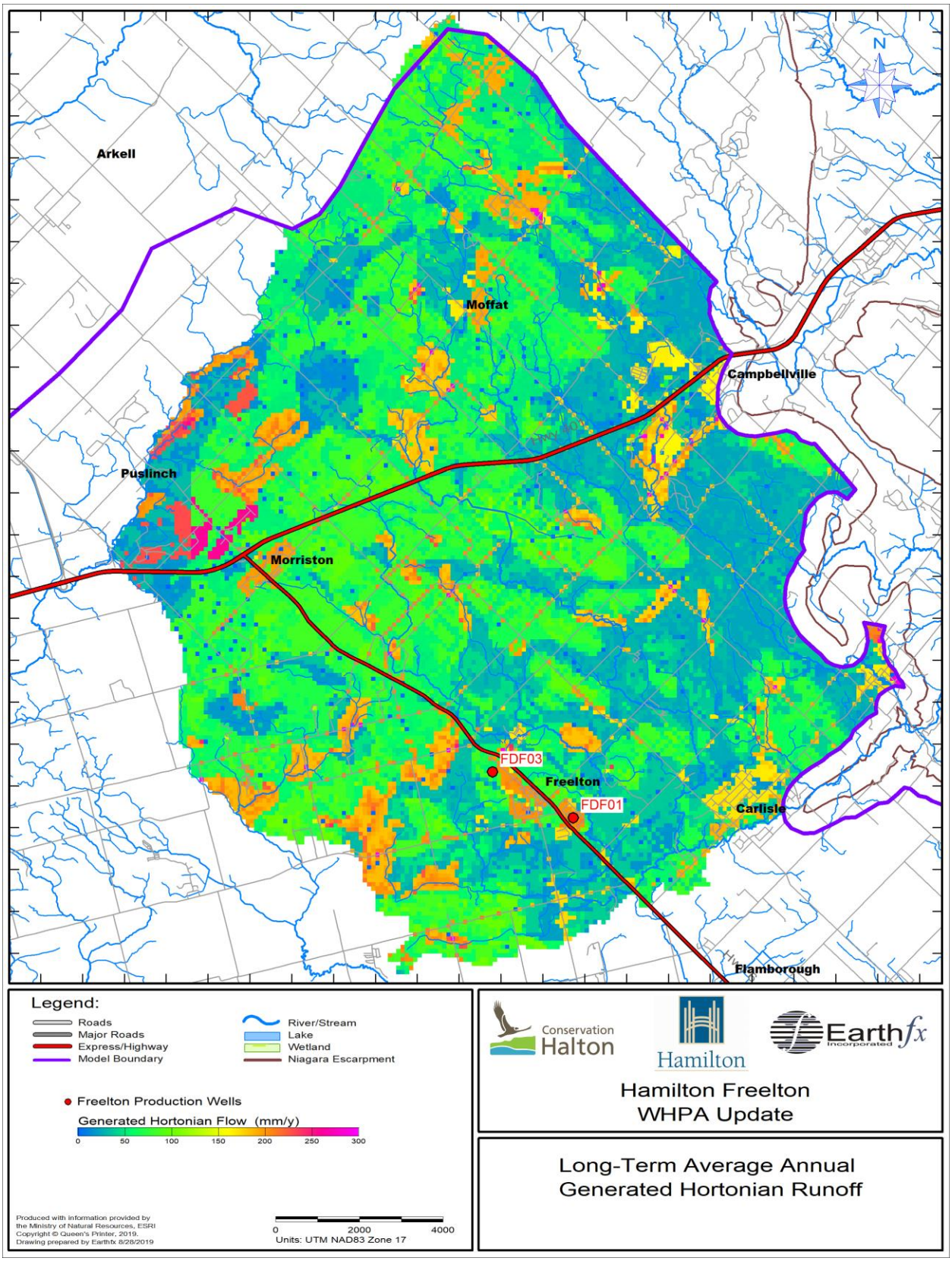

Figure 4.20: Long-term average annual Hortonian generated runoff.

Figure 4.21 shows average annual actual evapotranspiration (AET). AET patterns are sensitive to land use/land cover and soil type. The model indicates highest ET rates over the lowest permeability soils in the west of the study area and lower ET rates in areas of higher groundwater recharge (e.g., over thinly-covered or exposed bedrock) where soil water retention is lowest, and in areas classified as extraction or developed- impervious.

Lastly, Figure 4.22 shows average annual groundwater recharge which is affected by all the factors noted previously as well as by the permeability of the underlying soil and partitioning rates between interflow and gravity drainage. Greater recharge tends to occur on sand and gravel units as compared to till-covered areas. Recharge also increases towards the end of the overland flow path as more surface runoff and interflow accumulates down the cascade. Areas of high recharge correspond to the Flamborough plain where weathered bedrock is found at or near surface, and south and east of Freelton where outwash deposits and Norfolk Sands are found.

4.8 *Limitations of the PRMS Groundwater Recharge Estimates*

Groundwater recharge is defined as the amount of water percolating from the PRMS gravity soil zone to the linear groundwater reservoir. It should be noted that recharge cannot easily be measured directly over large areas. Instead, surface water models are used to estimate the primary components of the water balance (interception, overland runoff, ET, and recharge) and are calibrated to stream discharge measurements. The assumption is that if the model matches the observed streamflow, then the components of the water budget have been estimated in a reasonable manner. We attempted to reduce the uncertainty of this assumption by applying the calculated recharge to a groundwater flow model (discussed in Section 5) and comparing average observed separated baseflow with the simulated baseflow from the groundwater model. This was done previously for 23 locations across the model area; however, this update focuses mainly on the Bronte Creek at Carlisle stream gauge.

It should also be noted that the PRMS model, on its own, provides little feedback from the groundwater reservoir. Some feedback was obtained by calibrating the groundwater and surface water models in parallel, such as limiting recharge in areas of simulated groundwater discharge (e.g., near the Mountsberg reservoir). Higher levels of feedback can best be obtained through the use of integrated surface water/groundwater models (e.g., the USGS GSFLOW model which directly couples the PRMS and MODFLOW models). However, constructing an integrated model was beyond the scope of the current study.

As with all models, it must be recognized that there are inherent simplifications in the model conceptualisation of distributed hydrologic processes and in the simplified assignment of parameters. There are also limitations and uncertainty in the climate input and calibration target data. Accordingly, it is possible to achieve a reasonable calibration but not a perfect or unique calibration.

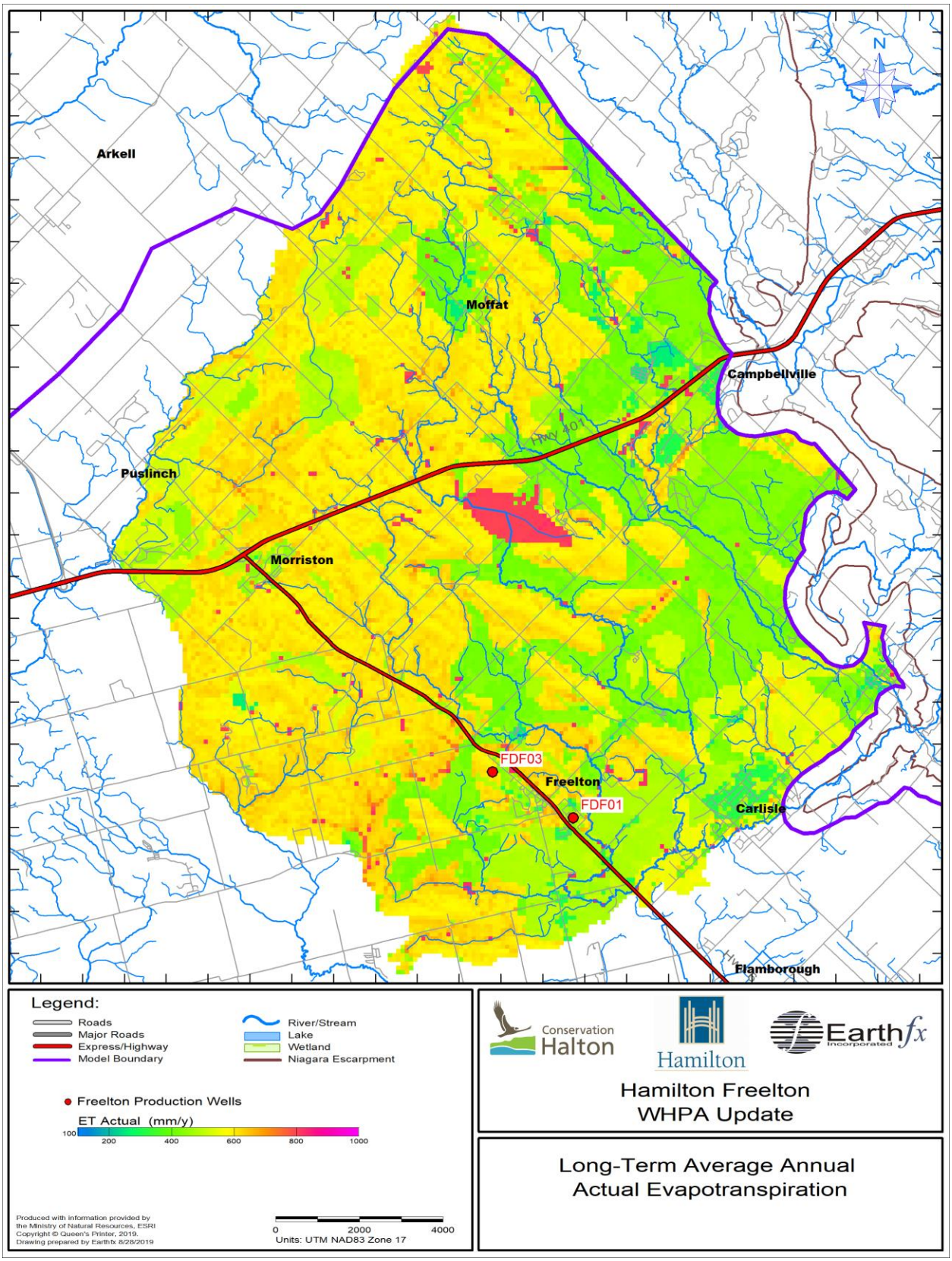

Figure 4.21: Long-term average annual actual ET.

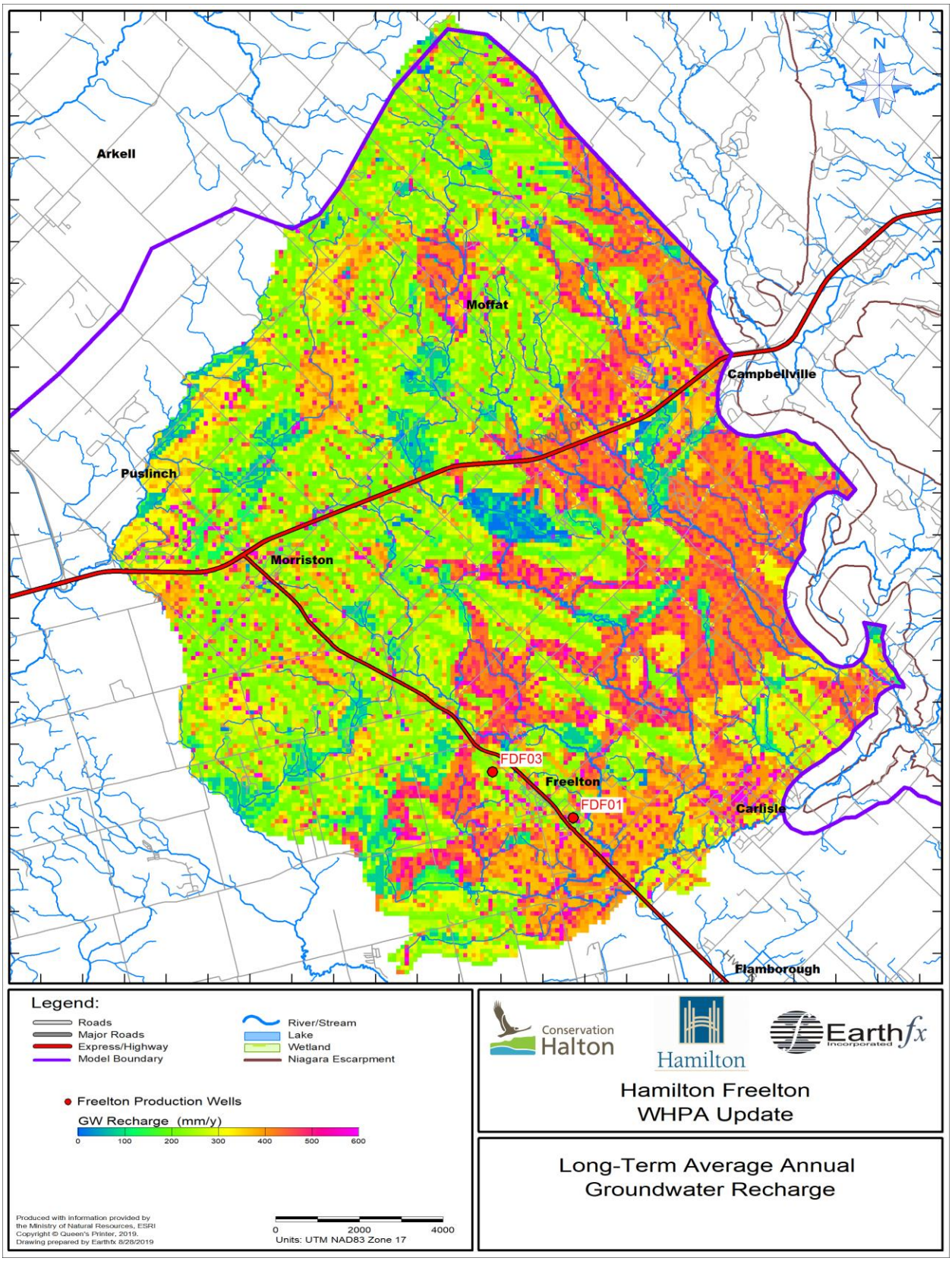

Figure 4.22: PRMS groundwater recharge estimate.

5 Groundwater Flow Model

5.1 *Scope of Model Update*

The original NH Model was converted from MODFLOW 96 (Harbaugh and McDonald, 1996) to MODFLOW-NWT (Niswonger *et al*., 2011). In doing so, several of the modules used in the NH Model have been upgraded to reflect advances in the model code. The most significant changes relate to how streamflow, groundwater recharge, and surface discharge processes are represented.

A review of recent studies completed in the Freelton area was also conducted and new borehole and water level data were incorporated into the project database. The hydrostratigraphic model was updated locally to reflect new borehole information. The model was re-calibrated under transient and steady-state conditions and changes were made to hydraulic conductivity values to match water level patterns. The following sections describe the model construction and calibration and highlight areas where updates were completed. The updated model is referred to as the NH 2019 Model in the remainder of this report.

5.2 *Model Description*

A groundwater model is a simplified representation of a complex physical, hydrologic, and hydrogeologic system where natural and anthropogenic processes affect the rates and direction of groundwater flow. MODFLOW solves the groundwater flow equations using the finite-difference method, which requires that the study area be subdivided into a grid of small square or rectangular cells. Local refinements can be made to the grid where a higher resolution is required, such as near a wellfield. The NH 2019 model employed the same grid as the original NH model, which was refined around the Freelton, Carlisle and Lynden wellfields. 25 m square cells were used around the municipal supply wells, whereas a maximum cell size of 200 m by 200 m was used near the outer edges of the model grid. The refined model grid is shown in Figure 5.1 and consists of 699 rows and 683 columns, for a total of 477,417 grid cells for each of the 10 model layers.

MODFLOW works in a local, grid coordinate system based on row and column numbers, and their individual widths and lengths. The VIEWLOG-GIS preprocessor (Kassenaar, 2013) was used to help translate geo-referenced map data into MODFLOW coordinates. The local origin for the model grid is at UTM coordinates 549000 E and 4775000 N. All digital data for the study area were referenced using NAD83 (UTM Zone 17) grid coordinates.

5.3 *Boundary Conditions*

Boundary conditions were specified for cells that lie along lines corresponding to the physical boundaries of the groundwater flow system. Three general types of boundary conditions were utilized in the NH 2019 groundwater flow model: constant head; no-flow; and head-dependent discharge boundaries (i.e., streams, surface leakage).

Figure 5.2 shows the location of constant head and no-flow boundaries. Constant head cells are located along the portion of the eastern model boundary adjacent to the Niagara Escarpment. The boundary was set back 500 m so as not to include the highly weathered zone that occurs near the escarpment face. Control elevations in the upper layers were set equal to 1 metre (m) above the elevation of the top of the upper till unit while the deeper units were set to the elevation of the top of the basal sand unit. No updates were made to the constant head model boundaries. It should be noted, however, that MODFLOW-NWT is much more stable than MODFLOW-96 in areas of steep topography and the model extents could be expanded at some future time.

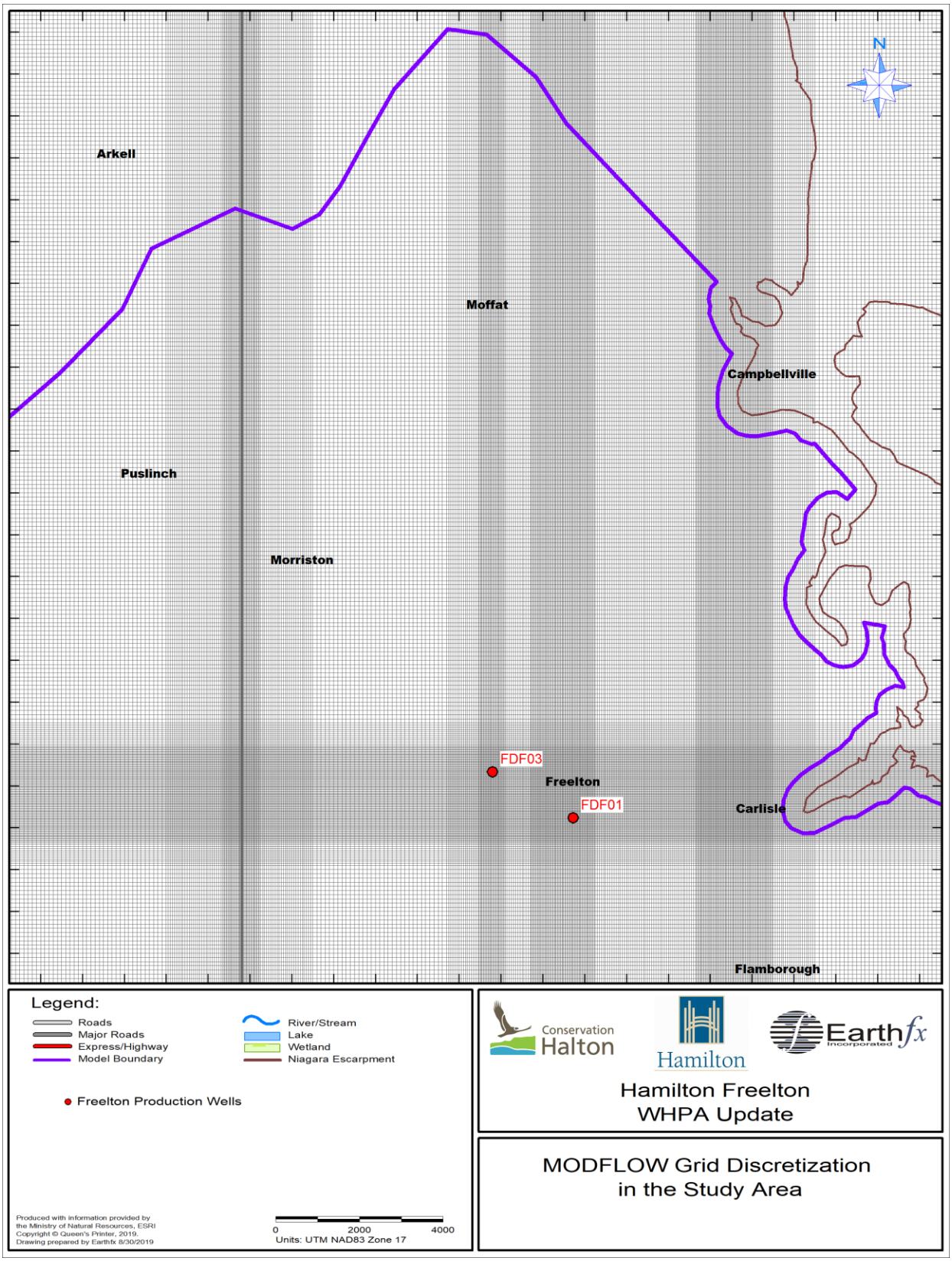

Figure 5.1: Finite difference grid with higher resolution in the wellfield areas.

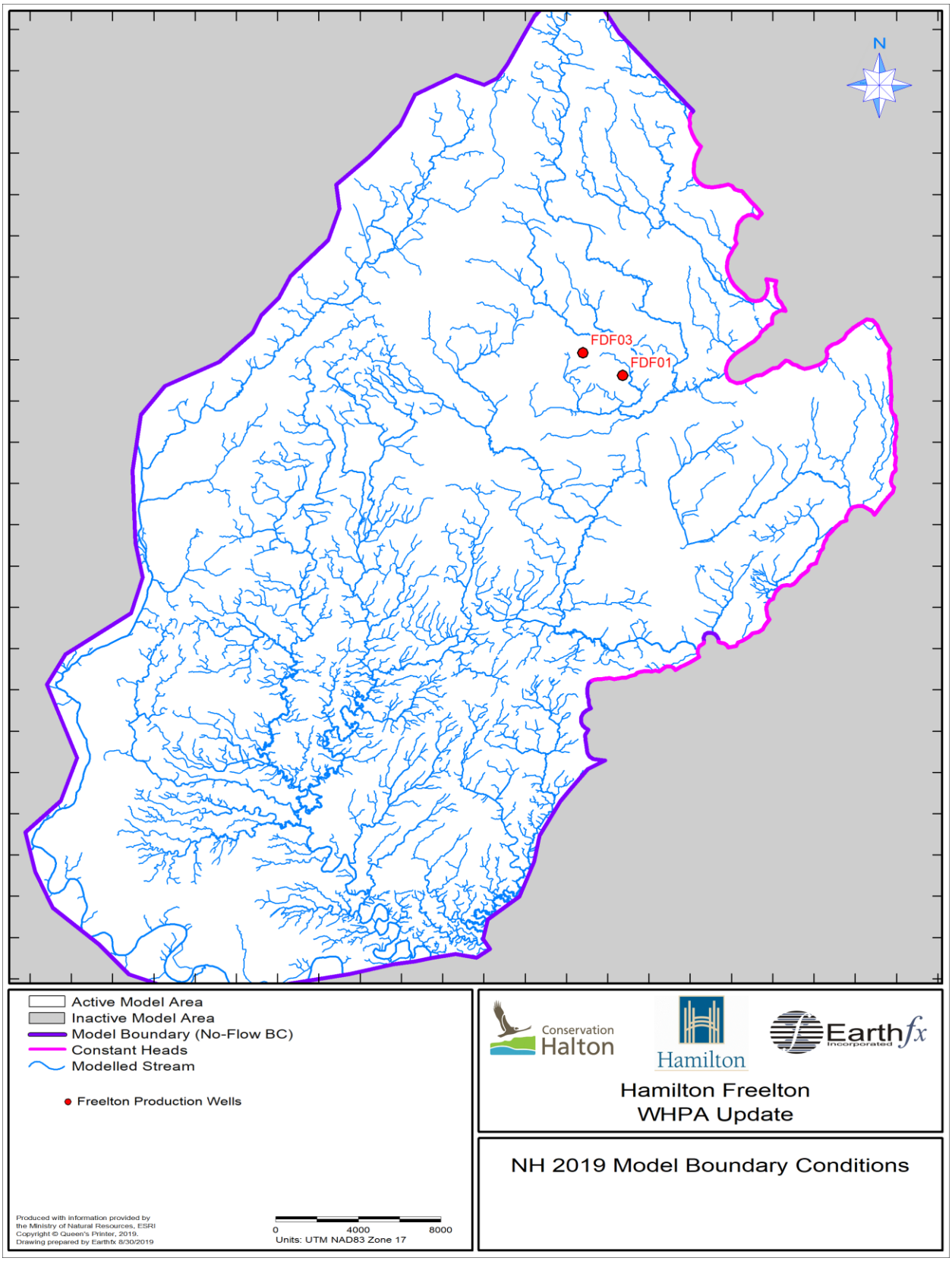

Figure 5.2: Model boundary conditions.

No-flow boundaries are located everywhere else along the external boundary assuming that cross watershed flow across these boundaries would be relatively small and would not affect the dominant regional groundwater flow patterns. A no-flow boundary was imposed along the base of the model flow assuming that flows across the Queenston Shale would be negligible. No updates were made to the no-flow boundaries.

5.3.1 Streamflow

Streams were previously represented through either the RIVER or DRAIN modules in the MODFLOW code. These boundaries only represent seepage processes and assign stream stage as a constant, user-specified value. Stream representation in the NH 2019 Model has been upgraded to the SFR2 module (Niswonger and Prudic, 2005). To implement the SFR2 module, the dendritic stream network was first translated from the MNR WRIP watercourse GIS layer into modelled "segments" and “reaches”. Stream segments are numbered from upstream to downstream and represent the distance between two “junctions” or “nodes” typically representing the confluence of two stream tributaries.

A stream “reach” is defined as the portion of a stream segment within a model cell. As such, a single stream segment may be made up of one or more stream reaches. The key difference between SFR2 and the RIVER module is that SFR2 determines the stage in each reach based on the sum of inflows and outflows (i.e., streamflow, stream leakage, and overland runoff), streambed roughness, slope, and channel geometry. Streamflow from the headwater reaches is then routed downstream through the dendritic network.

Rainfall/runoff events cannot be simulated in the steady-state simulations, so a key component of streamflow represented in the model is the long-term average groundwater discharge to the stream channels. Another, component is “surface discharge” which occurs in areas where the water table intersects land surface, primarily in riparian areas. Surface discharge is conveyed directly to the nearest stream channel or lake and routed down the stream network.

5.3.1 Hydrostratigraphy

The conceptual three-dimensional hydrostratigraphic model, (i.e., the layers representing the sequence of aquifers and aquitards encountered in the study area) was taken from Earthfx (2010). While there are often many similarities between the stratigraphic and hydrostratigraphic layers, there are several important differences. Multiple stratigraphic layers can be combined, if the properties are sufficiently similar, into a single hydrostratigraphic unit to simplify groundwater model development. Alternatively, a single stratigraphic formation can be split into multiple layers if the properties are significantly different. For example, the upper part of the bedrock units are often weathered and, therefore, more permeable than the rest of the underlying unit. Accordingly, the upper 5 metres of the bedrock were represented as a separate aquifer unit in this study. Similarly, many local and regional studies have identified a permeable unit within the Gasport Formation (e.g., Brunton, 2007; Brunton, 2009; Wood, 2018a) and therefore we subdivided this unit into an upper, middle and lower layer, each with different properties.

The hydrostratigraphic model layers of the NH 2019 model are the same as that of the original model described in Earthfx (2010). A cross section, locally equivalent to the geologic cross section presented earlier (Figure 3.8), is shown in Figure 5.3.

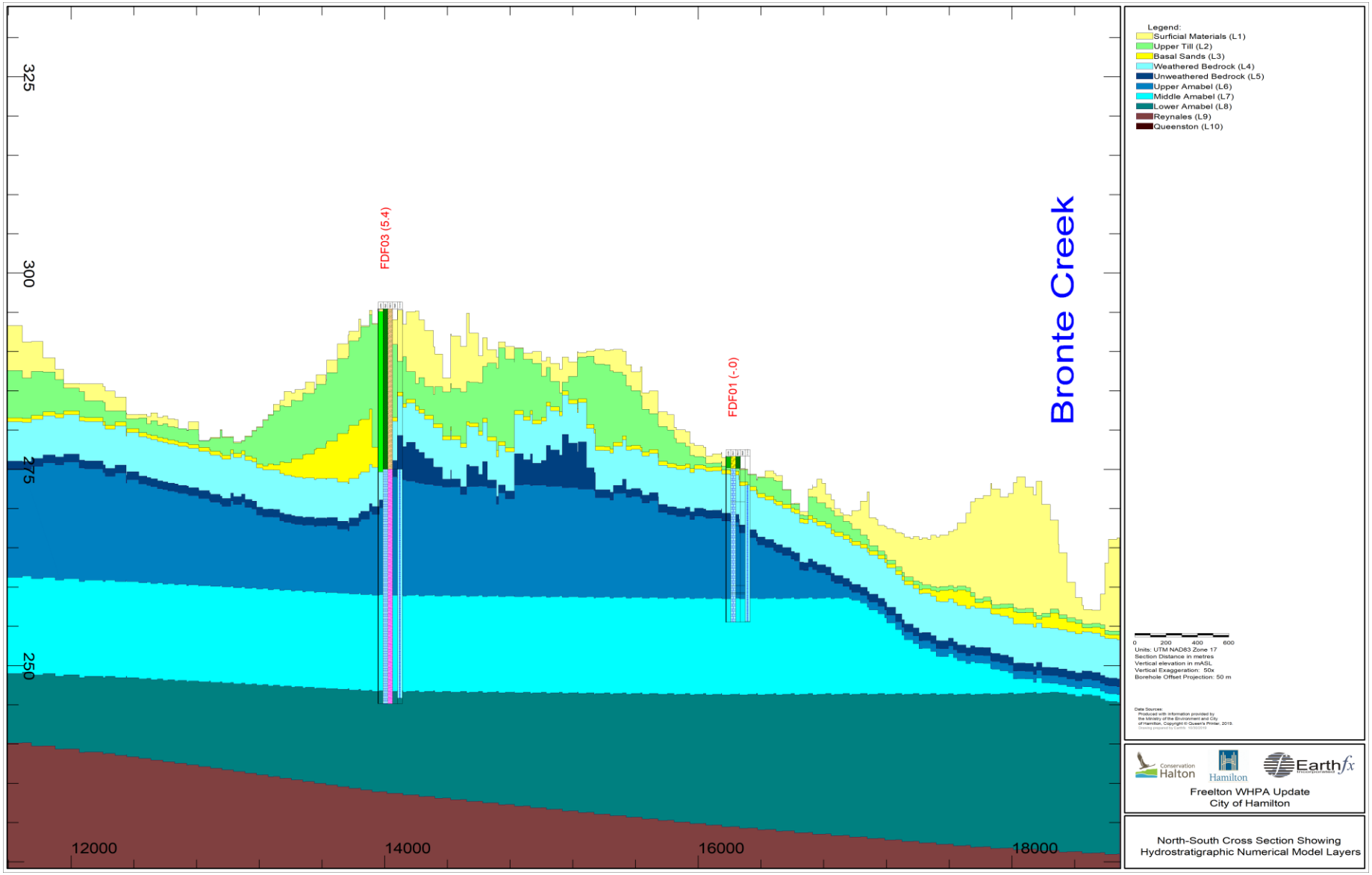

Figure 5.3: North-south cross section showing hydrostratigraphic numerical model layers.

The hydrostratigraphic model layers through Freelton are described briefly in Table 5.1 below:

Table 5.1: Description of the numerical model layers.

Layer	Hydrogeologic Unit Name	Description
1	Surficial Materials	Layer 1 includes overburden materials, bedrock valley infill sands and gravels, and weathered bedrock (where mapped at surface). Material selection and property assignment was based on surficial geology mapping. The layer may be very thin or absent and may also be unsaturated in places. Although not a significant aquifer, the layer was added to be consistent with the surficial geology represented in the PRMS recharge model.
2	Upper Till	Layer 2 represents the Wentworth Till, where present. The sandy silt to silty sand till outcrops in the northwestern part of the study area and underlies the glaciolacustrine or glaciofluvial sediments elsewhere in the study area except where the bedrock outcrops.
3	Basal Sands	Layer 3 represents the mainly glaciolacustrine deposits of silt and fine sand in the Hamilton area and both glaciolacustrine sediments and coarse-grained glaciofluvial sediments further north.
4	Weathered Bedrock	Layer 4 represents the upper 5 m of the bedrock. The assumption made was that exposed bedrock was likely to exhibit enhanced hydraulic conductivity due to weathering. Hydraulic properties of the weathered unit were varied based on which stratigraphic unit was at surface.
5	Eramosa	Layer 5 included the Eramosa and Vinemount shale beds, and possibly the chert layers associated with the Goat Island Formation. The unit confines the Amabel Formation west of Brookville and Mountsberg. The confining unit is mostly absent in the eastern portion of the model area and it dips and thickens to the southwest.
6	Upper Amabel/ Gasport	Layer 6 represents the upper Amabel. The unit is more permeable than the overlying Eramosa but less permeable than the middle Amabel except where near surface.
7	Amabel/Gasport Production Zone	Layer 7 is represents a zone within the Amabel/Gasport believed to be more permeable than the upper and lower parts of the formation and can be highly permeable locally especially where it subcrops or in highly fractured zones.
8	Lower Amabel/ Gasport	There is little evidence of significant permeability in any of the bedrock units below the middle Amabel zone. Layer 8 includes the lower part of the Amabel formation and the Rochester and Irondequoit Formations.
9	Reynales	Layer 9 contains the relatively low permeability units extending from the Reynales to the Queenston Formation.
10	Queenston Shale	Finally, Layer 10 represents the Queenston Shale down to the top of the Georgian Bay Formation shales. The Queenston Shale represents the uppermost bedrock unit below the Niagara Escarpment

5.3.1 Recharge and Surface Leakage

Recharge and groundwater discharge to land surface (also referred to as “surface leakage”) were previously represented through the use of the RCH and DRAIN modules, respectively. Recharge was supplied to the 2010 NH Model using the estimate derived from the previous PRMS model (now updated for this study), as described in Section 4. The PRMS recharge estimate was re-sampled to the MODFLOW grid and was incorporated with the previous estimate (outside the update area) to form an updated composite recharge map (Figure 5.4).

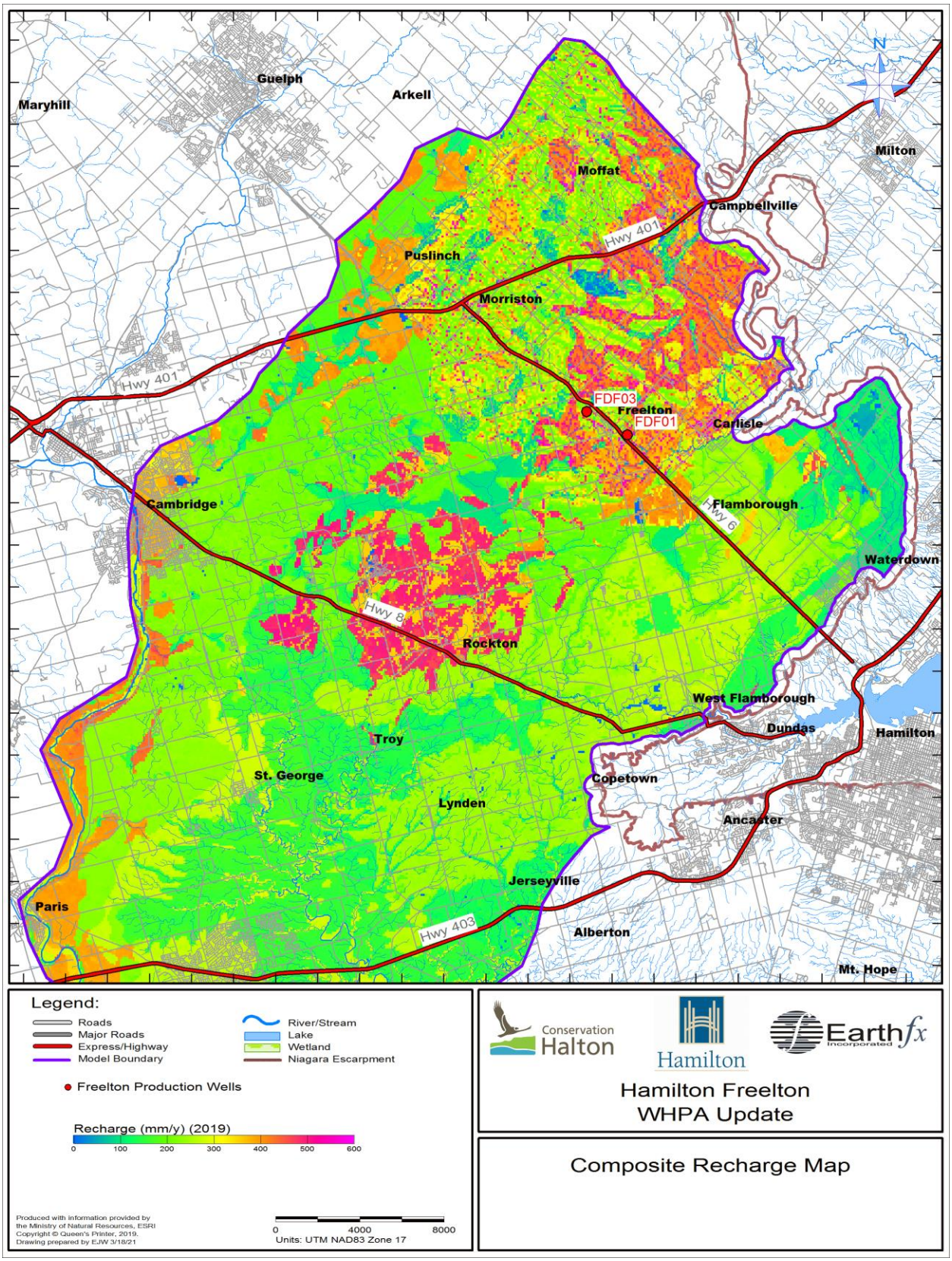

Figure 5.4: Composite recharge map.

Not only have recharge quantities been updated but the NH 2019 model was upgraded to the more advanced Unsaturated Zone Flow (UZF) module (Niswonger *et al*., 2006), which simulates both recharge and surface discharge and eliminates the need for drains to represent areas with high water-table . It should be noted; drains were only replaced by the UZF package where they were assumed to represent areas of natural groundwater discharge like wetlands, riparian areas, and low-order streams. There are multiple quarries that had their dewatering operations represented using drains and these have been left in the model. A major benefit of the UZF module over the DRAIN module is the ability to route surface discharge to SFR2 where it then becomes streamflow. It also has the ability to reject recharge in the instance that there is not enough capacity for the groundwater system to accept it.

5.4 *Simulated Groundwater Takings*

Simulated groundwater takings included the municipal supply wells of Freelton, Lynden and Carlisle. Lynden and Carlisle wells were simulated at their maximum permitted rates during calibration and WHPA delineation. The Freelton municipal wells were simulated at different combinations of their maximum permitted rates described in Section 2.2 for the WHPA delineation, however, during calibration, the average day demand (ADD) from June 2011 to November 2014 of 335 m^3/d was used (WSP, 2016). The ADD was divided between FDF01 and FDF03 at 118.37 m^3/d and 216.63 m^3/d, respectively, based on the ratio of their permitted maximum rates during the time period of 2011-2014.

5.5 *Groundwater Flow Model Calibration*

5.5.1 Calibration Targets for the Steady-State Groundwater Model

The overall goal of model calibration is to improve the match between simulated and observed values (i.e., the calibration targets) by systematically refining the estimates of model parameters, such as hydraulic conductivity, vertical anisotropy, and recharge, within reasonable ranges. Steady-state calibration targets were the observed water levels in the bedrock and overburden and the estimates of baseflow.

The primary source of observed static water levels was the MECP Water Well Information System (WWIS) database. All MECP wells within a 10 km radius of the municipal wells were included in the calibration dataset. Long-term average water levels measured at the Freelton monitoring wells were also included in the calibration dataset. Well data were screened to eliminate wells with obvious location or elevation inaccuracies. The model layer containing each well was determined based on the reported depth of the well screen. Wells less than 20 m and greater than 20 m, along with their water levels, are shown in Figure 5.5 and Figure 5.6. A visual inspection of both figure shows that the static water level of one well may vary significantly from another well nearby. This may be due to the fractured nature of the bedrock, differences in time when the measurements were taken and/or due to other systemic errors in the dataset. Therefore, we cannot expect to achieve a calibration that reduces the error to less than that of the intrinsic error of the data. The WWIS water level data for the bedrock and overburden were found to have a standard error of between ±4 m to ±10 m even after statistical outliers were removed.

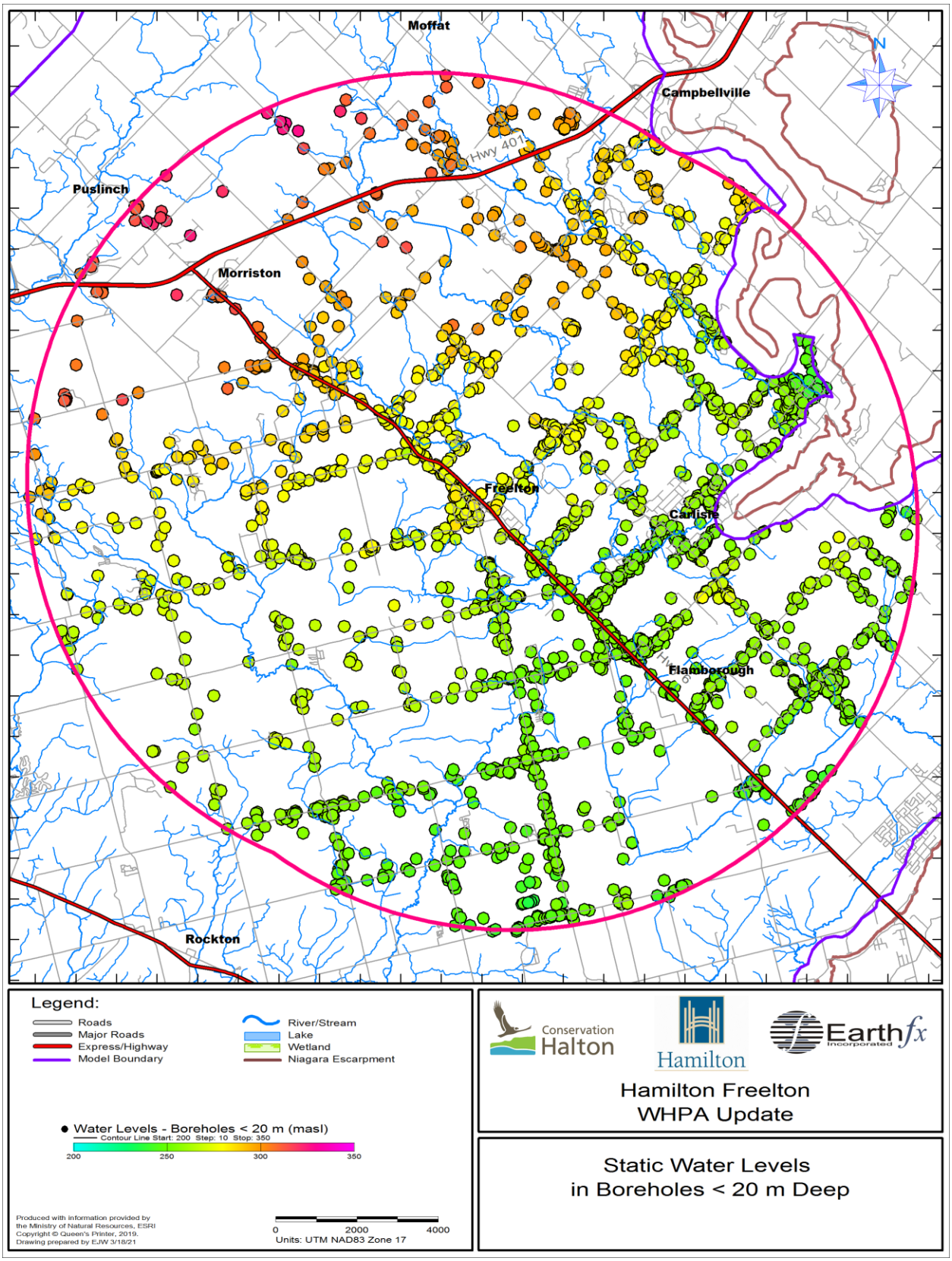

Figure 5.5: Static water levels in Boreholes less than 20 m deep.

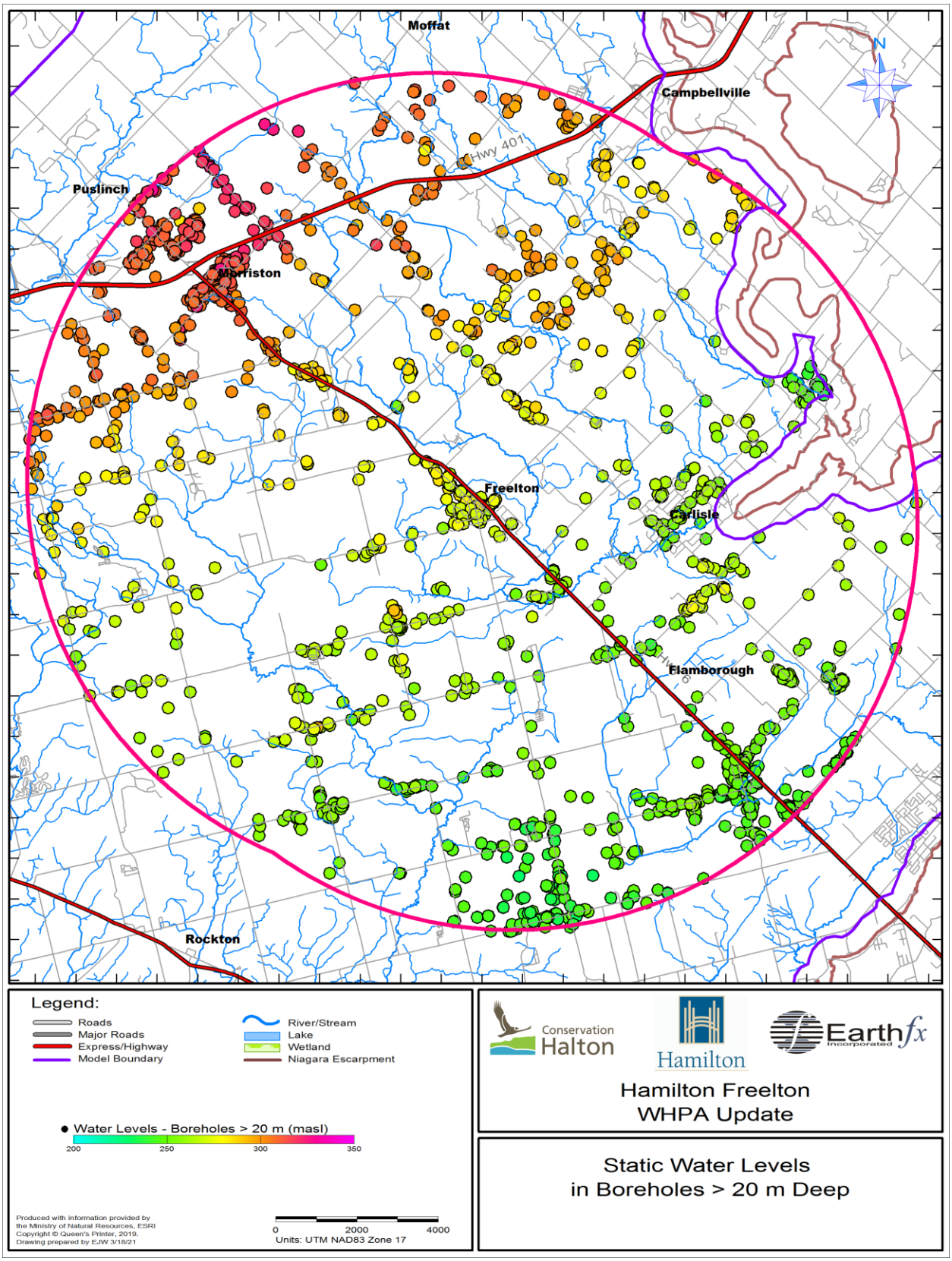

Figure 5.6: Static water levels in boreholes greater than 20 m deep.

5.5.2 Model Hydraulic Conductivity Values

Initial estimates for hydraulic conductivity were taken from the original NH Model (see Earthfx, 2010). An equivalent porous medium (EPM) assumption was used for all bedrock units rather than attempting to define fracture-dependent hydraulic conductivity values. The model was already quite well calibrated using the properties from the original NH Model; however, some refinements were completed during the calibration process as summarized below:

1. At the outset of the study, water levels in the north, atop the Galt Moraine were overpredicted by the model. The Galt Moraine is composed primarily of Wentworth Till, which is known to have a high degree of sand content. It was initially assigned a value of $5x10^{-7}$ m/s in Layer 1 and $2x10^{-7}$ m/s in Layer 2. Both layers were increased by a factor of ten within the footprint of the moraine according to physiographic mapping. This resulted in lower simulated water levels and a better match to observed data.

2. The weathered bedrock (Layer 4) was locally modified in the Freelton area where the Eramosa member was mapped in the hydrostratigraphic model. Additional confinement was added to the local area. This was done to improve the consistency with the Wood (2018a) pump test findings, which reported FDF01 to be highly confined. Accordingly, the vertical anisotropy ratio was decreased to 0.01 locally around Freelton.

3. Hydrogeologic investigations in the Freelton area were also used to locally update the hydraulic conductivity distribution of the production zone within the middle Gasport/Amabel hydrostratigraphic unit (Layer 7). Discrete transmissivity measurements of the bedrock aquifer in Freelton derived from pump tests (see Table 3.1) were interpolated and then converted to hydraulic conductivity by dividing by the thickness of the model layer. The result was a locally increased hydraulic conductivity distribution for Layer 7 that was more consistent with the pump test data.

The hydraulic conductivity and vertical anisotropy values applied to the hydrostratigraphic model units are summarized in Table 5.2. The green highlighted areas in the table represent areas where changes were made to the original NH Model. Maps showing the spatial distribution of the final hydraulic conductivity values are presented in Figure 5.7 to Figure 5.16.

Table 5.2: Aquifer and aquitard properties for the hydrostratigraphic units.

Hydrostratigraphic Unit	Hydraulic Conductivity (m/s)	Anisotropy (K_v/K_h)
Surficial Deposits	$5x10^{-7}$ – $1x10^{-3}$	1.0
Upper Till	$2x10^{-7}$ – $1x10^{-3}$	0.3
Basal Aquifer	$5x10^{-6}$ – $1x10^{-4}$	1.0
Weathered Bedrock (Guelph, Eramosa, Gasport, Goat Island/Amabel)	$5x10^{-6}$ – $1x10^{-3}$	0.01-0.3
Unweathered Bedrock (Guelph, Eramosa, Gasport, Goat Island/Amabel)	$1x10^{-6}$ – $1x10^{-3}$	0.01-0.1
Upper Gasport/Amabel	$5x10^{-6}$ – $1x10^{-3}$	0.3
Middle Gasport/Amabel	$9x10^{-5}$ – $5x10^{-3}$	0.3
Lower Gasport/Amabel	$5x10^{-7}$	0.3
Reynales	$1x10^{-8}$	0.3
Queenston	$2x10^{-9}$	0.3

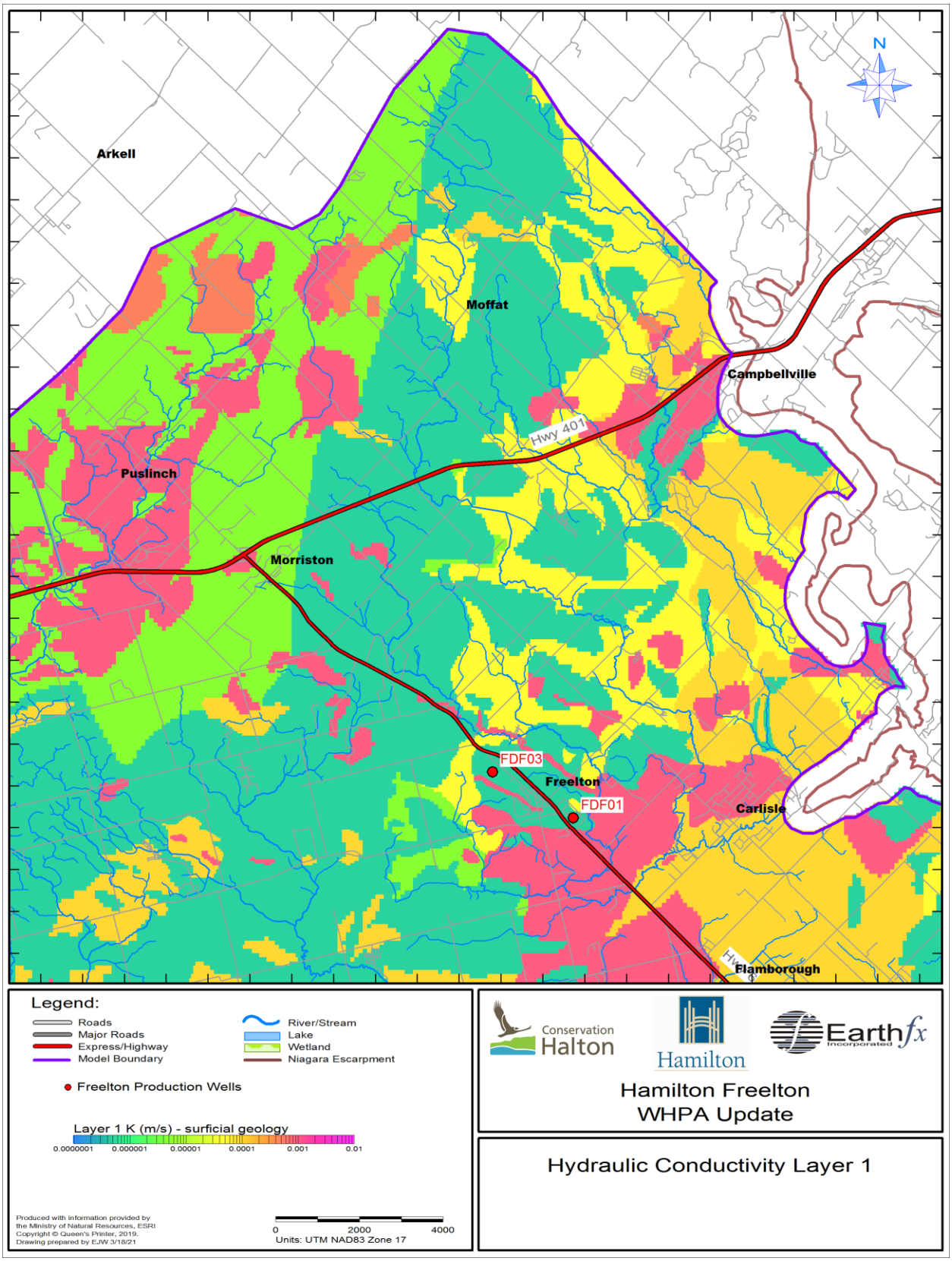

Figure 5.7: Hydraulic conductivity distribution in model Layer 1.

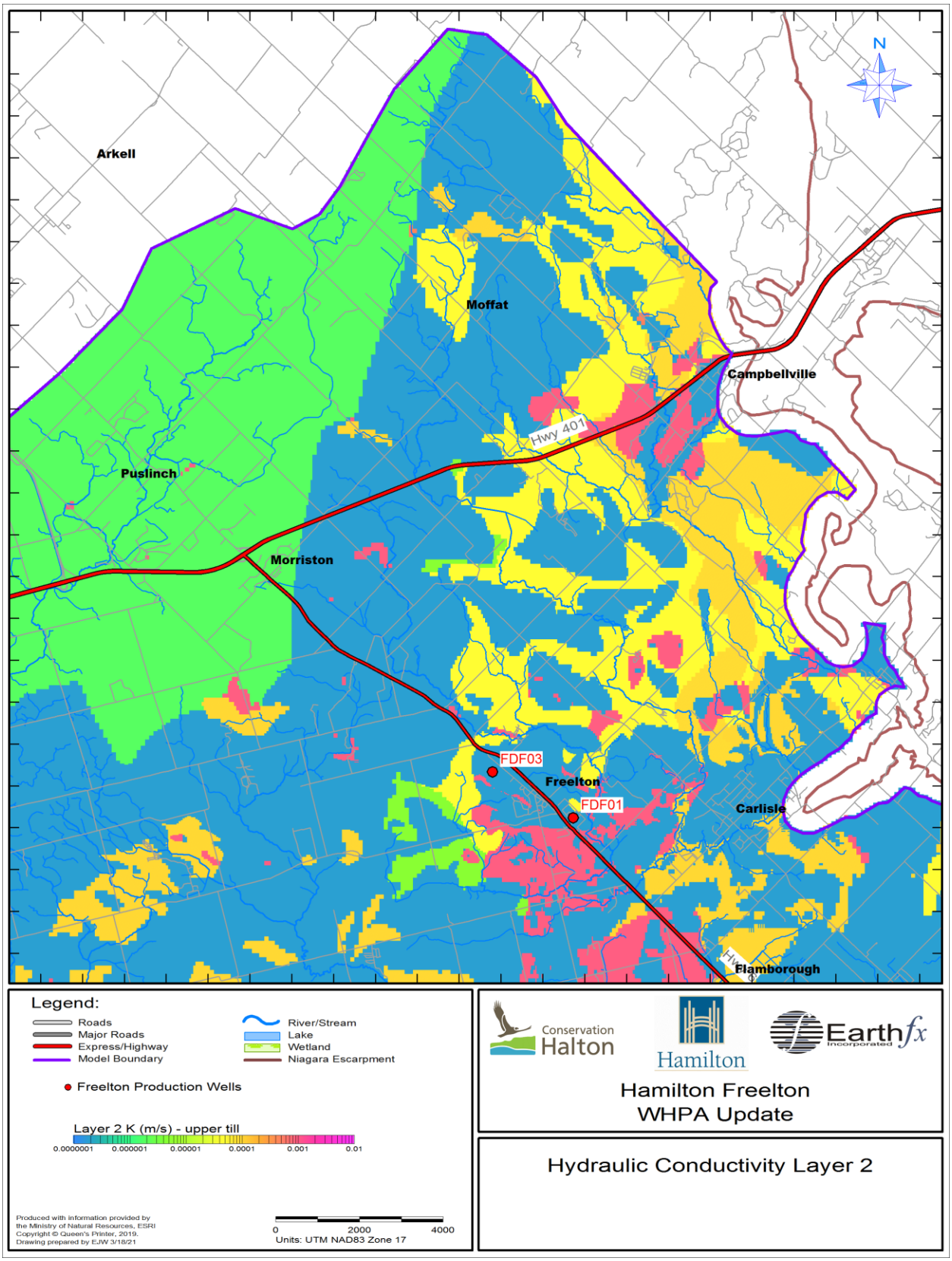

Figure 5.8: Hydraulic conductivity distribution in model Layer 2.

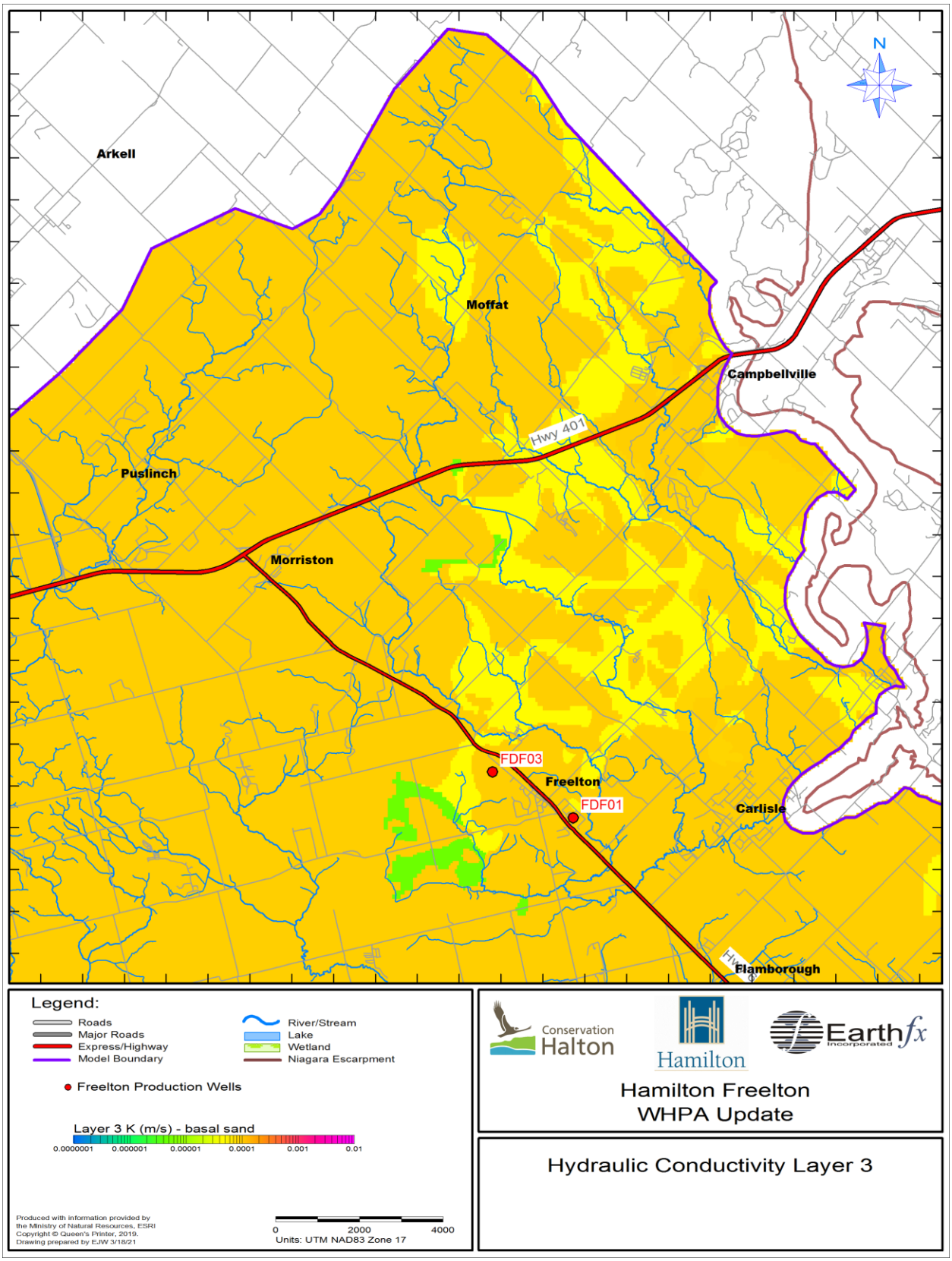

Figure 5.9: Hydraulic conductivity distribution in model Layer 3.

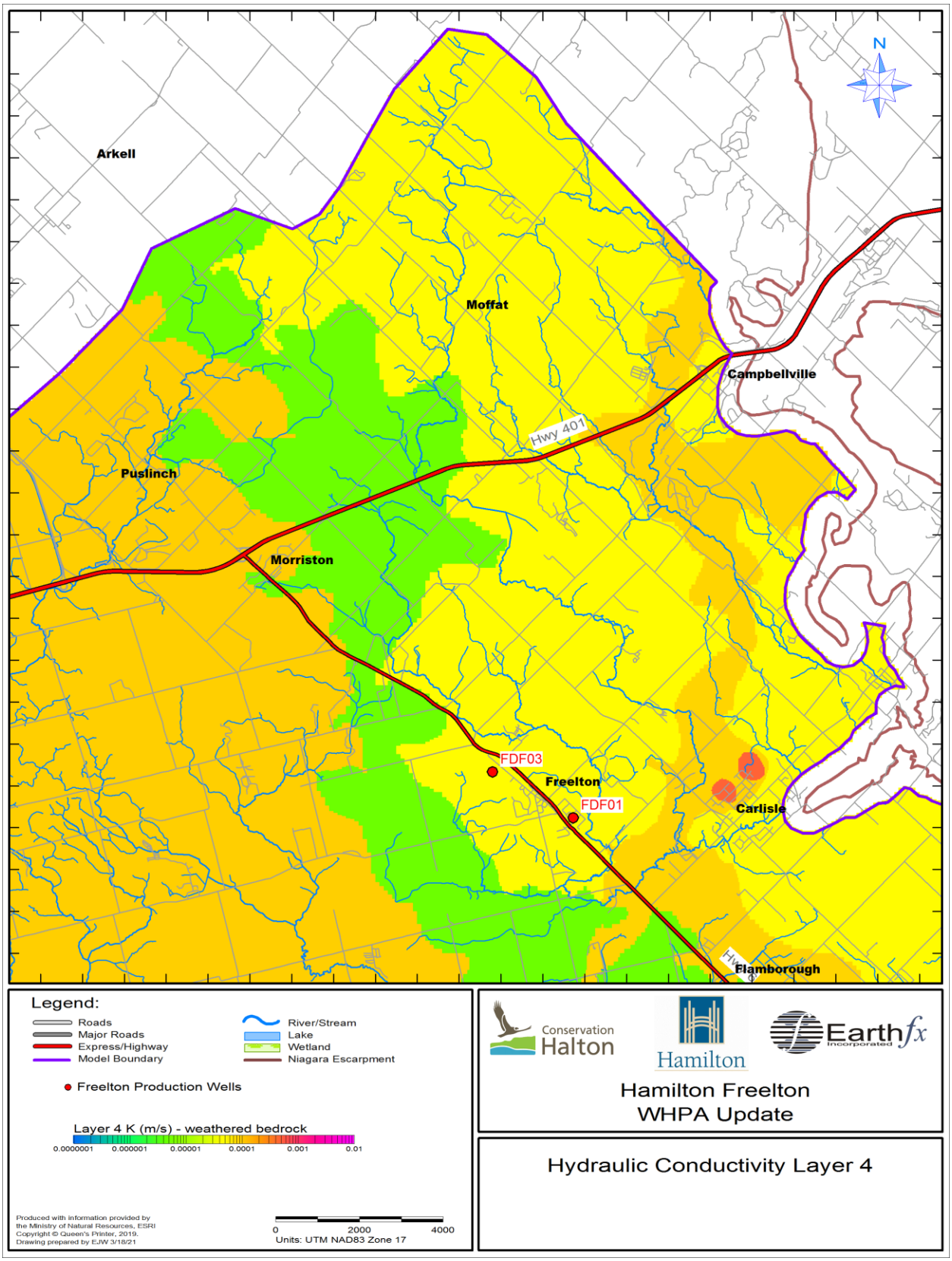

Figure 5.10: Hydraulic conductivity distribution in model Layer 4.

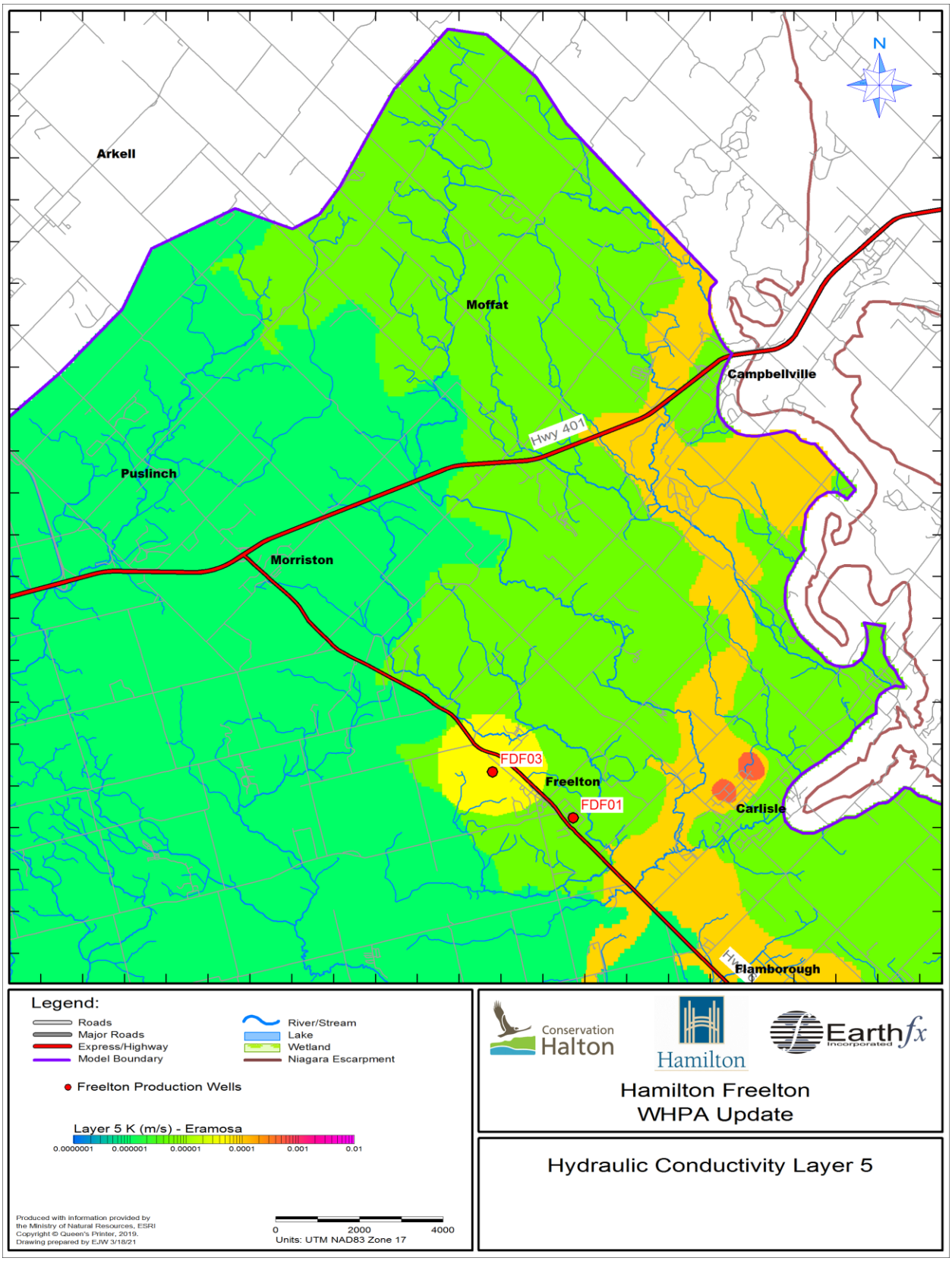

Figure 5.11: Hydraulic conductivity distribution in model Layer 5.

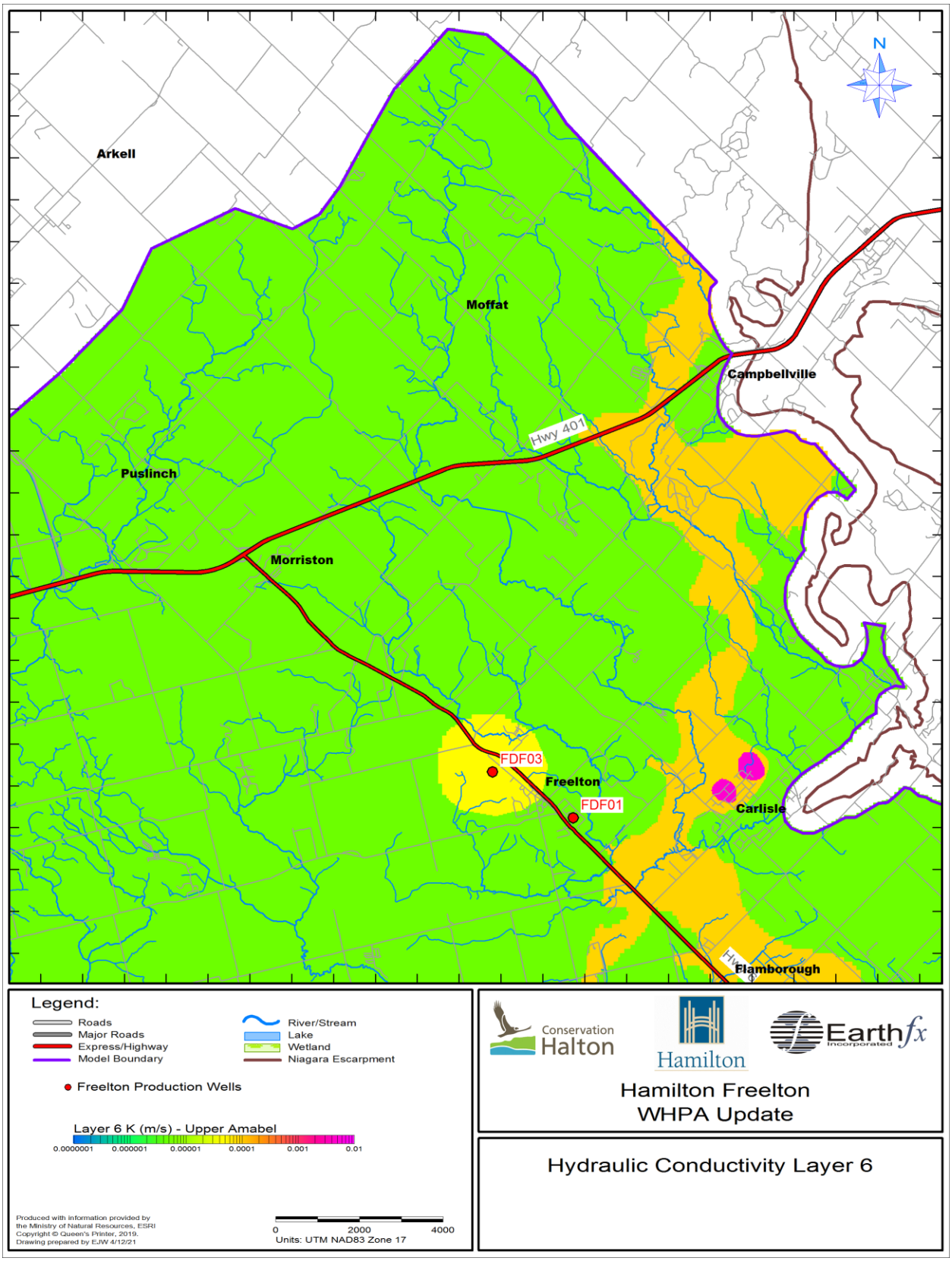

Figure 5.12: Hydraulic conductivity distribution in model Layer 6.

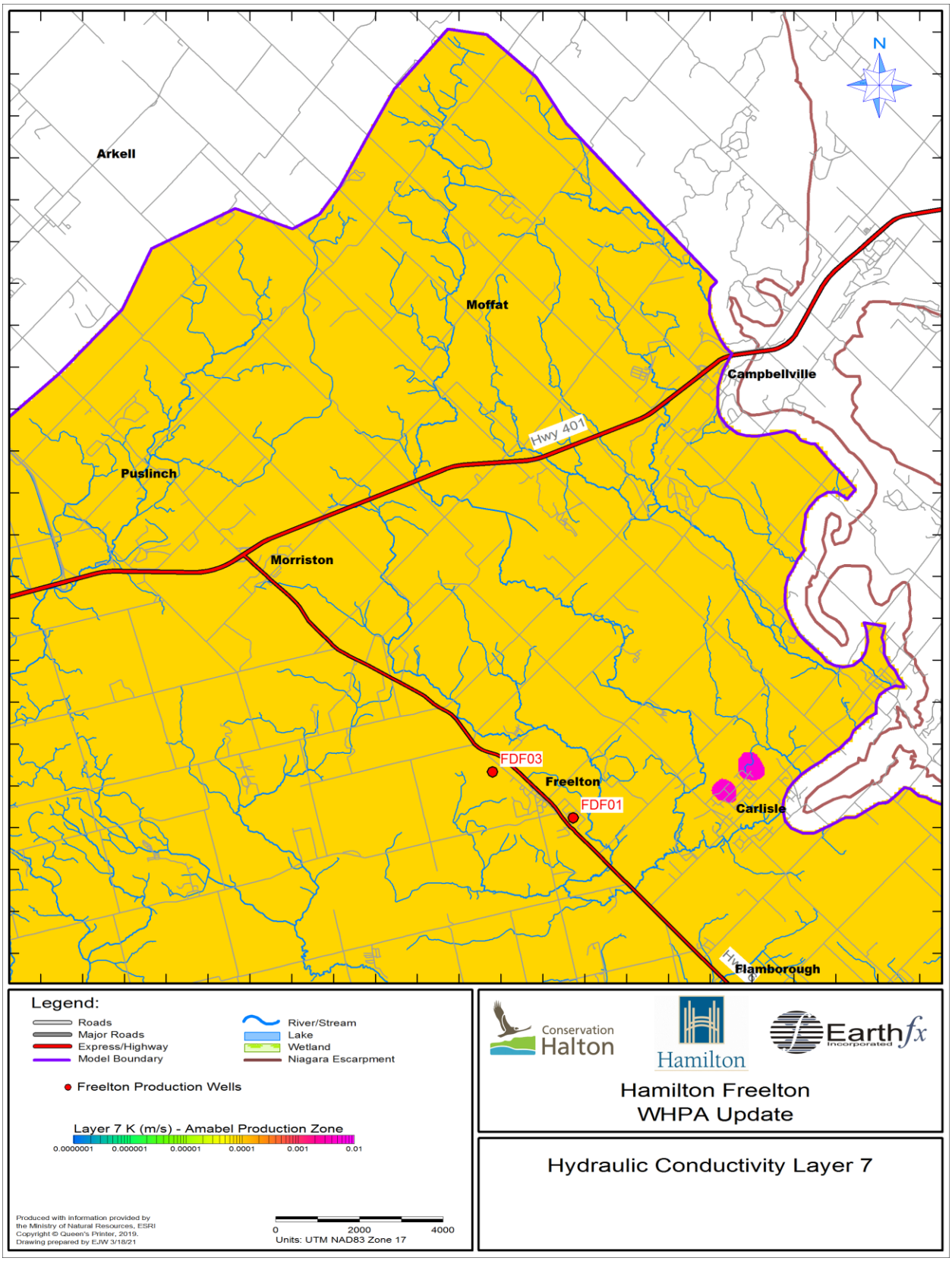

Figure 5.13: Hydraulic conductivity distribution in model Layer 7.

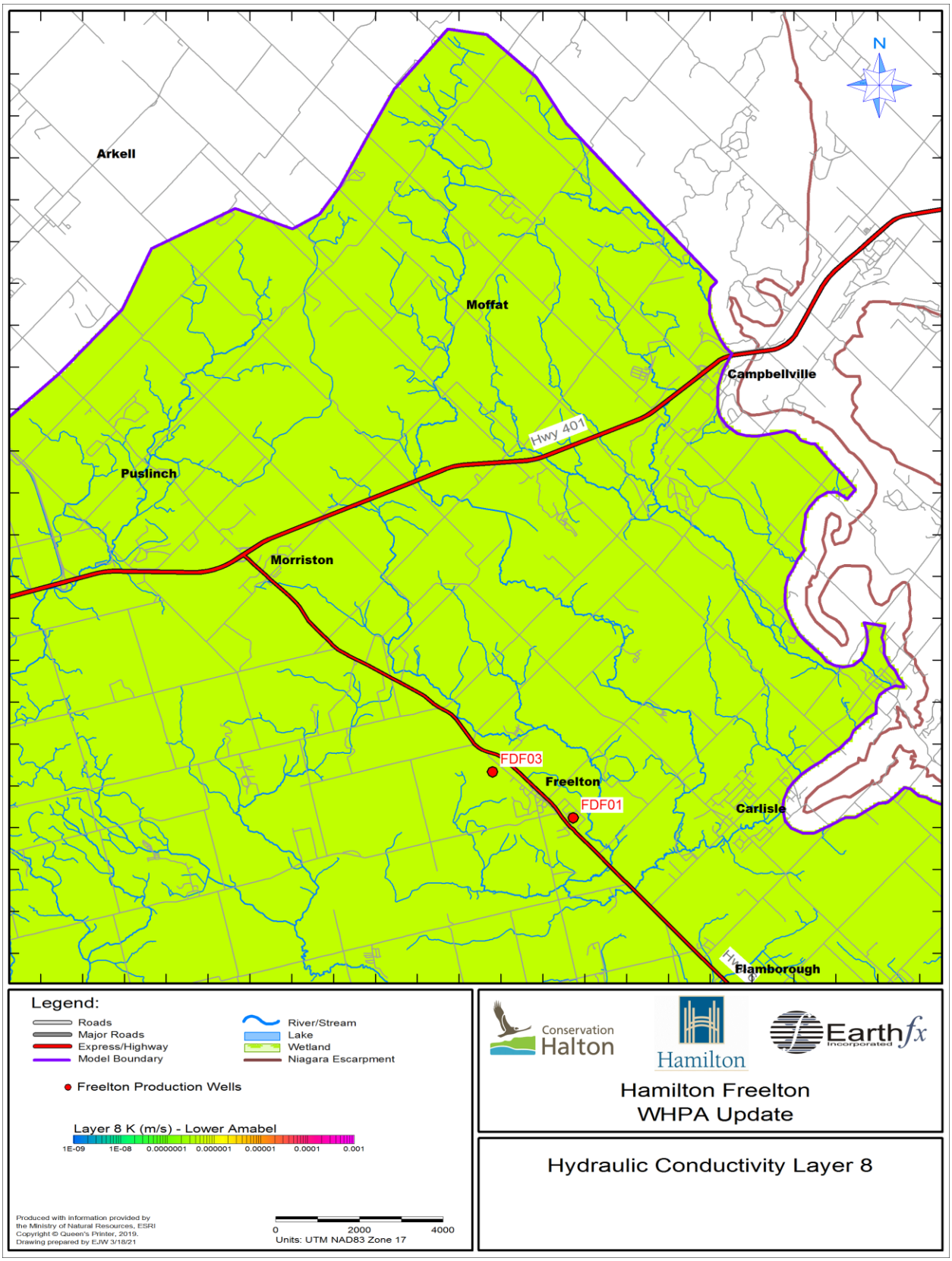

Figure 5.14: Hydraulic conductivity distribution in model Layer 8.

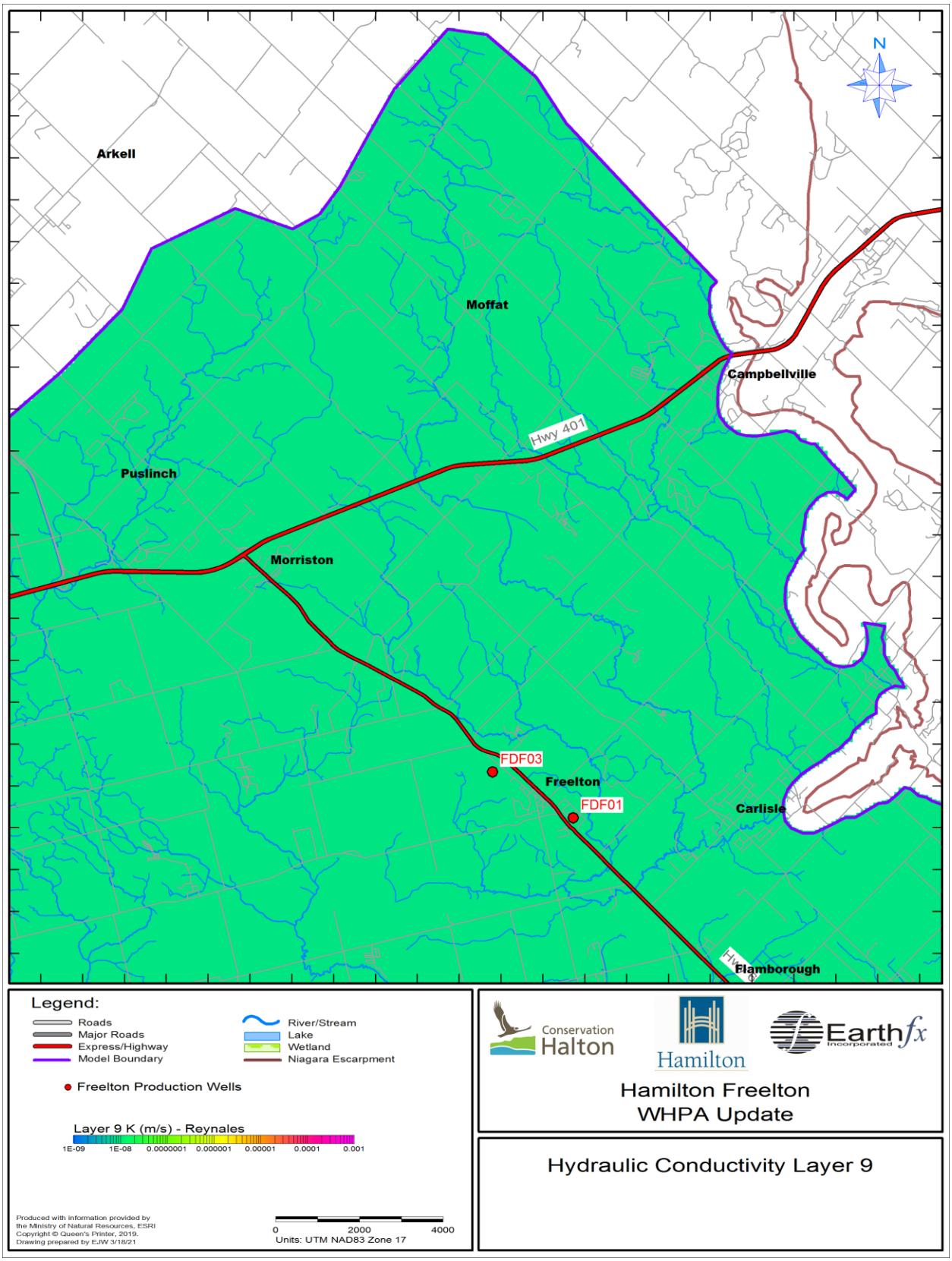

Figure 5.15: Hydraulic conductivity distribution in model Layer 9.

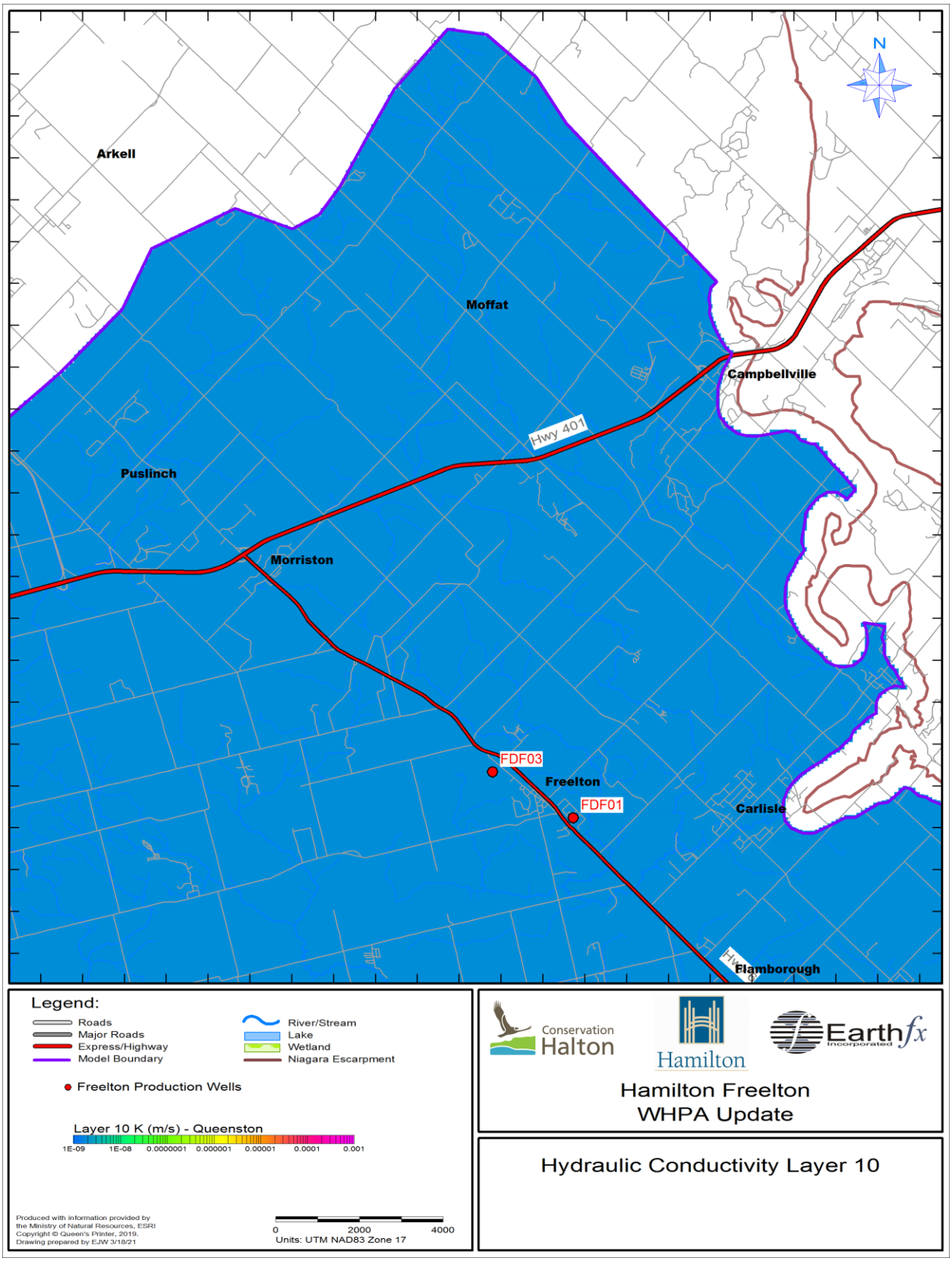

Figure 5.16: Hydraulic conductivity distribution in model Layer 10.

5.5.3 Groundwater Level Comparisons and Calibration Statistics

Figure 5.17 and Figure 5.18 compare the simulated steady-state water levels in model Layer 3 and Layer 7 and interpolated static water levels in the shallow and deep systems, respectively. A reasonable match was achieved to the interpolated data, particularly to wells screened less than 20 m below ground surface (mbgs), which makes up the vast majority of observations. Simulated and observed groundwater contours show the general two-dimensional flow direction through Freelton is from the northwest to the southeast with some local variation due to the presence of streams and low-lying wetlands. Some discrepancy is present between simulated heads and the interpolated water levels for wells screened deeper than 20 mbgs where the model tends to over-predict the heads in the deeper system through Freelton. Boreholes sampling this depth are scarcer and the static water levels in Freelton, alone, vary by up to 20 m within a small area make it difficult to rely on the absolute values of the interpolated water levels in this area. Nevertheless, the inferred two-dimensional flow patterns are consistent between the simulated and interpolated heads.

Statistical analyses were applied to test the quality of the calibration. A scatterplot comparing the WWIS water levels to the simulated steady-state heads for boreholes less than and greater than 20 m in depth is shown in Figure 5.20. Higher quality observations from Freelton monitoring wells are highlighted with green symbols. Ideally, all data points should fall on the 1:1 line; however, due to intrinsic error present in the MECP WWIS dataset and due to model simplifications, a perfect match cannot be achieved. Generally, the data fall within ±10 m, as shown by the dashed red lines.

Three calibration statistics were used to assess and demonstrate model accuracy: the mean error (ME), mean absolute error (MAE), and root mean squared error (RMSE) defined as:

$$\text{Mean Error} = \frac{1}{n}\sum_{1}^{n}(h_O - h_S)_i$$

$$\text{Mean Absolute Error} = \frac{1}{n}\sum_{1}^{n}\left|(h_O - h_S)_i\right|$$

$$\text{Root Mean Squared Error} = \sqrt{\frac{1}{n}\sum_{1}^{n}(h_O - h_S)_i^2}$$

where h_o are the observed heads, h_s are the simulated, and n is the number of observations. Calibration statistics for the 3,786 observed heads are presented in Table 5.3. The negative value for ME indicates that simulated values are biased to the high side by 0.88 m on average. The MAE and RMSE provide a measure of the average magnitude of variance between observed and simulated values. An MAE of 3.4 m and RMSE of 4.96 m are quite good considering the intrinsic error in the observations is approximately 4 m.

Table 5.3: Summary of calibration statistics.

Number of Wells	ME (m)	MAE (m)	RMSE (m)
3,786	-0.88	3.40	4.96

Another target for model calibration was matching simulated baseflow to baseflow estimates for the Bronte Creek at Carlisle stream gauge. Estimated baseflows were presented in Earthfx (2010) for 23 stream gauges across the Halton-Hamilton region. The estimated average baseflow at the Bronte Creek at Carlisle gauge is 0.82 m³/s, which compares well to the simulated baseflow of 0.87 m³/s. The good match between the estimated and the observed baseflow is further evidence that the model is well calibrated in the Freelton study area.

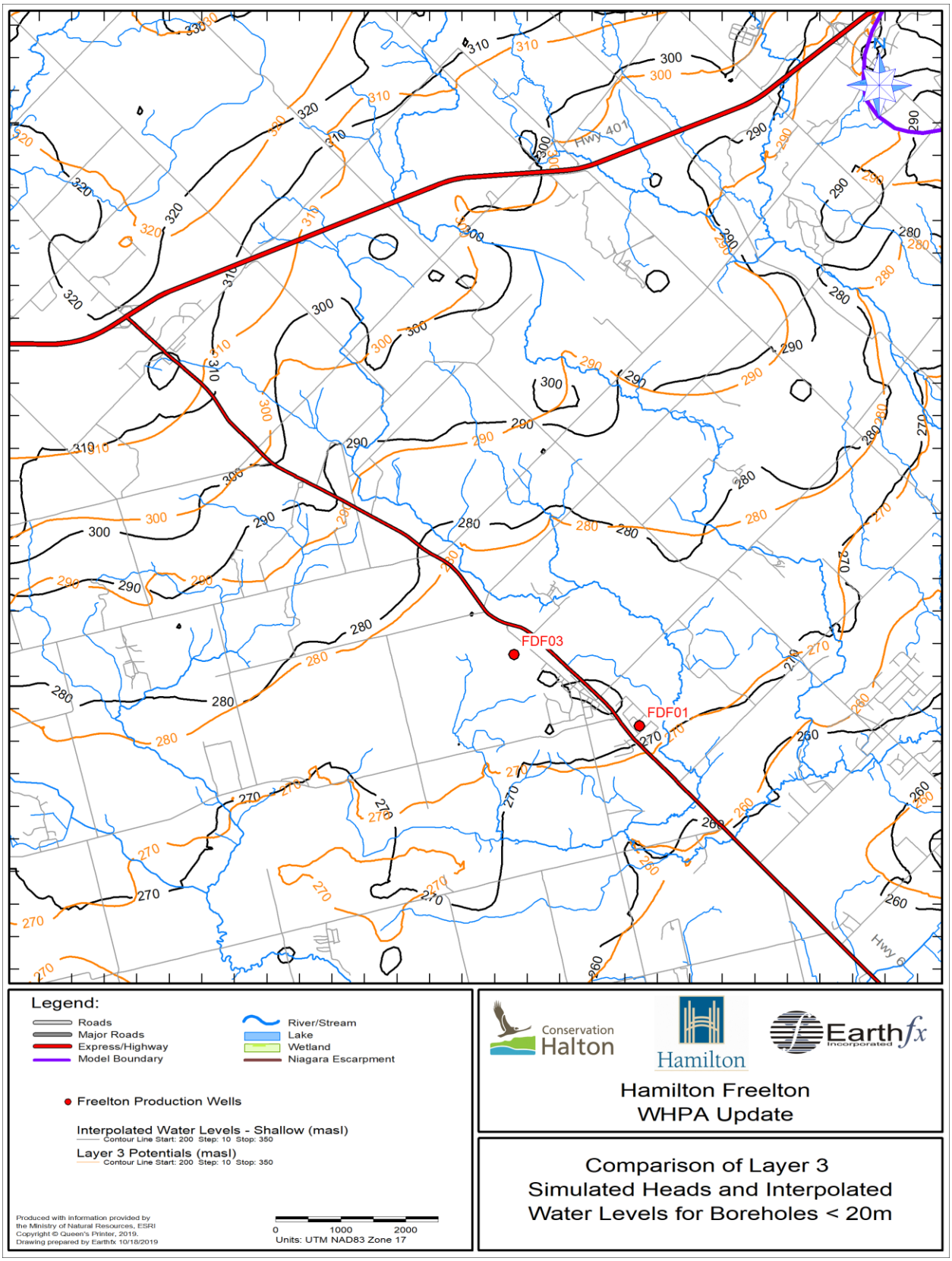

Figure 5.17: Comparison between interpolated WWIS water levels and simulated heads in model Layer 3.

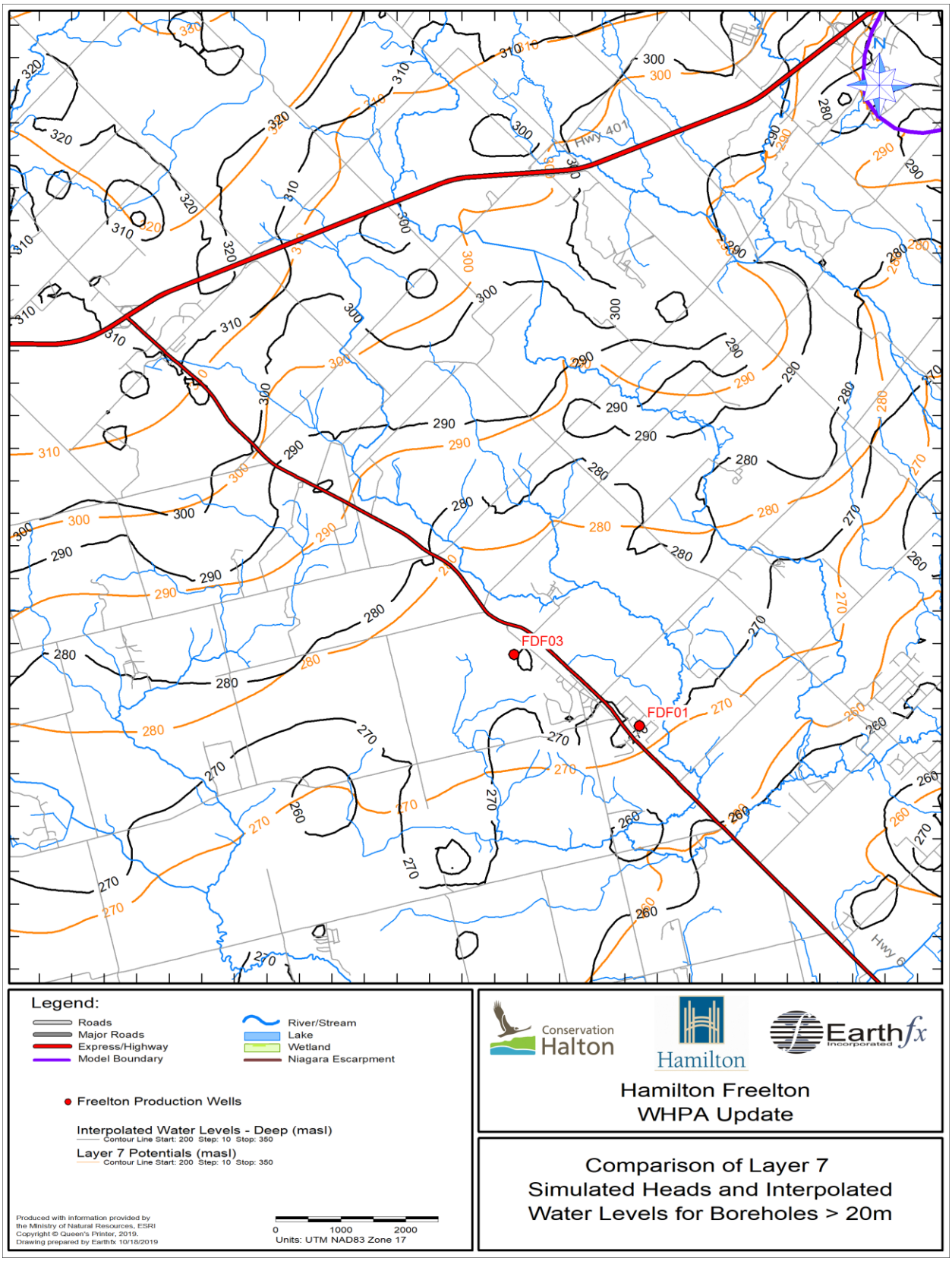

Figure 5.18: Comparison between interpolated WWIS water levels and simulated heads in model Layer 7.

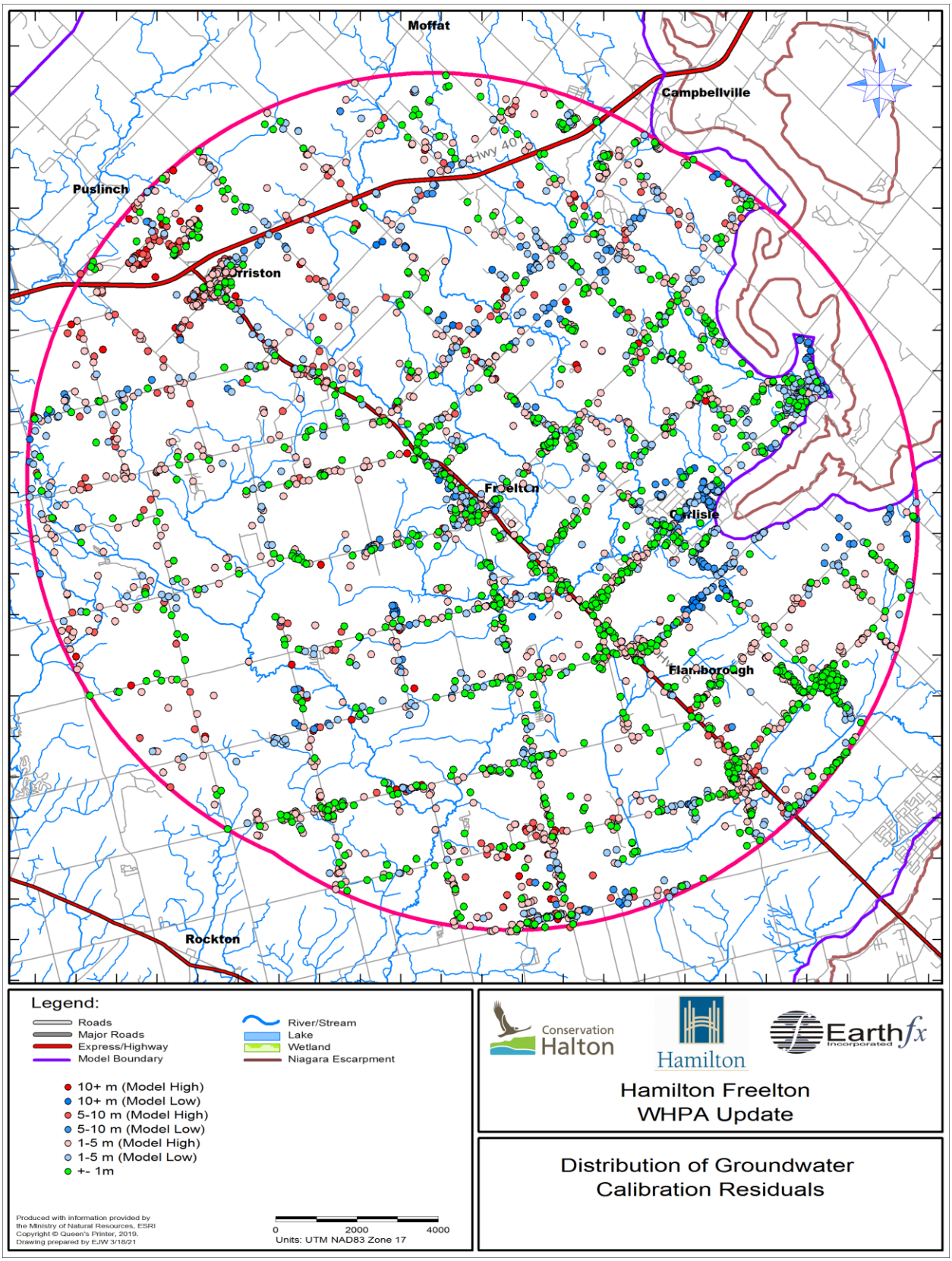

Figure 5.19: Distribution of overburden groundwater calibration residuals.

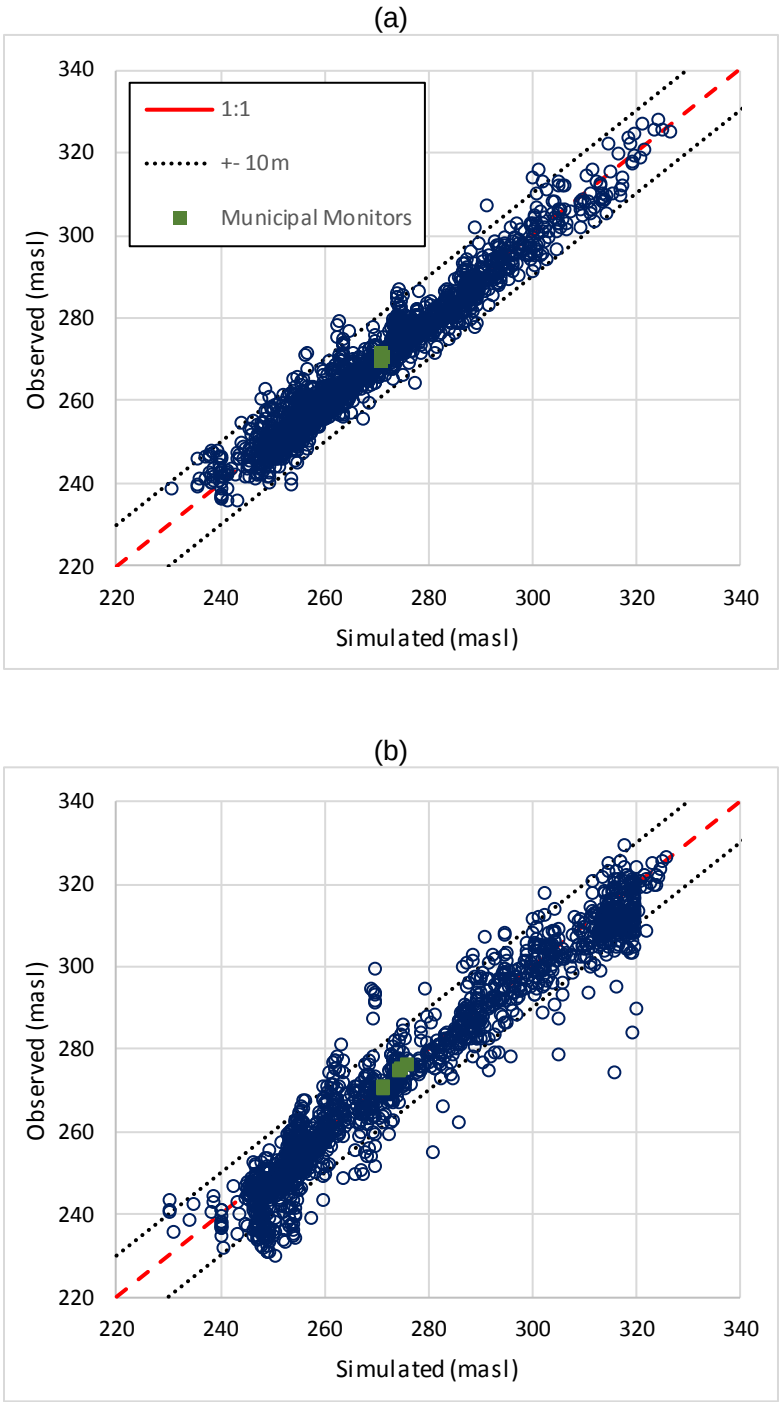

Figure 5.20: Scatterplots of calibration residuals in the (a) shallow wells (less than 20 m deep) and (b) deep wells (greater than 20 m deep).

5.5.4 Transient Validation

The model was also calibrated in transient mode to match the 92.5-hour pump-test completed in September of 2017 (Wood 2018a). The pump test was completed at FDF01 as part of an application to increase the PTTW average daily maximum pumping rate from 10.2 L/s to 18.3 L/s. It should be noted, however, that the model resolution is not sufficient to exactly represent spacing between wells in the vicinity of FDF01 and therefore it cannot be expected to exactly match drawdowns at the specified monitoring wells. The primary focus of the transient calibration was to illustrate that the model parameters were reasonably consistent with the pump-test results. In doing so, we can be reasonably certain that the model is adequately representing the bulk hydrogeologic properties in the vicinity of the pumping well.

As mentioned in Section 3.6.1, Wood (2018a) describes the aquifer as highly productive and highly confined. However, monitoring data during the pump test show that shallow monitors FM-01-17sb and FDF-01-02 behaved in a similar manner monitor FM-01-17d, screened at a similar depth to the production well. Wood (2018a) concluded that this behaviour was due to vertical leakage through the well seal at FM-01-17sb or vertical leakage through the formation at FDF-01-02. While we agree that the system is confined; we cannot not rule out the possibility of enhanced vertical connectivity in the vicinity of FDF01.

Figure 5.21 through Figure 5.23 show a comparison between the observed and simulated water levels. The model time units were “days” and therefore the pumping stress period could not be exactly 92.5 hours. Instead it was set to 4 days or 96 hours. As a result, the recovery period occurs 3.5 hours later than the observed results. There is also a slight offset between the simulated and the observed water levels. A close match was achieved between the heads in FM-01-17d and with simulated heads in model Layer 7 during pumping and recovery. The model underpredicted the drawdown in the shallow bedrock (Layer 6) at FM-01-17sb and to a lesser degree at FDF-01-02. As mentioned above, it is believed that vertical leakage, whether it is through the formation or through a leak in the well seal, causes the shallower monitors to behave similarly to FM-01-17d (Wood 2018a). Nevertheless, the smaller drawdowns simulated in the shallow bedrock are consistent with the conceptual model that assumes the aquifer behaves in a confined manner. Overall, the assigned model parameters appear to adequately represent the aquifer properties.

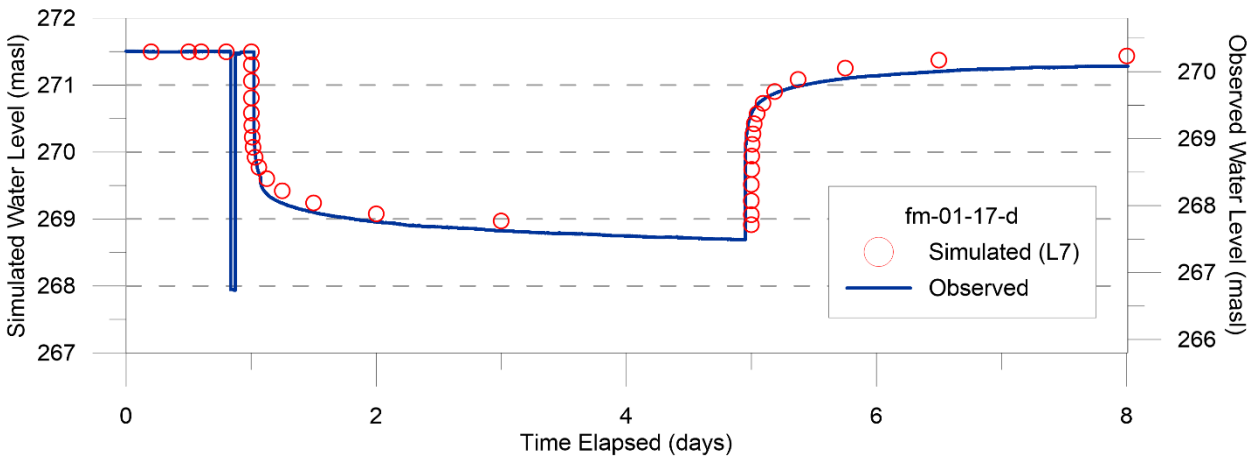

Figure 5.21: Observed and simulated heads during Wood (2018a) pump test at FM-01-17-d.

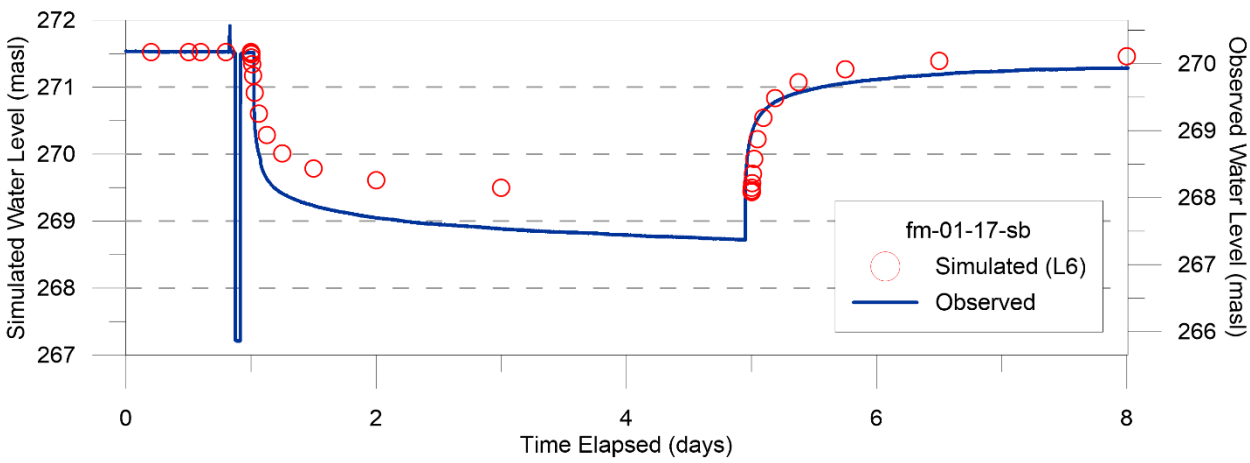

Figure 5.22: Observed and simulated heads during Wood (2018a) pump test at FM-01-17-sb.

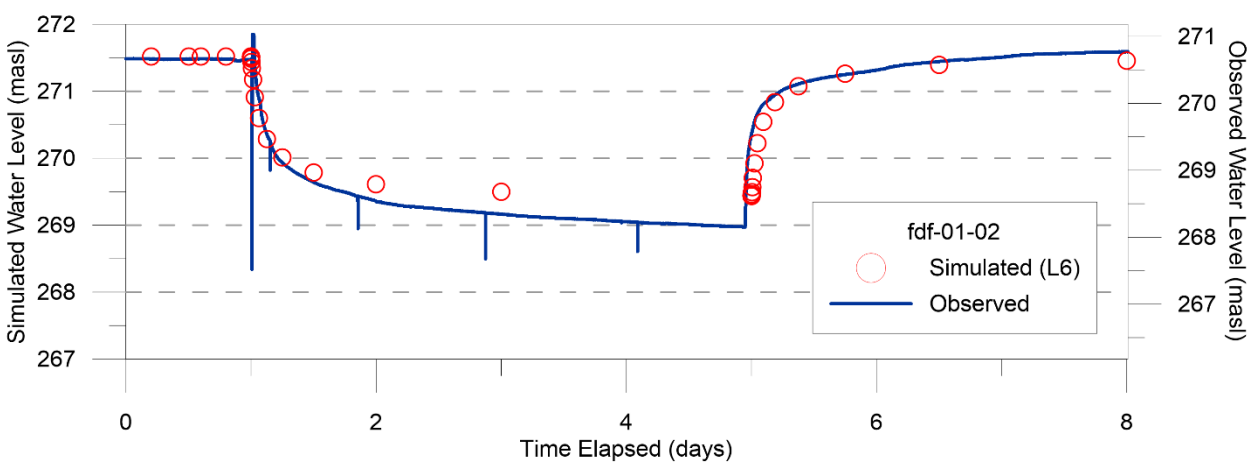

Figure 5.23 Observed and simulated heads during Wood (2018a) pump test at FDF01-02

6 Aquifer Vulnerability Assessment

6.1 *Wellhead Protection Areas (WHPAs)*

6.1.1 WHPA Delineation Methodology

Requirements for delineating WHPAs and aquifer vulnerability zones are defined in the Ontario Ministry of Environment, Conservation, and Parks (MECP) Technical Rules for Assessment Reports (MECP, 2017). The approach used in this study closely followed these guidelines. WHPAs were delineated based on time-of-travel (TOT) determined through the application of a three-dimensional groundwater flow model. This is the "preferred method" according to the Technical Rules because numerical models can represent spatial variability of aquifer and aquitard properties and recharge rates. The following mapped zones were delineated

- WHPA-A (i.e., the surface area within a 100-m radius of the well),
- WHPA-B (the surface area within a 2-year Time of Travel (TOT) zone)
- WHPA-C (the surface area within a 2 to 5-year TOT zone)
- WHPA-D (the surface area within a 5 to 25-year TOT zone)

Time-of-travel zone analyses were conducted using the USGS MODPATH v6.0 code (Pollock, 2012). MODPATH uses simulated groundwater levels (heads) from the MODFLOW-NWT model along with estimates of aquifer porosity to calculate average groundwater velocities (magnitude and direction) within each cell in the model grid. MODPATH was used to track virtual particles backwards from the municipal supply wells to their point-of-entry to the groundwater flow system.

Porosity values for the geologic units are needed to calculate the groundwater velocities. Values assigned to the geologic units are listed in Table 6.1. MODPATH analysis was conducted by releasing 100 virtual particles on each of the six sides of the cells containing the production wells. Particles were released in model Layer 7 (Amabel/Gasport Production Zone) for FDF01 and FDF03. In total, 1200 particles were tracked backwards in time from each well as they moved through the aquifers and aquitards.

Table 6.1: Porosity values assigned to geologic units.

Geologic Unit	Porosity		Geologic Unit	Porosity
Recent Deposits	0.15		Upper Amabel/Gasport	0.01
Upper Till	0.20		Amabel/Gasport Production Zone	0.01
Basal Sands	0.05		Lower Amabel	0.01
Weathered Bedrock	0.05		Reynales	0.01
Guelph/Eramosa	0.01		Queenston	0.01

As noted in Section 2.2, several pumping scenarios were considered in this analysis, including having all pumping from FDF01 (18.3 L/s), all pumping from FDF03 (18.6 L/s), and various combinations of pumping from the two well. The five pumping rate configurations used in the WHPA analysis were shown in Table 2.3. WHPAs were delineated for the first two scenarios and then adjusted slightly based on the results of the remaining scenarios to delineate a composite WHPA.

Simulated water levels in Layer 7 are shown for pumping scenarios 1 and 2 in Figure 6.1 and Figure 6.2, respectively. The differences in water levels are significant in the vicinity of the individual wells but are negligible at distances greater than 1.5 km.

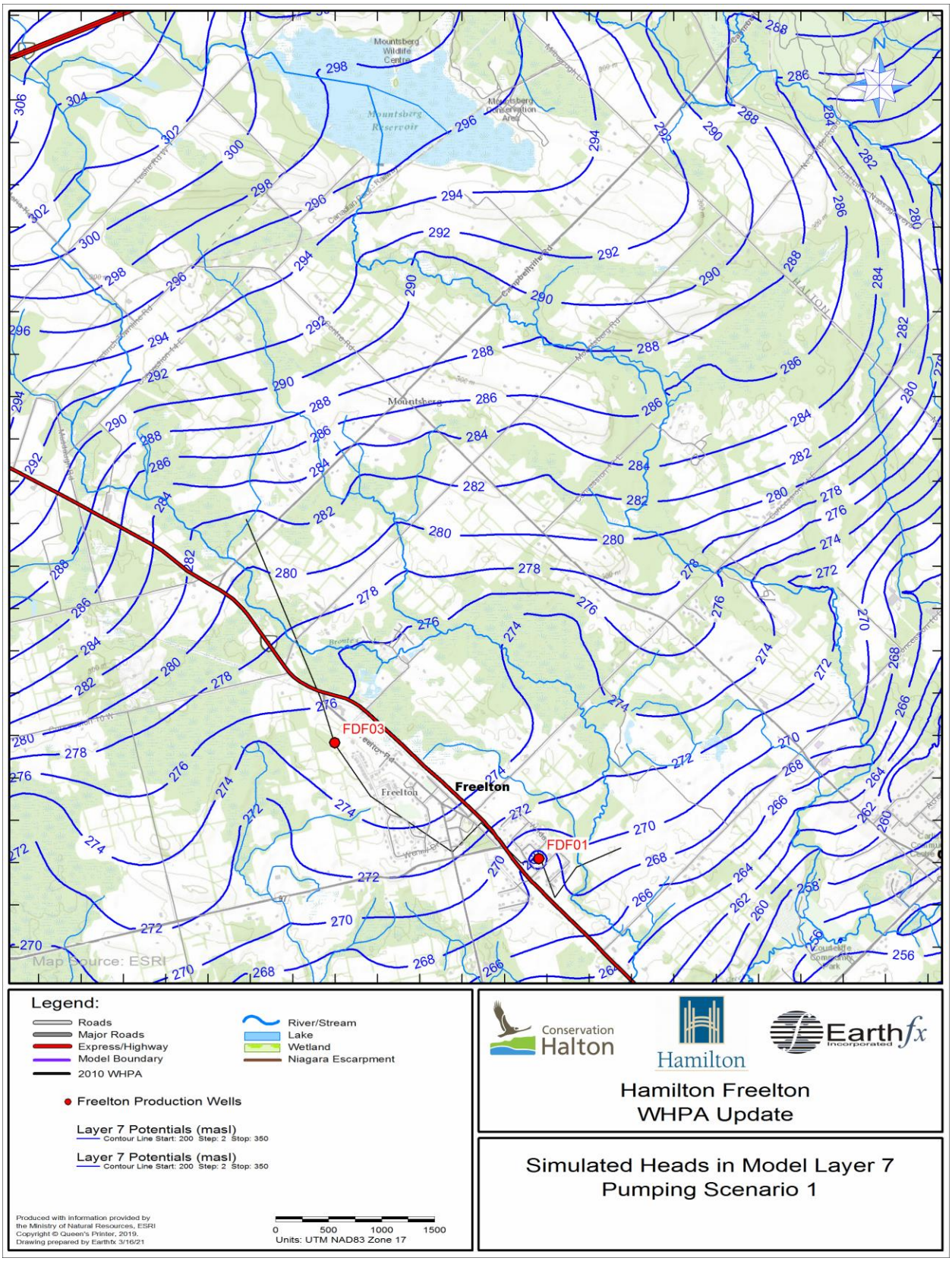

Figure 6.1: Simulated water levels in numerical model Layer 7 – Pumping scenario 1.

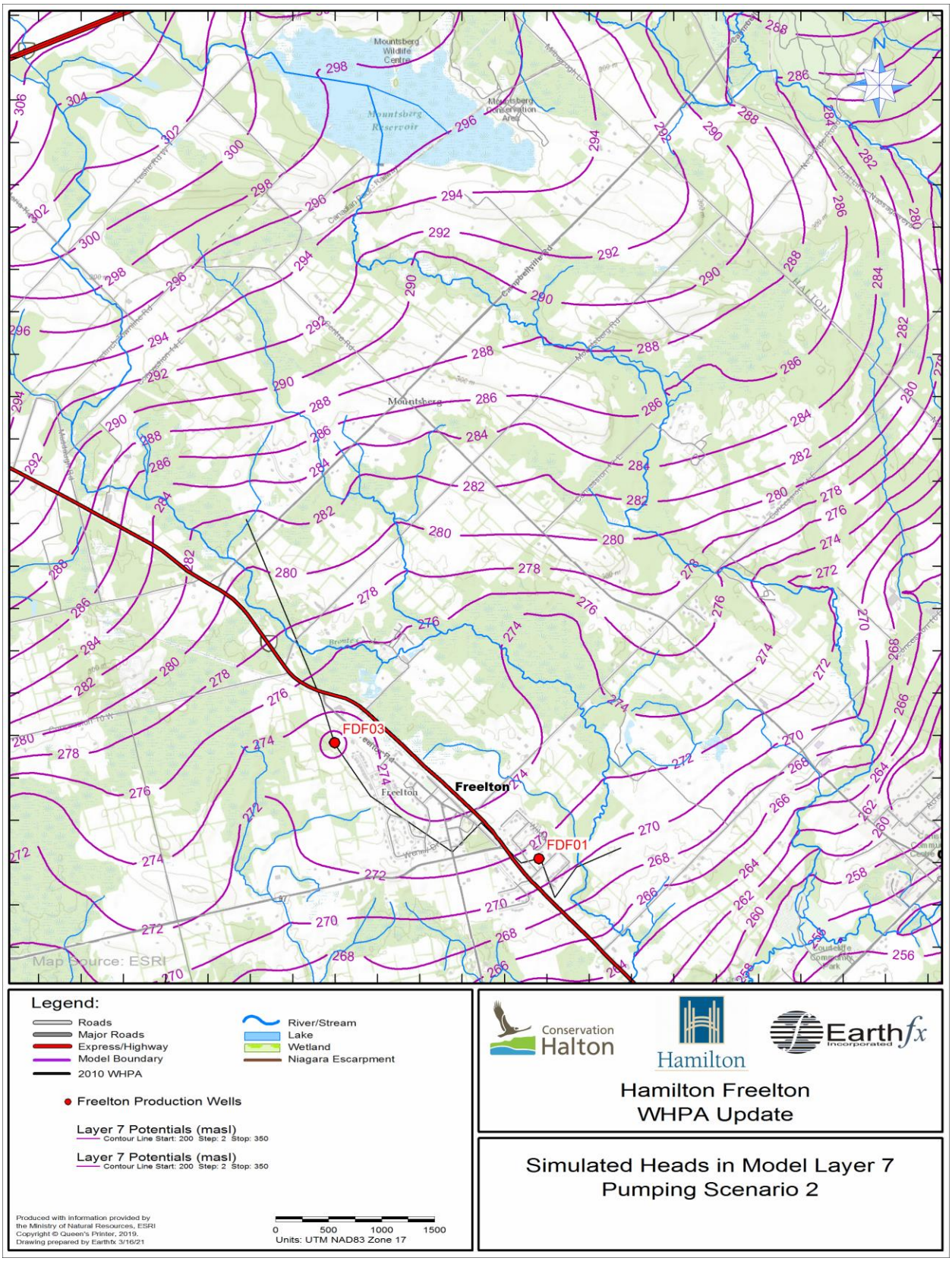

Figure 6.2: Simulated water levels in numerical model Layer 7 – Pumping scenario 2.

6.1.2 WHPA Delineation

Capture zones for all pumping scenarios were analyzed together in order to produce the most conservative WHPA delineation. Backward particle tracks from the supply wells at the maximum time of travel (25 years) under Scenario 1 and 2, the most extreme pumping configurations, are shown in Figure 6.3. The particle tracks for all five scenarios are compared to the interpolated shallow water table in Figure 6.4 and show good agreement in the flow directions as the pathlines generally intersect the groundwater elevation contours at right-angles. The particles tracks for Scenarios 3 to 5 generally fit within the WHPA outlines for Scenarios 1 and 2 with some minor differences at the far ends of the FDF03 capture zone in Scenario 4.

The capture zone for FDF01 (in Scenario 1, for example) has a typical teardrop shape pointing upgradient. This would indicate that local recharge and leakage through the overlying formations is sufficient to sustain the well. While much of the flow to FDF03 is also derived locally (in Scenario 2, for example), a higher degree of confinement exists, and the well pulls additional flow from as far away as the Galt Moraine. These extended pathlines skirt areas of groundwater discharge as they travel backward to their point of recharge. As a result, the pathlines tend to follow subtle groundwater flow divides in between streams and wetlands resulting in the two long and narrow arms. Recharge to either side of the lines likely is captured as direct discharge to the stream channels or as surface leakage.

WHPA delineations for the Freelton supply wells were based on the composite TOT zones (i.e., the 2, 5, and 25 year zones) and the 100 m radius around the wells. These are shown in Figure 6.5. The WHPA-B occupies a large proportion of the composite capture zone around FDF01 and FDF03. This is due to the high permeability of the bedrock aquifer in the vicinity of the supply wells. The long, tailing WHPA-C and WHPA-D for FDF0-03 are the result of a small number of pathlines that travel long distances through the bedrock aquifer with relatively high velocity owing to the high hydraulic conductivity and low porosity.

Finally, Figure 6.6 shows the 25-year capture zone determined in the Earthfx (2010) study compared to that for the current study. Given the changes in the model construction and supporting hydrostratigraphic model, the distribution of recharge, and changes in the pumping rates, the two results are very similar. This indicates that both models were able to replicate the critical features of the physical system that control the shape and extents of the capture zones.

6.1.3 WHPA-E and WHPA-F Delineations

Under Technical Rule 49 (1), all wells that are identified as groundwater under the direct influence of surface water (GUDI) are required to have additional wellhead protection areas delineated, known as the WHPA-E and WHPA-F. The Freelton municipal wells are both classified as non-GUDI (Dillon, 2008; Wood, 2018b) and hence the WHPA-E and WHPA-F were not necessary.

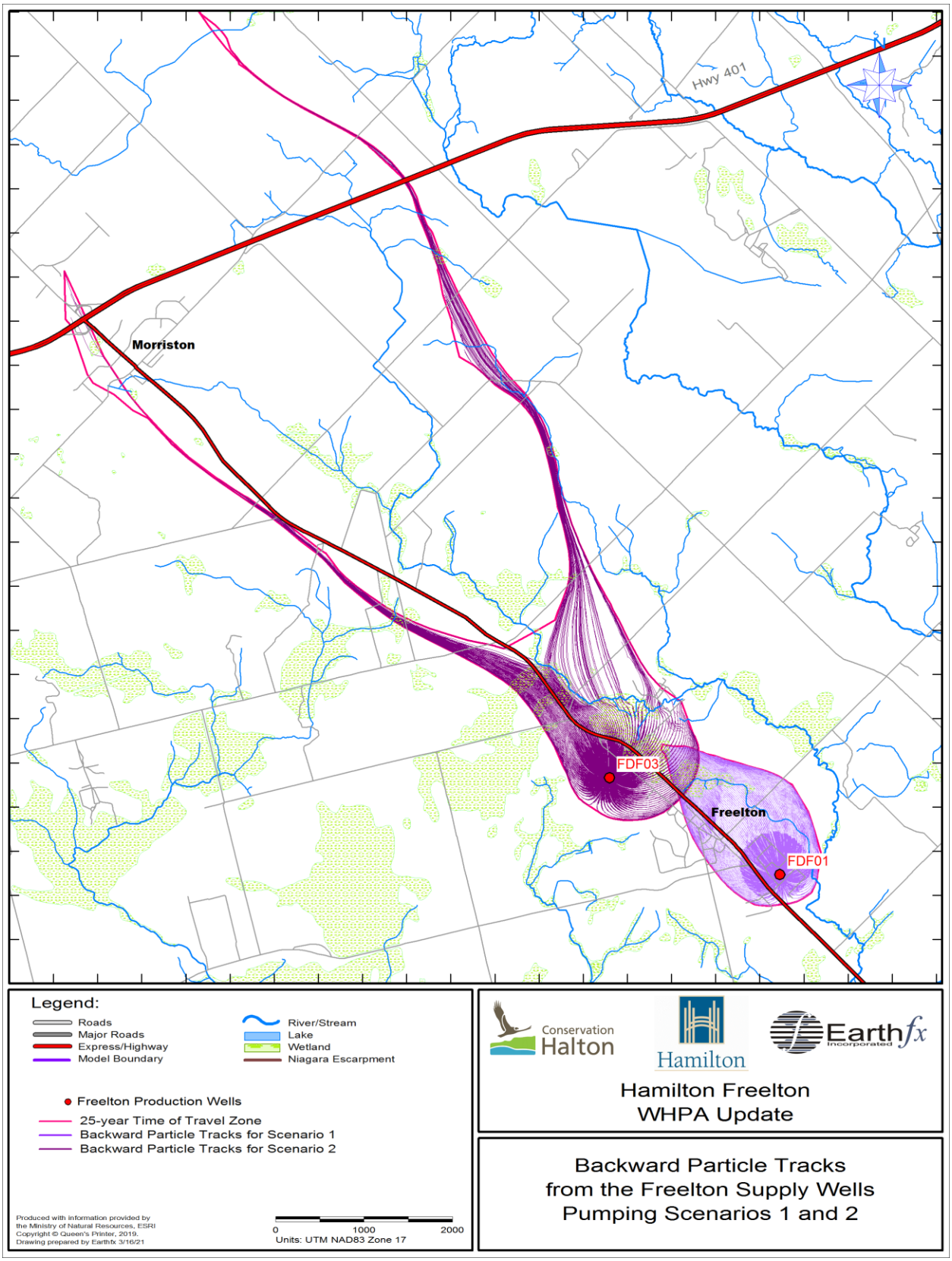

Figure 6.3: Backward particle tracks from Freelton supply wells under Scenarios 1 and 2 and the composite 25-year Time of Travel zone.

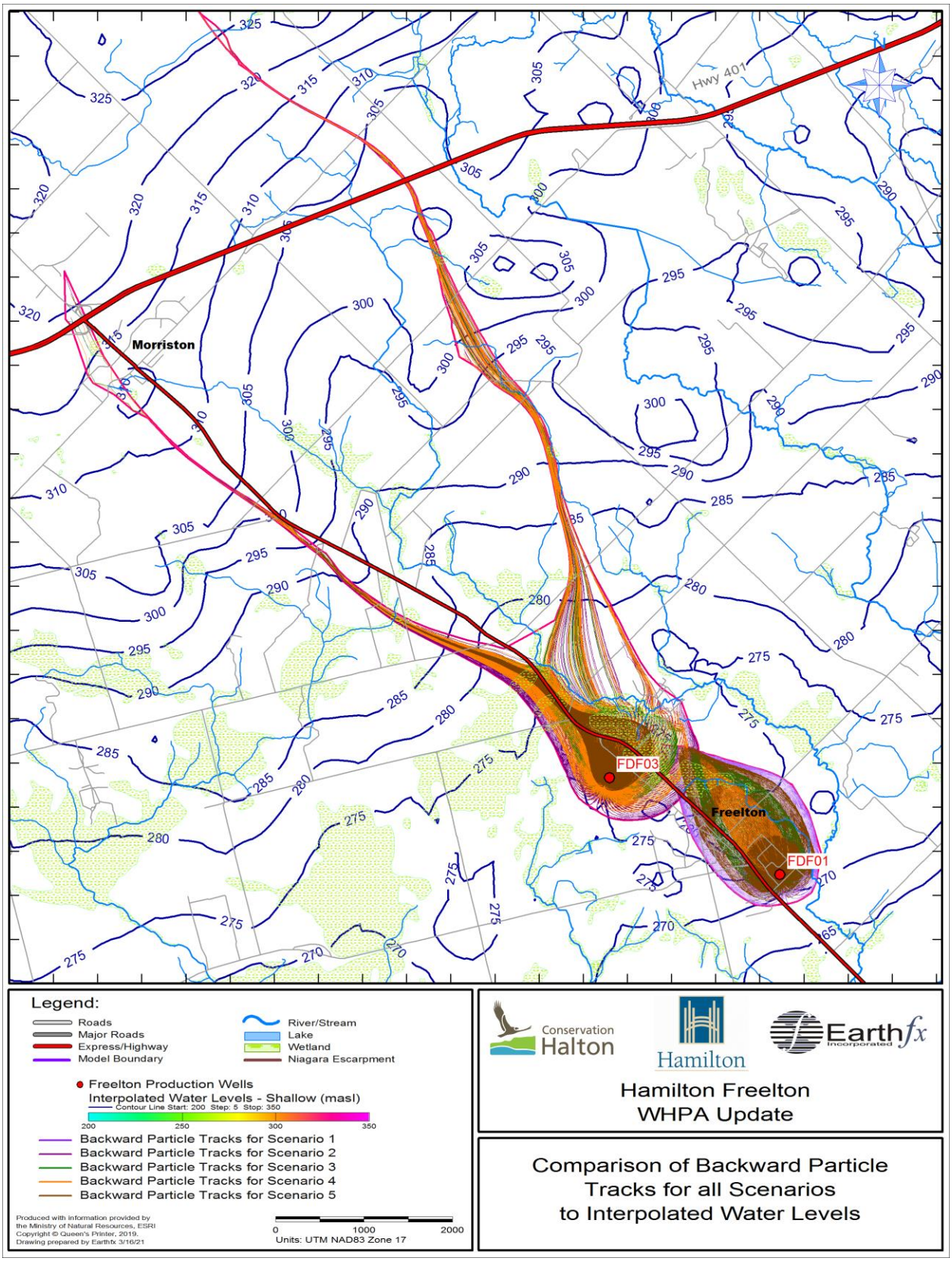

Figure 6.4: Comparison of backward particle tracks for all scenarios to interpolated water levels.

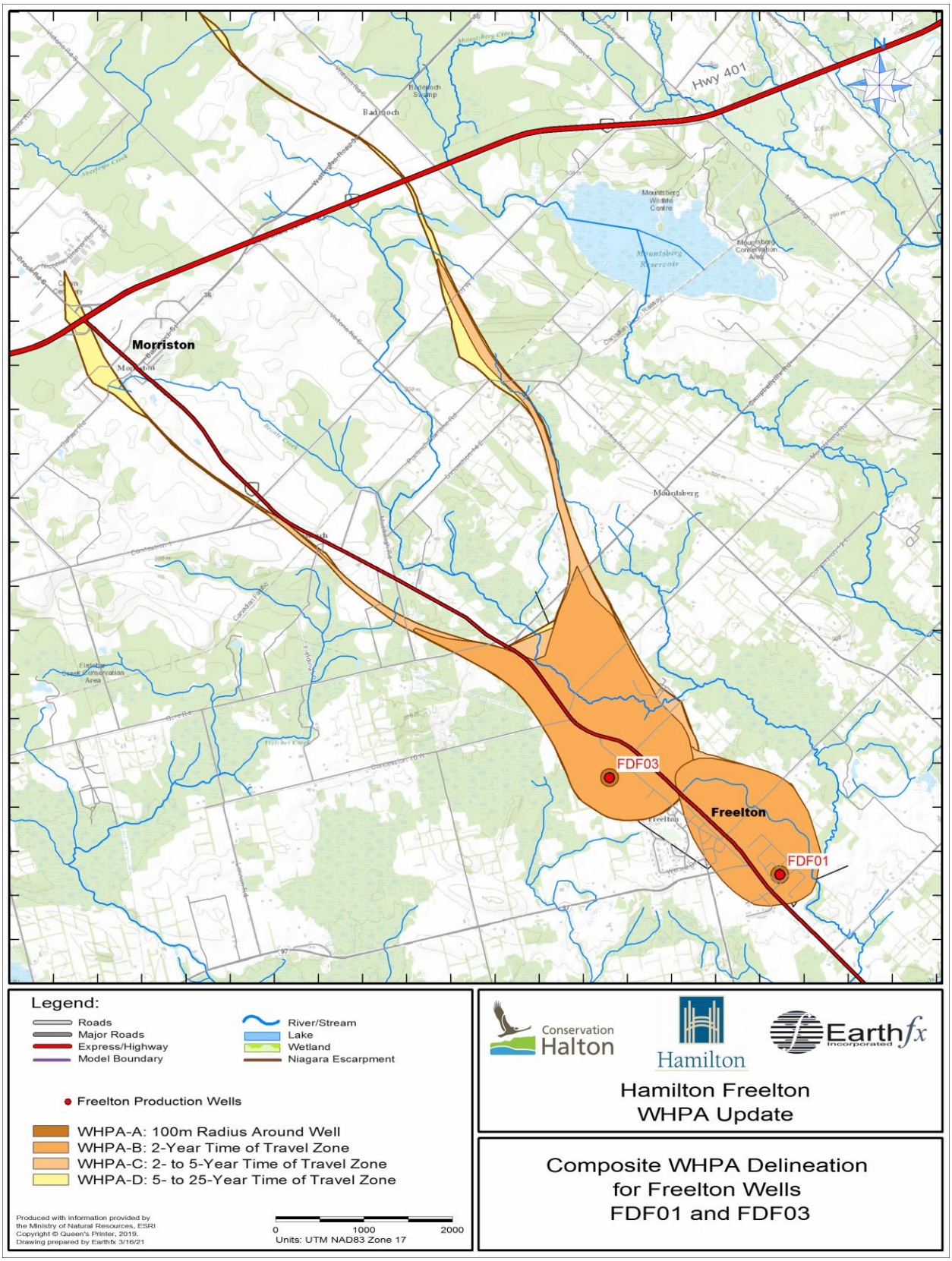

Figure 6.5: Composite WHPA delineation for Freelton Well FDF01 and FDF03.

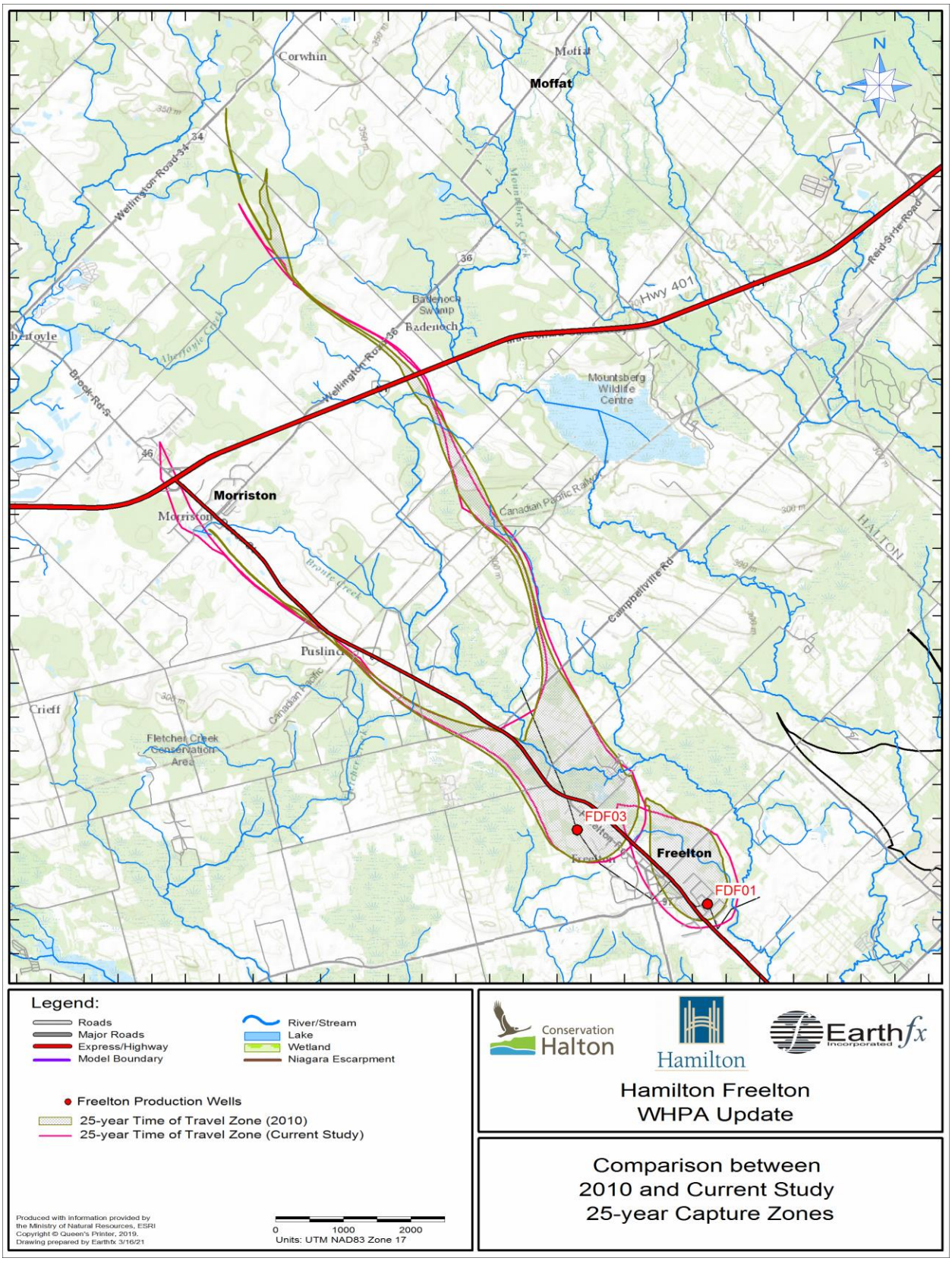

Figure 6.6: Comparison between the 25-year time-of-travel zone from Earthfx (2010) and that for the current study.

6.2 *High, Medium, and Low Vulnerability Zones*

6.2.1 Vulnerability Assessment Methodology

According to the Technical Rules (MECP, 2017) for Assessment Reports, aquifer vulnerability within the WHPA-A to WHPA-D zones must be assessed by one or more of the following groundwater vulnerability assessment methods (Rule 37):

1. intrinsic susceptibility index (ISI);
2. aquifer vulnerability index (AVI);
3. surface to aquifer advection time (SAAT); or
4. surface to well advection time (SWAT).

The surface to well advective time (SWAT) method was used in this study to delineate low, medium, and high vulnerability zones. From a technical perspective, a time-based method is preferred because the units of vulnerability are then the same as for the TOT estimates.

Part IV of the Technical Rules for Assessment Reports defines areas of high, medium, and low groundwater vulnerability for each of the assessment methods. For the surface to well advection time (SWAT) method, the classification is based on travel times from the surface to the well as:

a. areas of high vulnerability are those with travel times to a well less than 5 years;
b. areas of medium vulnerability are those with travel times greater than or equal to 5 years but less than or equal to 25 years; and
c. areas of low vulnerability are those areas with travel times greater than 25 years.

Surface to well advective travel time (SWAT) consists of two components: (1) the vertical travel time through the unsaturated zone above the water table (UZAT); and (2) the travel time from the water table to the well through the saturated zone (WWAT) as shown schematically in Figure 6.7. These components are discussed in the next two sections.

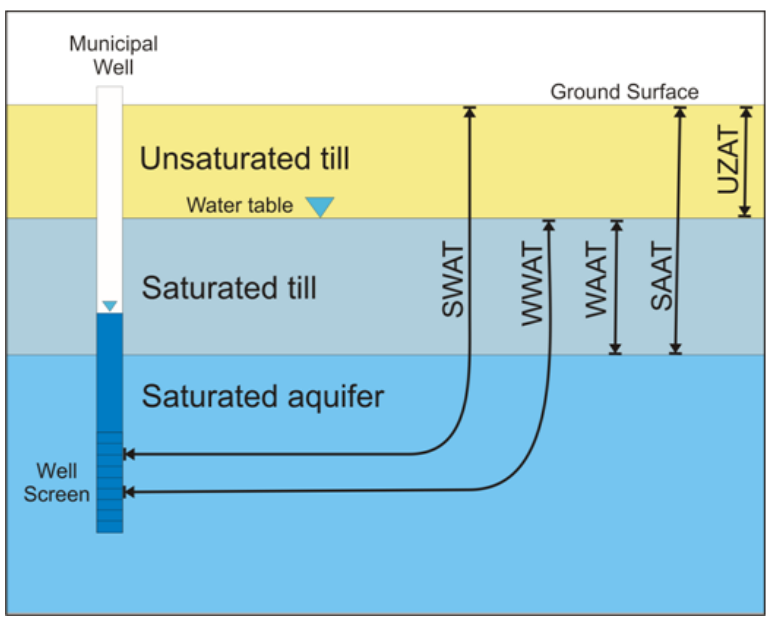

Figure 6.7: Schematic section showing definitions of time-of-travel terms for SWAT analysis.

6.2.1 Unsaturated Zone Advective Times

Estimating the time of travel through the unsaturated zone is highly complex and depends on the unsaturated hydraulic conductivity of the soil, soil moisture, and pressure-head gradients in the unsaturated zone. Unsaturated hydraulic conductivity and pressure-head can be related to moisture content through characteristic curves developed for each soil type. Unfortunately, data on unsaturated soil properties are generally unavailable, so as an alternative, the guidance modules supporting the Technical Rules suggest a simplified method. This method assumes that the annual rate of groundwater recharge is a good approximation for the average flux of moisture through the unsaturated zone and can be used to approximate the advective contaminant travel times through the unsaturated zone. The estimate is given by:

$$UZAT = \frac{d_{wt} \cdot \theta_m}{q_z}$$

where UZAT is the time of travel through the unsaturated zone, d_{wt} is the depth to the water table, θ_m is the "mobile moisture content", and q_z is the infiltration rate (equivalent to the groundwater recharge rate, as defined in this study).

Depth to water table, d_{wt}, at all points in the study area was computed by subtracting the simulated water-table surface from land-surface elevation (Figure 3.1). The values were checked against the depth to water obtained by subtracting the interpolated shallow water levels (Figure 5.17) and found to be reasonably similar. Negative depth-to-water values, indicating heads above land surface, were set to zero so that there would no negative UZAT values.

The mobile moisture content, θ_m, represents the pore space through which gravity drainage occurs under steady-state drainage at the infiltration rate. The average moisture content of the soil under this condition should lie somewhere between field capacity (f_c) and porosity (n) for the particular soil. Flow will not readily occur through the bound water, which is measured by the wilting point for the soil. For this study, we assumed that the average moisture content was equal to the midpoint full saturation (porosity) and field capacity (fc) and that the mobile moisture content was equal to this value minus the wilting point. Porosity values, field capacity, and wilting point were assigned through lookup tables for all soil classes as part of the PRMS model parameterization. Estimated values for mobile moisture content ranged mostly from 0.03 to 0.18

It was assumed for this study that infiltration rate, q_z, was equal to the recharge rate (i.e., the infiltration rate after taking losses to ET and interflow). Recharge rates were determined from the PRMS results for long term simulations and converted to metres per year.

Final UZAT values were determined on a cell-by-cell basis. High recharge values and small depth to water result in very short, near zero, UZAT values. On the other hand, very low recharge rates create larger UZAT values. Figure 6.9 shows the calculated UZAT values in the Freelton area which ranged from 0 to over 35 years. Values above 25 years represent areas of low risk. Final vulnerability scores depend on the combined UZAT and WAAT scores.

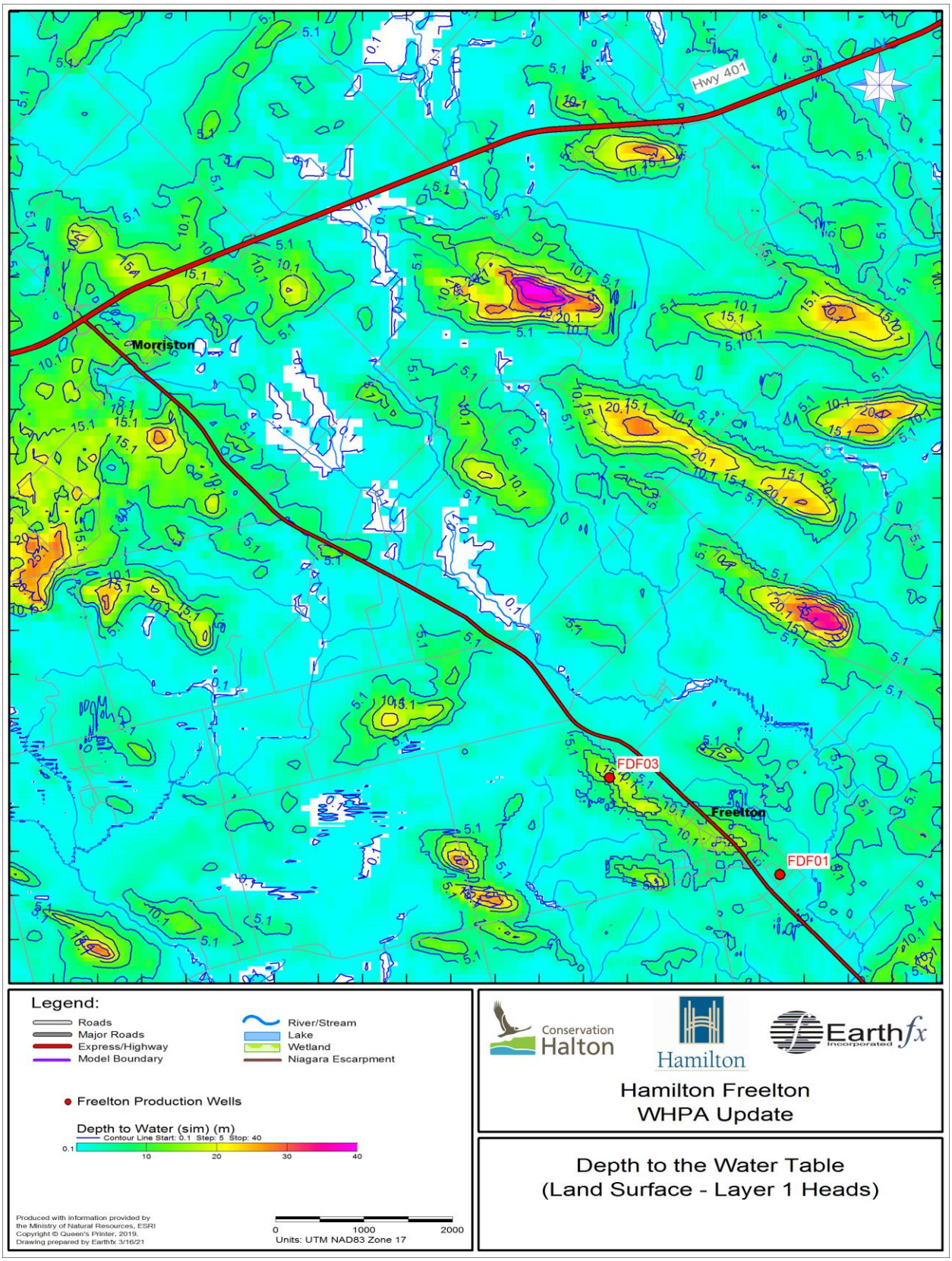

Figure 6.8: Depth to the water table, based on subtracting the simulated heads in Layer 1 from land surface topography.

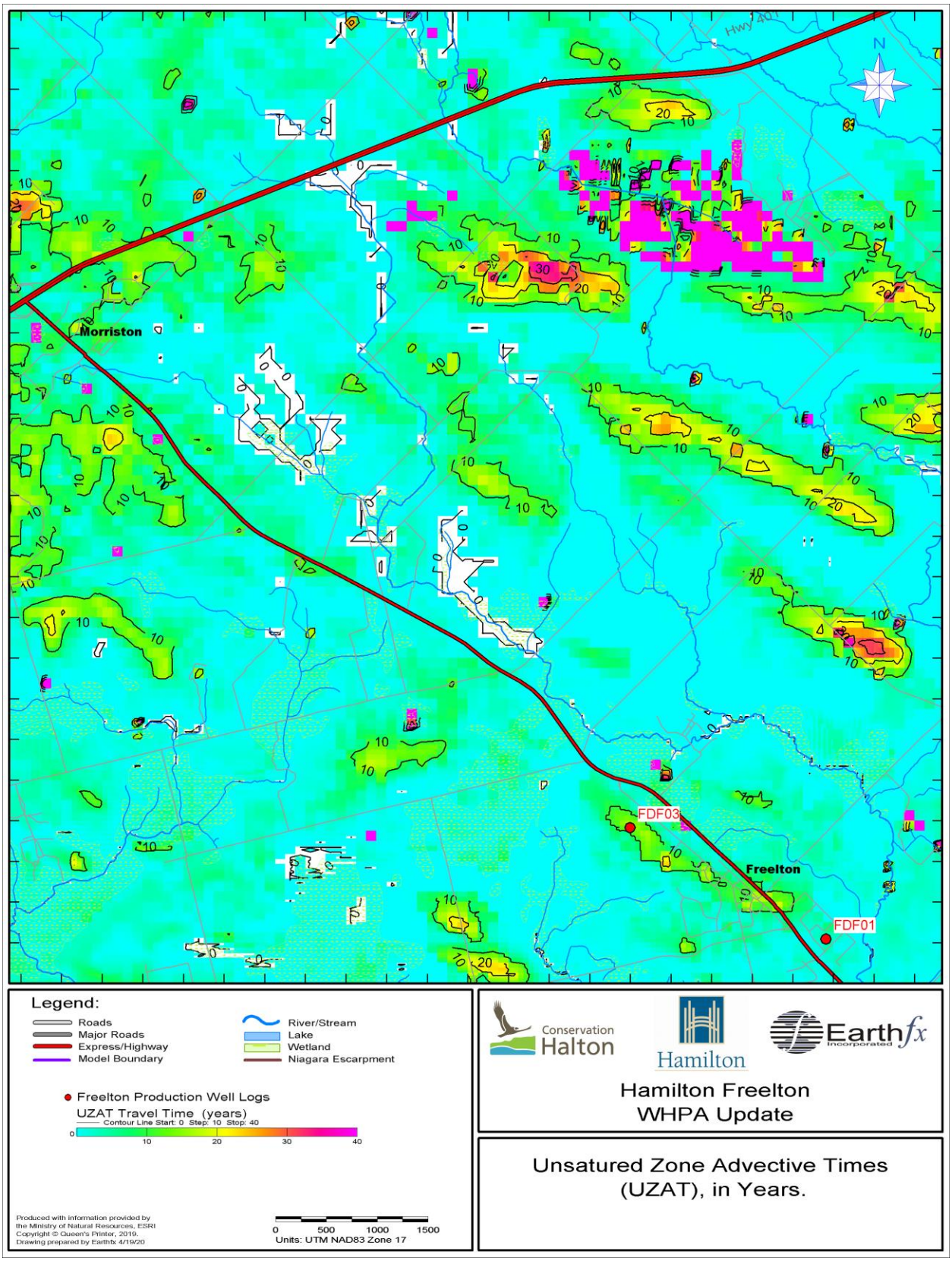

Figure 6.9: Unsaturated zone advective times (UZAT), in years, in the Freelton area.

6.2.1 Water Table to Well Advective Times

WWAT values were determined by releasing four virtual particles from each cell in the uppermost active groundwater model layer (i.e., the layer containing the water table) within a larger area surrounding the 25-year time-of-travel zones. The particles were forward-tracked from the water table, using MODPATH, to their point of discharge, corresponding to either the municipal well or another discharge point, such as a nearby stream. The forward particle tracking was completed for all pumping configurations.

As an example, Figure 6.10 shows the forward pathlines of particles released under pumping Scenario 4. The figure shows particle tracks ending up in the supply wells. The travel times for these particles were assigned back to the originating cell. It should be noted that most particles did not reach the well and ended up in nearby wetlands and streams. This result is not surprising and reflects the subtle conceptual differences between forward and reverse particle tracking, particularly for confined or semi-confined systems like the one present in Freelton.

Figure 6.11 shows the composite WWAT values, in years, for particles reaching FDF01 or FDF03 for all scenarios. Because multiple particles were released from each cell for each scenario, the TOT was selected based on the minimum travel time from each cell, again resulting in a more conservative outcome. WWAT values ranged from less than 1 year o greater than 25 years. Blank areas within the 25-year TOT zones indicate that the particles did not reach the municipal wells but discharged elsewhere. These areas were ultimately treated the same as areas in which particles took longer than 25 years to reach the well. It should be recognized that the advective travel times were calculated without consideration of the nature of the potential contaminants, release mechanisms, and attenuation processes (e.g., diffusion, dispersion, adsorption, and chemical transformation).

6.2.2 High, Medium, and Low Vulnerability Zone Delineation

UZAT values (in years) were added to the WWAT values (also in years) for the Freelton supply wells to determine the composite total surface to well advective travel times (SWAT). These are shown in Figure 6.12. Large areas within the 25-year capture zone for FDF03 remain at zero because surface recharge in these areas does not reach the supply wells.

Maps of High, Medium and Low groundwater vulnerability were developed for the Freelton supply wells based on the SWAT values and thresholds of 0 to 5 years (high), 5 to 25 years (medium), and greater than 25 years (low), as outlined in the Technical Rules. The vulnerability index mapping is shown in Figure 6.13. Areas that do not contribute to the wells were assigned the lowest possible score, equivalent to that of a SWAT value greater than 25 years.

6.3 *Preferential Pathways Analysis*

6.3.1 Transport Pathways

Adjustments to the vulnerability levels were undertaken to account for the presence of transport pathways (i.e., constructed preferential pathways) that may bypass the natural protective geologic layers. Preferential pathways can include improperly constructed or decommissioned wells, pits and quarries, ditches, and pipeline bedding for storm and sanitary sewers. According to Technical Rule 39, the vulnerability of an area identified as low vulnerability can be increased from low to medium or medium to high vulnerability due to the presence of a transport pathway that is anthropogenic in origin (Rule 40).

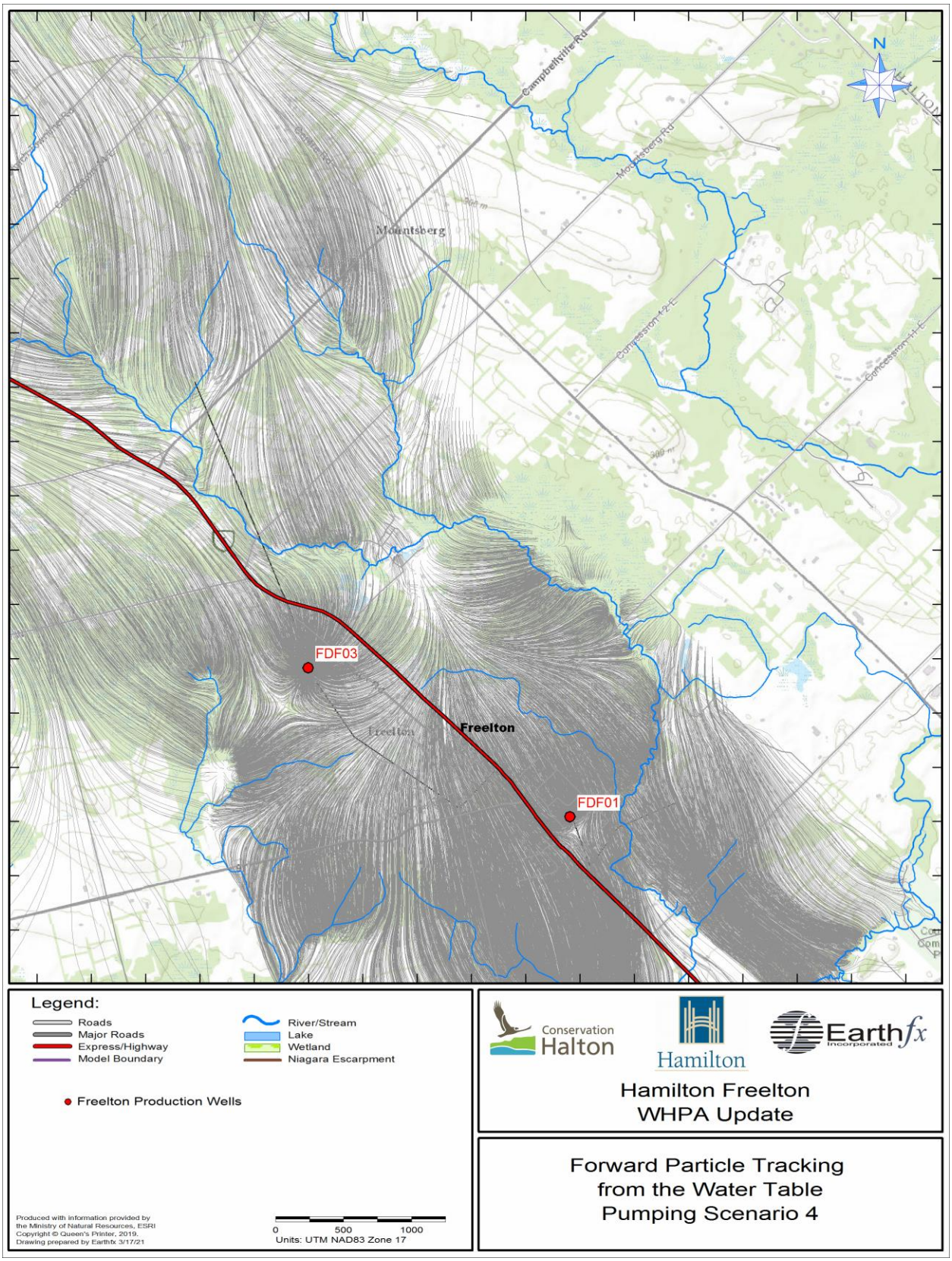

Figure 6.10: Forward particle tracking from the water table for pumping Scenario 4.

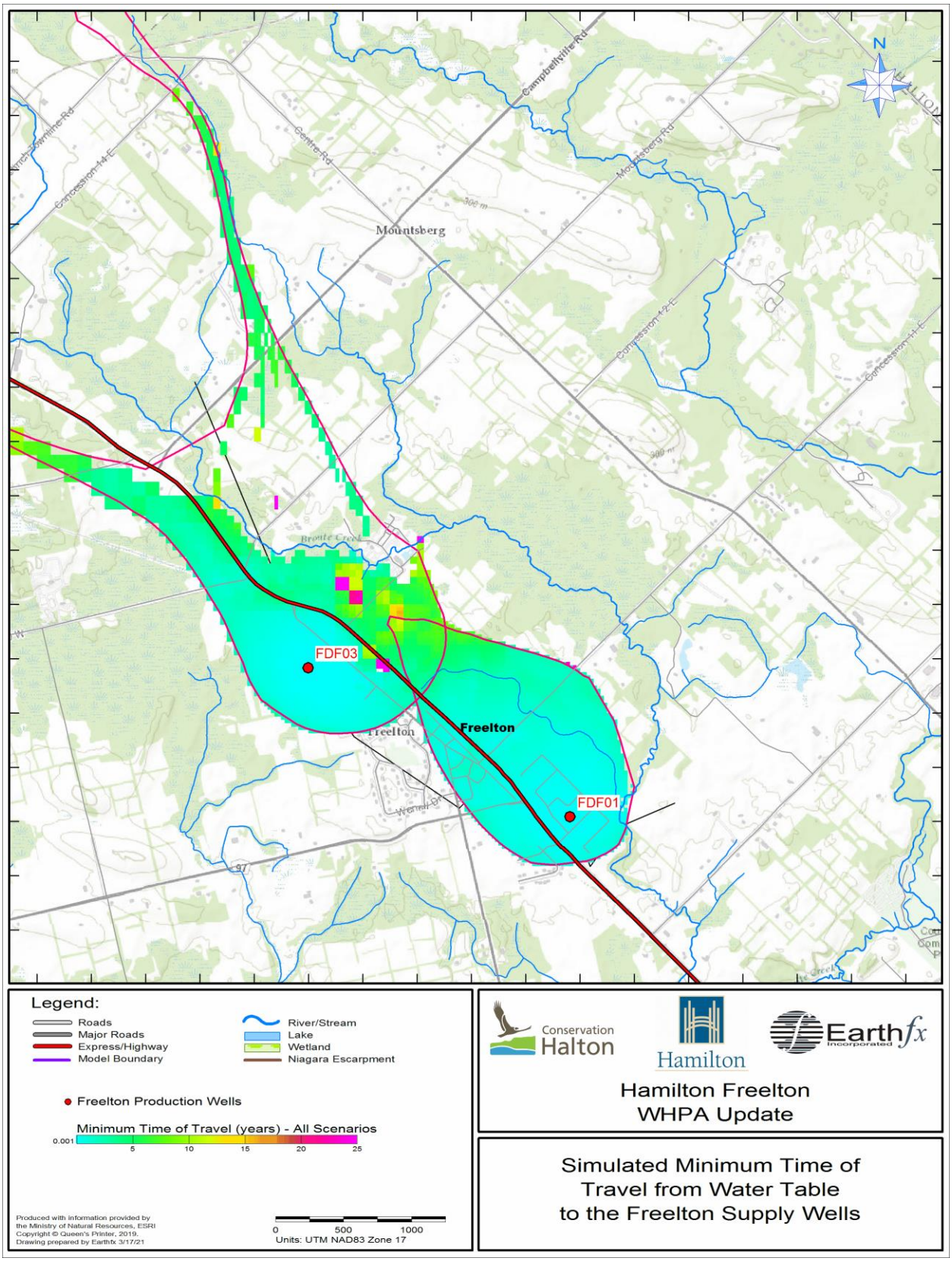

Figure 6.11: Simulated minimum time of travel from the water table to the Freelton supply wells (WWAT), in years, for all scenarios.

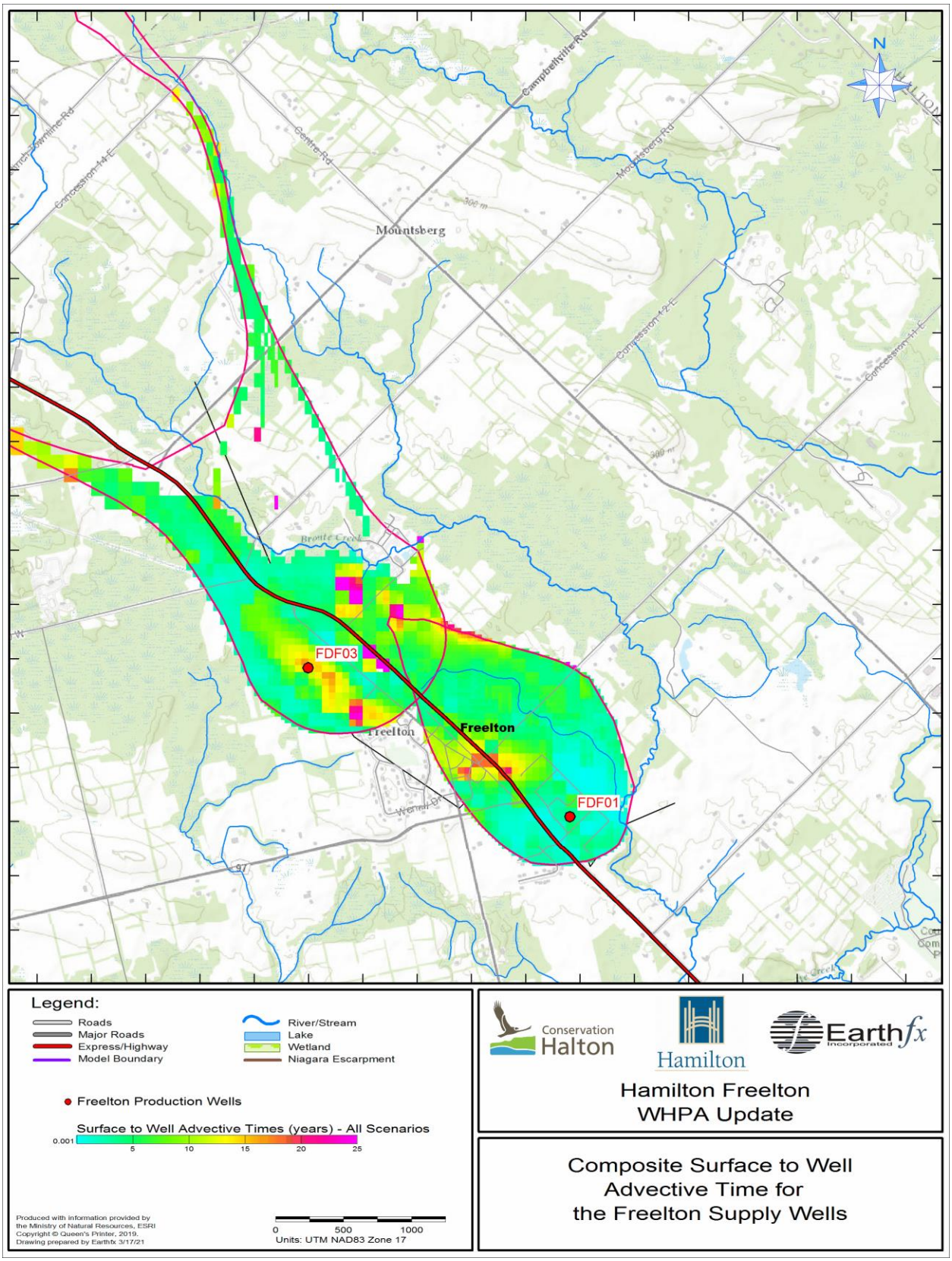

Figure 6.12: Composite time of travel from the surface to the Freelton supply wells (SWAT), in years, for all scenarios.

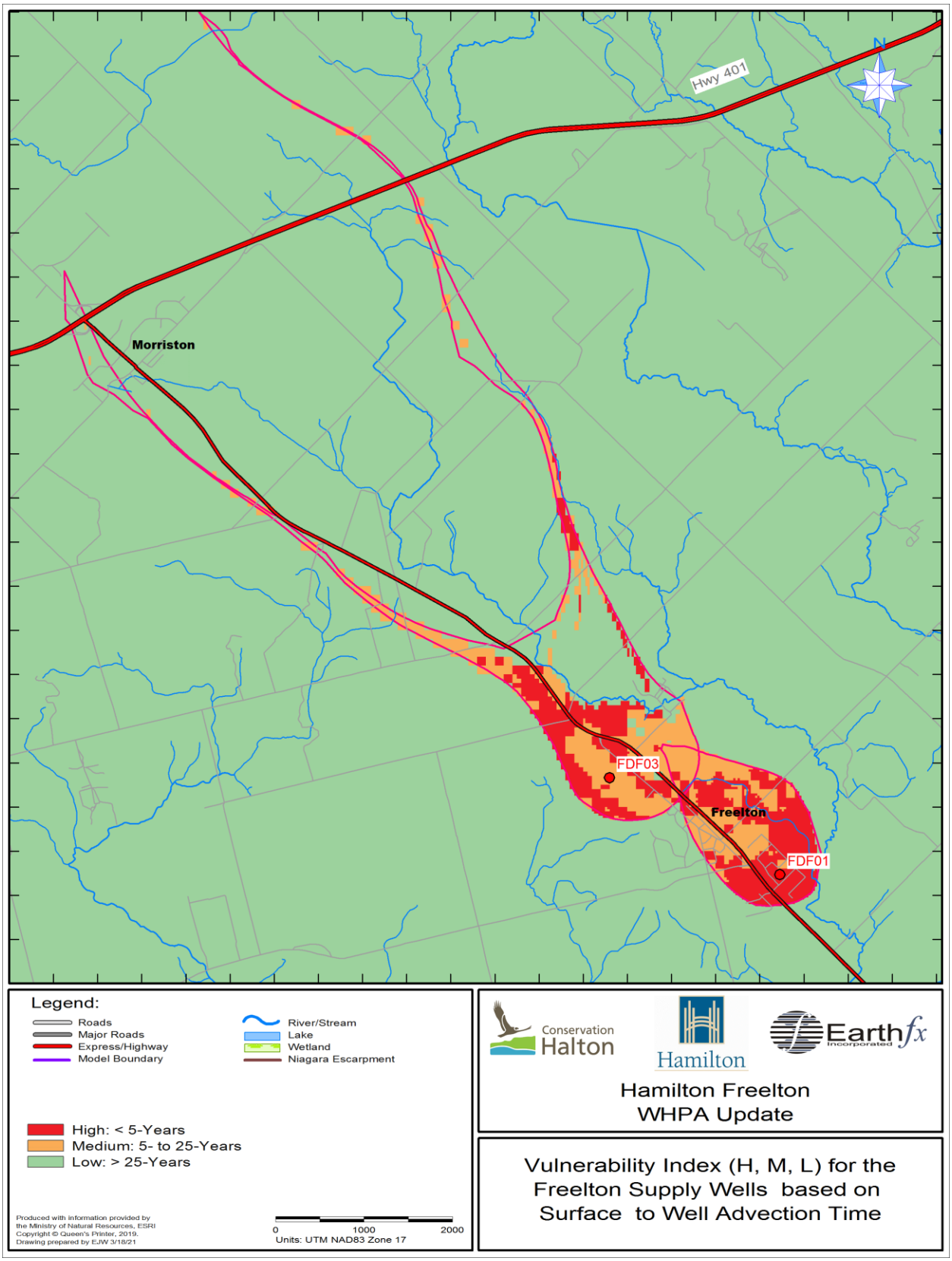

Figure 6.13: Vulnerability Index (H, M, L) for the Freelton supply wells based on surface to well advection time (SWAT).

The assessment of increased vulnerability considers:

a. hydrogeological conditions;
b. the type and design of the transport pathways;
c. the cumulative impact of the transport pathways; and
d. assumptions used in the assessment of groundwater vulnerability.

Unsaturated zone travel times (UZAT) were calculated using relatively conservative assumptions. Therefore, constructed pathways that could possibly reduce unsaturated zone travel times, such as pipeline bedding and excavations above the water table, would not likely increase the vulnerability scores already assigned. Accordingly, areas with land use classified as urban or transportation were considered for increasing the vulnerability index.

An additional area of focus was on identifying those constructed pathways that could reduce travel times in the saturated zone. These included:

- wells that may leak or have been improperly abandoned;
- pits and quarries that breech the upper confining unit;
- lakes in connection with the municipal aquifer system
- landfills located in former pits or quarries that may breach the upper confining unit; or
- other deep excavations.

Of these possible pathways, only the abandoned wells required further investigation.

6.3.2 Private Water Wells

Discharge of contaminants to improperly constructed or decommissioned wells could provide a pathway to deeper zones within the unconfined aquifers or to the underlying confined aquifers. The risk posed by water wells in the area was assessed using the MECP WWIS database.

The potential for a water well to impact the Freelton supply wells was determined based on two main considerations: (1) whether the well is connected to the production aquifer, and (2) the interpreted condition and quality of the well construction, with respect to preventing contaminants from reaching the aquifer. To evaluate the potential connection between a well and the municipal aquifer, the screened interval listed for each well record was reviewed. Any well that was reported to penetrate bedrock was considered to represent a potential connection to the supply aquifer.

Ontario Regulation 903 (Wells) under the Ontario Water Resources Act was enacted in 1990 and set minimum standards for the construction and proper decommissioning of all types of wells. Wells installed after 1990 were assumed to be of higher quality construction and, therefore, less likely to have failures of the casing or annular seals. On the other hand, dug wells and wells that were constructed prior to the introduction of pitless adaptors (in the early 1980s) were considered to represent higher risk locations for the introduction of contaminants; these wells are categorized as being of poor construction. Wells that fall between the construction dates of 1980 and 1990 are considered to be of moderate construction quality. Wells were assigned a risk level of high, medium, or low according to the framework presented in Table 6.2.

Table 6.2: Framework for risk level assignments to other wells.

	Poor Construction	Moderate Construction	Proper Construction
No Connection to Aquifer	Low	Low	Low
Likely Connection to Aquifer	High	Medium	Medium

A total of 137 wells were identified within the delineated WHPA-A through WHPA-D areas for the Freelton water supply wells (Figure 6.14) including some in nearby Morristown and Puslinch. Wells with poor location quality flags were not considered. The numbers of wells with low, medium, and high-risk ratings are summarized below in Table 6.3. There were 103 wells in the capture zone constructed before 1980 and an additional 2 with no construction date. These were considered higher risk wells that likely do not meet the current MECP well standards and are expected to be in connection with the aquifer used for municipal supply.

Table 6.3: Number of wells assigned to each risk level within the WHPA zones.

	Risk Levels		
	High	**Medium**	**Low**
WHPA-A	0	0	0
WHPA-B	70	33	10
WHPA-C	6	3	2
WHPA-D	2	1	10
Totals	78	37	22

6.3.3 Adjustment of Vulnerability Zone Ratings

In previous studies, the vulnerability index within a 30 m radius of each of the wells was adjusted based on the risk level assigned to each well. While this has been an accepted conservative approach, it becomes difficult to manage these areas from a source protection standpoint, particularly when there are a large number of wells. In addition, the medium and high-risk wells are generally older and their location accuracy tends to be inconsistent. Visual inspection showed that the older wells fell within areas having urban or transportation land use classes. Given the concerns regarding excavations and pipeline and sewer bedding in the urban areas and along roadways, cells scored as low vulnerability within these areas were increased to medium and cells scored as medium vulnerability within these areas were increased to high. The vulnerability indexes adjusted for transport pathways are shown in Figure 6.15.

It should be noted that the City of Hamilton has partnered with local Conservation Authorities to subsidize the cost for homeowners to decommission abandoned wells. This program should be continued and possibly expanded to help remove or recondition older private wells in the wellfield area.

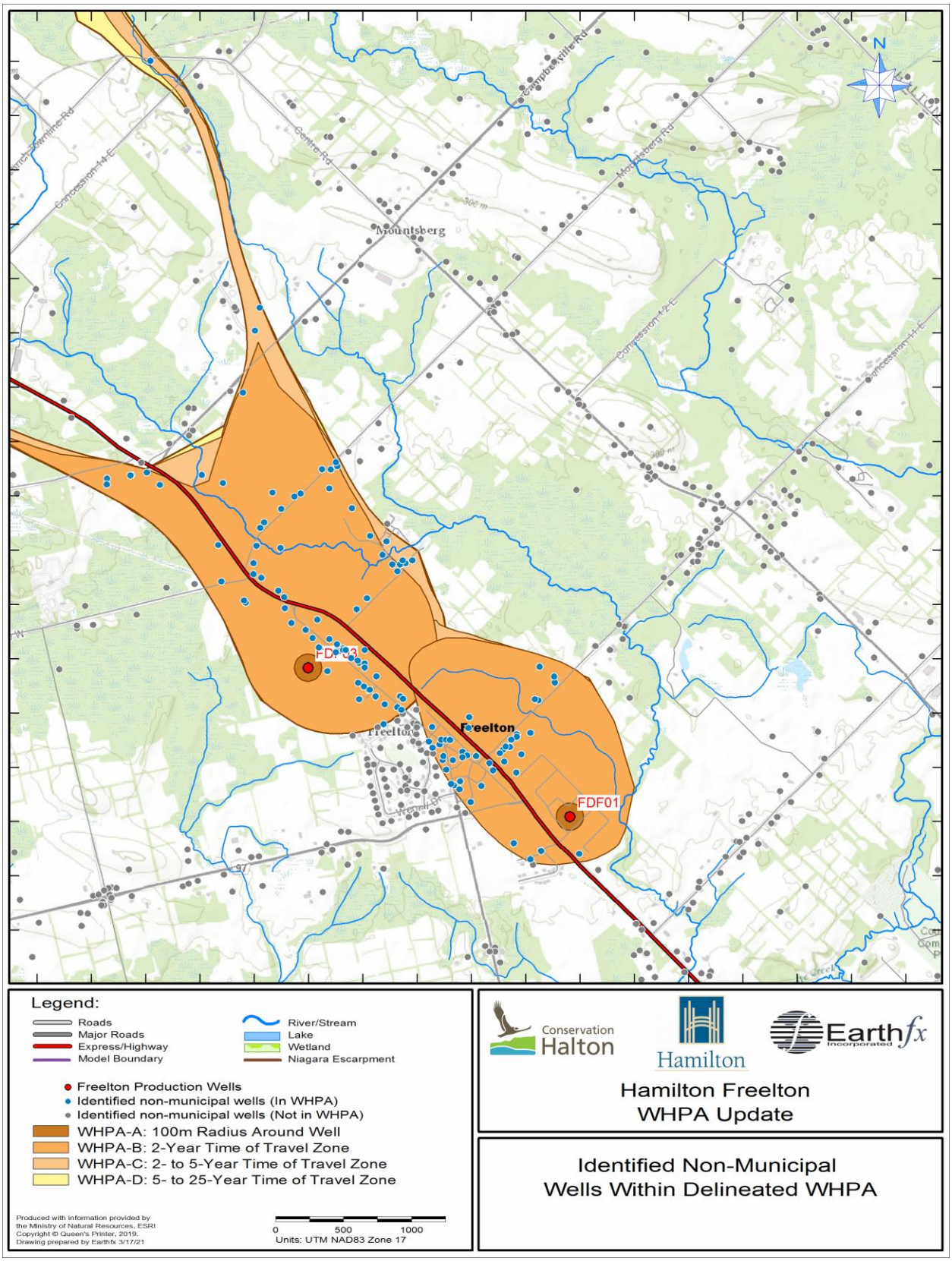

Figure 6.14: Identified non-municipal wells within the Freelton WHPAs.

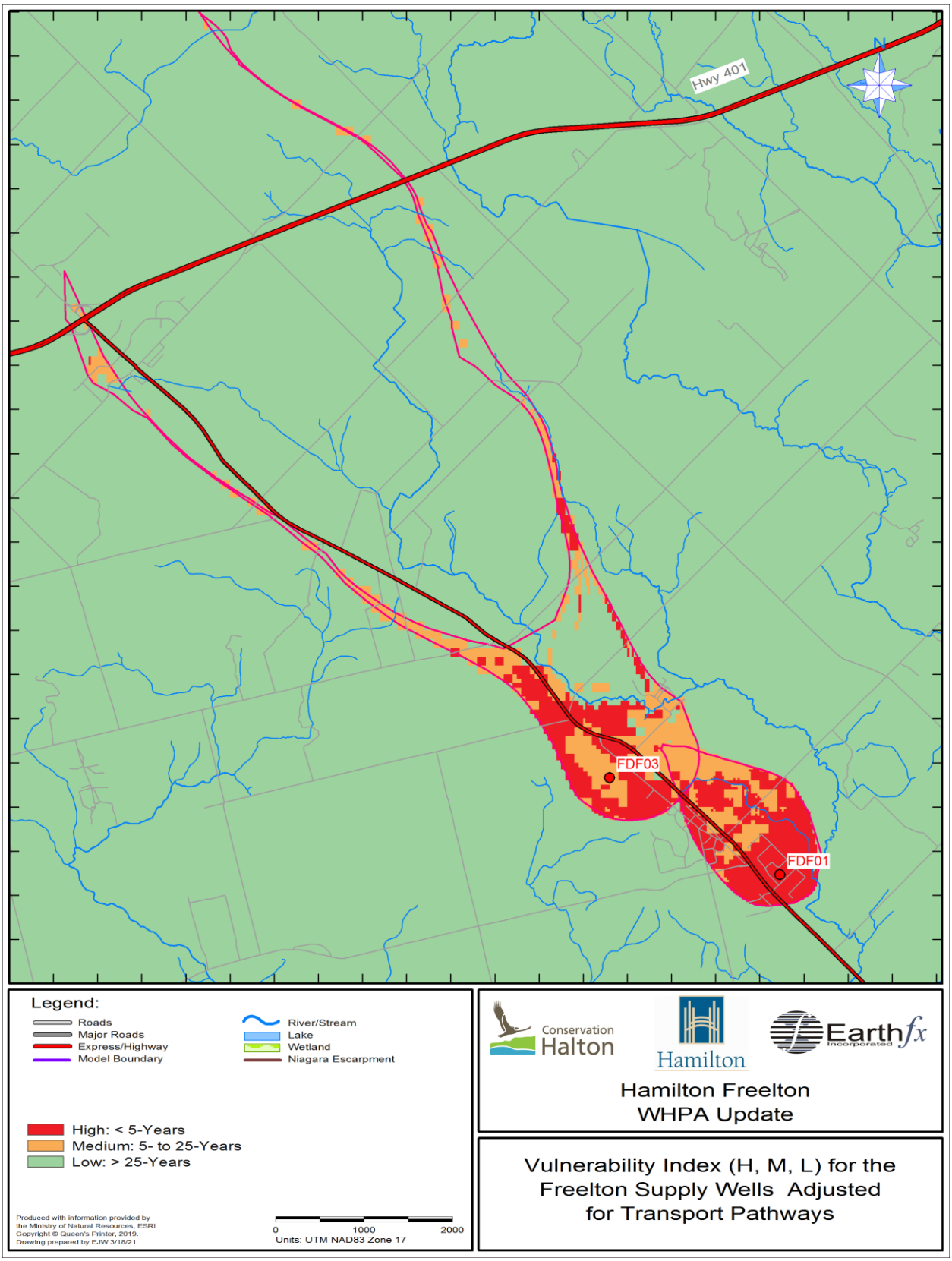

Figure 6.15: Vulnerability Index (H, M, L) for the Freelton supply wells after adjusting for potential transport pathways.

6.4 *Vulnerability Scores*

Vulnerability scoring is a mapping exercise in which the WHPA outlines are intersected (overlain) on the vulnerability map showing the low, medium and high vulnerability zones. Each subzone created is assigned a value based on a numerical scoring system defined in the Technical Rules (MECP, 2017) and listed in Table 6.4. Vulnerability scores for the subzones within each WHPA can range from 2 (low vulnerability) to 10 (high vulnerability). The purpose is to identify subzones within the WHPAs that are more or less vulnerable to contamination from land surface.

Table 6.4: Vulnerability scoring matrix.

	Surface to Well Advective Time (SWAT)		
	High 0 to 5 years	Medium 5 to 25 years	Low > 25 years
WHPA A	10	10	10
WHPA-B	10	8	6
WHPA-C	8	6	2
WHPA-D	6	4	2

Composite vulnerability scores were calculated for the Freelton capture zones. Results showing vulnerability scores before adjusting for transport pathways are shown in Figure 6.16. Final results showing vulnerability scores after adjusting for transport pathways are shown in Figure 6.17.

The vulnerability score distribution is indicative of the complex hydrostratigraphy and spatially variable connection between the water table and the municipal supply wells. The most vulnerable areas correspond to the WHPA-A and WHPA-B. The vulnerability tends to be lower in the extended areas upgradient of FDF03 because the WWAT tends to be long and thin due to vertical confinement. In general, vulnerability tends to decrease with increasing distance away from the supply wells, in the direction of flow.

These analyses are a first, but very important, step in conducting a risk-based assessment of potential threats to the municipal supply wells from past, current, or future land-use activities. Further steps include listing of drinking water quality issues, listing of drinking water quality threats (both activities and conditions) and then identifying areas of low, moderate, and significant drinking water threats within the WHPAs as per Part XI of the Technical Rules (MECP, 2017). The identification of drinking water threats within the WHPAs was not within the scope of this study.

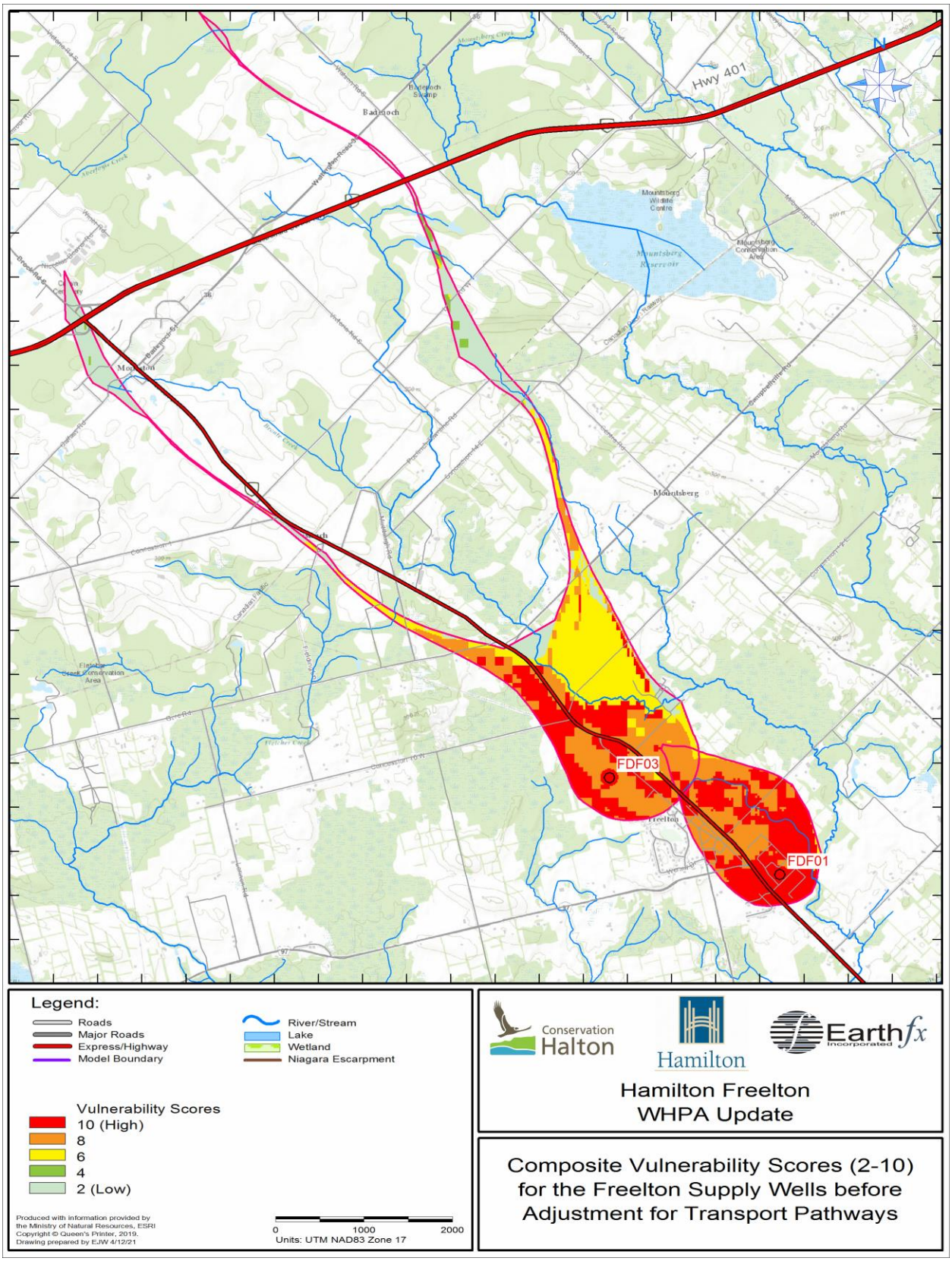

Figure 6.16: Composite vulnerability scores (2 – 10) for the Freelton supply wells before adjustment for transport pathways.

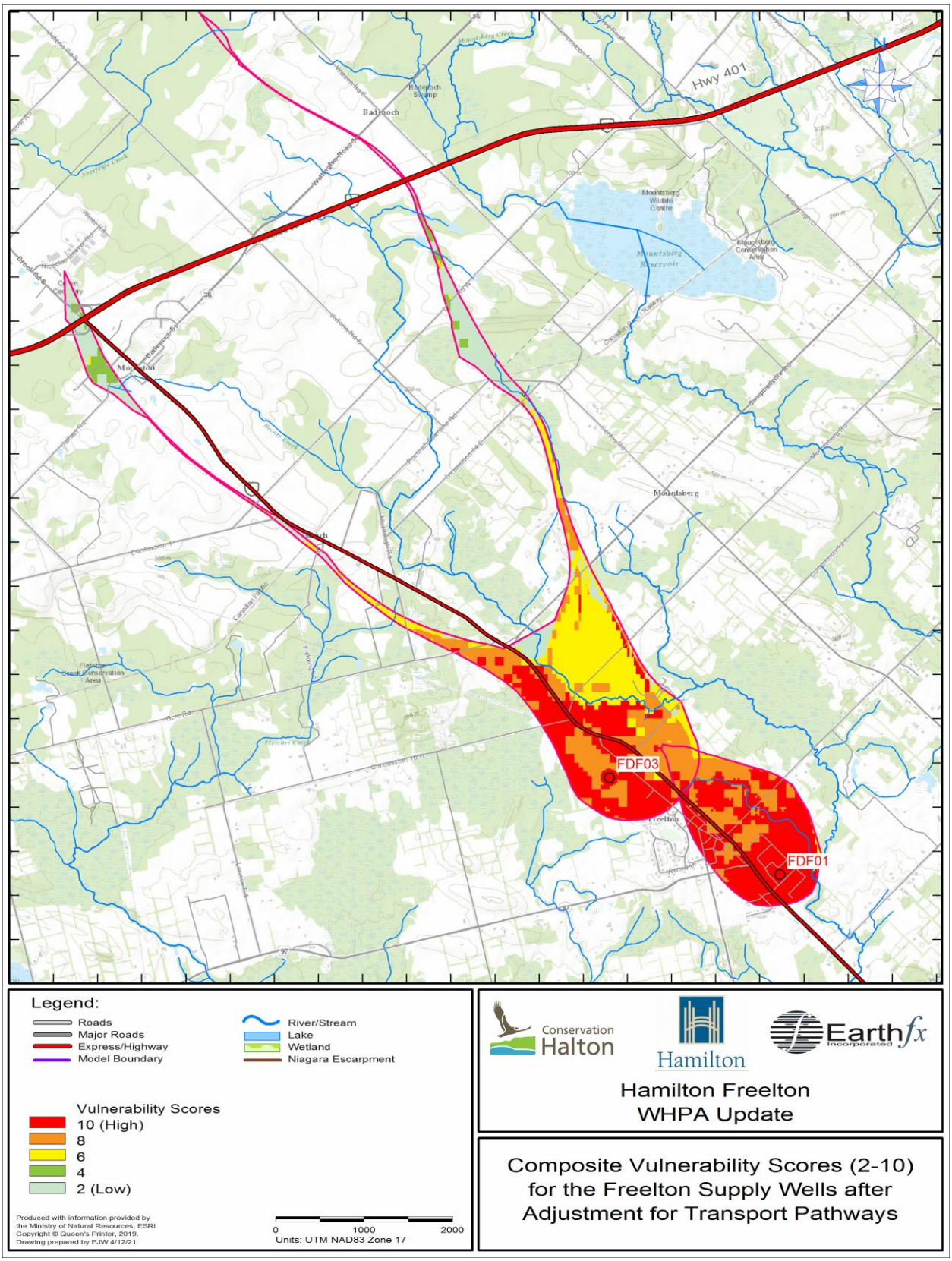

Figure 6.17: Final composite vulnerability scores (2 – 10) for the Freelton supply wells after adjustment for transport pathways.

6.5 *Uncertainty Assessment*

6.5.1 Overview

There is a degree of uncertainty associated with the TOT, SWAT, and vulnerability scoring analyses; however, it is difficult to provide a quantitative assessment of the level of uncertainty. The Technical Rules specify that the following factors should be considered in an uncertainty analysis for WHPA delineation and vulnerability assessments (Rule 14):

1. the distribution, variability, quality and relevance of data used in the preparation of the assessment report;
2. the ability of the methods and models used to accurately reflect the flow processes in the hydrological system;
3. the quality assurance and quality control procedures applied;
4. the extent and level of calibration and validation achieved for models used or calculations or general assessments completed; and
5. the accuracy to which the groundwater vulnerability categories effectively assess the relative vulnerability of the underlying hydrogeological features. (Item 5 applies only to the vulnerability scoring.)

An uncertainty factor of “high” or “low” was assigned to each vulnerable area delineated based on the results of the uncertainty analysis (as required by Rule 15). The uncertainty is smaller in the vicinity of the wells but higher in the extended areas away from FDF03. Overall, the analysis was considered to have a low uncertainty given the significant amount of work that went into the analysis, the repeatability of model results over several iterations of model development. This finding does not discount the unknowns associated with quantifying the local and regional-scale hydrogeology. Results of the uncertainty analysis are discussed below and final uncertainty factors for the WHPA delineation and vulnerability scoring are provided in Table 6.5 and Table 6.6, respectively.

Table 6.5: Summary of uncertainty analysis for WHPA delineation.

Uncertainty Element	Uncertainty
Distribution, variability, quality and relevance of data	Low
Ability of the methods and models used to accurately reflect the flow processes in the hydrological system	Low
Quality assurance and quality control procedures applied.	Low
Extent and level of calibration and validation achieved for models used or calculations or general assessments completed.	Low
Overall	**Low**

Table 6.6: Summary of uncertainty analysis for vulnerability scoring.

Uncertainty Element	Uncertainty
Distribution, variability, quality and relevance of data	Low
Ability of the methods and models used to accurately reflect the flow processes in the hydrological system	High
Quality assurance and quality control procedures applied.	Low
Extent and level of calibration and validation achieved for models used or calculations or general assessments completed.	Low
Accuracy to which to which the groundwater vulnerability categories effectively assess the relative vulnerability of the underlying hydrogeological features	High
Overall	**High**

6.5.2 Uncertainty related to Data Distribution Variability, Quality, and Relevance

Appendix 6 of the MOE Guidance Module indicates that it would be reasonable to expect a low level of uncertainty in areas where data density is high, where hydrogeologic studies have been conducted, and where numerical models have been developed. While it must always be recognized that all hydrogeologic analyses have an intrinsic level of uncertainty as one can never have enough data to fully know how conditions vary locally in the subsurface, this study generally satisfies the above criteria. Specifically, this study built on the previously completed Earthfx (2010) North Hamilton model, which was calibrated to a high standard. Furthermore, this model made use of new data, including the Wood (2018a) PTTW application for FDF01, which included a pump test. Local refinements were also completed to increase confidence in the hydrogeologic properties.

The density of MECP WWIS dataset was reasonably high with a large number of boreholes in the wellfield vicinity. This provided a higher level of confidence in the regional patterns of interpolated static water levels. The uncertainty was reduced by screening the MECP dataset to eliminate data with poor location accuracy or erroneous measurements. It is worth noting, however, that the aforementioned study by Wood (2018a) introduced some uncertainty into the local water level patterns in the vicinity of FDF01. Their local water table interpretation differed from the regional interpolated surface based on MECP data. Wood (2018a) concluded that groundwater flows from the north or northeast toward FDF01, contrary to the regional flow direction, which trends from the northwest to the southeast. We chose to put more weight behind the groundwater flow patterns inferred from the WWIS dataset because they represents decades of data collection and thereby provide more insight into the long-term average conditions.

6.5.3 Groundwater Model Uncertainty

With all numerical modelling studies, there is inherent variation in the level of confidence, which includes the quality of the input data as well as the uncertainty in model output due to computational assumptions within the model. In particular, there will always be a level of uncertainty related to the continuity and thickness of the hydrostratigraphic units and with the variability of hydraulic properties within each unit. While the level of confidence in the accuracy of the geologic surfaces used create the hydrostratigraphic model layers in this study is high based on the extensive study done by Earthfx (2010), the uncertainty can never be removed completely and must be acknowledged.

Overall, while the numerical model produced regional matches to the observed water levels, the ability of the flow model to exactly reproduce local flow patterns is not as certain. Intrinsic errors in

the WWIS data used to map the water table and potentiometric surfaces imply that one can never know the true water levels and flow patterns to a high level of certainty. Quality assurance checks (e.g., comparing reported static water levels to the bottom elevation of the well) and statistical analyses (outlier detection) were applied to the data to filter out many of these suspicious data points and improve the reliability of the calibration data points. Overall a good calibration was achieved to observed heads. The good match of the backward particle tracks to the flow directions inferred from the observed heads indicates that the model was able to match the complex flow patterns in the area.

6.5.4 Recharge Model Uncertainty

Average groundwater recharge, a common source of uncertainty in groundwater models, was estimated independently by developing and calibrating a separate hydrologic model. The uncertainty and limitations of the PRMS model were discussed in Section 4.8. These included the absence of field measured values for groundwater recharge, limited ability to represent groundwater feedback using an uncoupled surface water model, and uncertainty in the input and calibration target data. The match to observed streamflows at gauges in the calibration and validation periods was good with Nash Sutcliffe Efficiencies (NSEs) ranging from 0.50 to 0.59 for daily values and 0.65 to 0.75 for monthly values. The simulated flow volumes matched observed volumes well.

We attempted to validate the recharge quantity by applying it to the groundwater model and comparing the simulated baseflow to the estimated average separated baseflow at multiple locations. The model update, however, only focused on the Bronte Creek at Carlisle subcatchment. Recharge outside of this sub-area was previously validated in Earthfx (2010). Based on the calibration results, the hydrologic model was considered suitable for creating a regional recharge estimate for use in simulating groundwater flow in the Freelton area. The PRMS model was calibrated to streamflow data, with the implicit assumption that if the model matches the observed streamflow, then the components of the water budget have been estimated in a reasonable manner. This assumption is difficult to validate because there may be multiple solutions that produce an acceptable match to streamflow. For this reason, the recharge estimates are considered to have lower uncertainty than the other flow components (e.g., actual ET).

6.5.5 Time of Travel Analysis Uncertainty

While the application of a calibrated numerical groundwater model to delineate the WHPAs is considered to be the most robust and precise of the options available for determining the time of travel to a well, sources of uncertainty are introduced from both the groundwater flow model and the time of travel analysis itself. Subtle variations in the flow directions near the wells are caused by local variation in aquitard or aquifer thickness, aquifer and aquitard hydraulic conductivity values, and/or recharge rates and can lead to significant changes in the flow paths of the particles.

The time of travel values scale linearly with the porosity of the formations and are highly sensitive to the values assumed. Porosity values are not used in the flow model and are, therefore, not part of the normal model calibration process (the uncertainties of which are discussed in the previous section). No specific measurements of porosity were available for this study, so values for the various formations were estimated based on literature values from similar areas (e.g., Freeze and Cherry, 1979, p. 37). Low-end values were used for the porosity, resulting in greater velocities and larger capture zones. This approach produces results that are considered to be conservative and reduces the uncertainty that the resulting WHPA sizes will be underestimated. Overall, the uncertainty was considered high due to the difficulty in accurately predicting formation porosity, particularly in fractured bedrock, and the high degree of uncertainty surrounding the continuity and uniformity of geologic units.

6.5.6 Vulnerability Mapping Uncertainty

Of the recommended methods listed in the Technical Rules for Assessment Reports (MECP, 2017), the WWAT component of the SWAT method is by far the most defensible. It is based on assessing travel times using locally-determined hydraulic properties that have been adjusted and refined through model calibration. The model that the WWAT analyses was based on was developed using widely-accepted hydrogeologic and hydraulic principles and has been calibrated to match the observed heads and, more importantly, the model was calibrated to best match the observed directions of flow by carefully representing factors that influence flow patterns such as local variations in aquifer properties, recharge rates, aquifer and aquitard thickness, and continuity of the geologic units. However, as indicated by the discussions above, it is difficult to quantitatively assess the certainty of the TOT zones in an unbiased way and it is even more difficult to assess uncertainty in the WWAT values within the TOT zones.

Time of travel through the unsaturated zone (UZAT) is another source of uncertainty. While the method for assessing UZAT is reasonable, the range in likely values is high. In other Source Protection studies, we assumed that the time of travel, especially for a contaminant spill event, can be rapid. In these studies, we based the vulnerability scoring just on the WWAT values. The use of SWAT zones to subdivide areas within the TOT zones adds another level of uncertainty because the SWAT results cannot be field-verified or easily tested.

Water well records from the MECP WWIS dataset were used to evaluate possible transport pathways that could reduce the time of travel of contaminants to the municipal wells. This exercise relied heavily upon the location and construction details (depth and date of completion) within the database. As introduced in the previous sections, there is an inherent level of uncertainty that is to be expected when using this dataset, including missing information or erroneous data on locations and physical details (e.g., screen setting depth). While there was uncertainty in the dataset, all the older, higher risk wells were located in the developed area which also had increased risk due to excavations, ditching, pipelines, and sewers. The risks and uncertainty could be reduced by continue support of programs to decommission older wells.

The overall uncertainty of the vulnerability scoring has been assessed and is considered to be high. While we consider the uncertainty to be low relative to other, less detailed, WHPA delineation studies, the intrinsic uncertainty associated with hydrogeologic and contaminant transport investigations remains high.

7 Summary

Earthfx Incorporated was retained to conduct a groundwater study to evaluate and update the wellhead protection areas (WHPAs), vulnerability scores for the Rural Settlement Area RSA of Freelton. Freelton obtains the majority of its drinking water from two city-owned production wells (FDF01, and FDF03) both screened in a dolostone bedrock aquifer. The new PTTW for the Freelton water supply permits a maximum daily average taking of 18.3 litres per second (L/s) for FDF01 and 18.6 L/s for FDF03. Combined pumping for the two wells cannot exceed 18.6 L/s under the new permit. In addition, the average annual rate cannot exceed 7.5 L/s.

This study made use of the conceptual geologic model, the hydrogeologic model, and the hydrologic model previously developed for the City of Hamilton (Earthfx, 2010). New borehole data were incorporated into the project database and the bedrock surface in the Freelton area was re-interpolated. The hydrologic model was updated to a newer version of the USGS PRMS code and was further refined in the Freelton study area. The model was calibrated and validated by matching observed daily streamflow at the Water Survey of Canada gauge on Bronte Creek at Carlisle. A new long-term average groundwater recharge distribution was then created for the Freelton area based on a 25-year simulation.

The 2010 North Hamilton groundwater model was then upgraded from MODFLOW-96 to MODFLOW-NWT and modules for simulating streamflow routing and surface leakage were added. The long-term average annual recharge rates, estimated with the PRMS model, were used as input to the groundwater model. The updated groundwater model was calibrated to match observed static water levels obtained from the MECP WWIS database and a recent pump test (Wood, 2018a) was also used to refine the local estimates of aquifer hydraulic conductivity in the vicinity of FDF01.

The results of the groundwater model were then post-processed using the USGS MODPATH particle tracking code to define wellhead protection areas based on the reverse time of travel from the supply wells. Five different pumping configurations, based on the maximum permitted pumping rate at FDF01 and FDF03, were used to delineate the WHPAs. The most conservative WHPA was delineated by combining the different capture zones generated under different pumping configurations.

The vulnerability assessment of the WHPAs was conducted based on a Surface-to-Well Advection Time (SWAT) analysis. The groundwater recharge rates, depth to water, and estimates of mobile moisture content were used to calculate unsaturated zone travel times (UZAT). Forward particle tracking with the groundwater flow model was conducted for the five pumping scenarios to calculate the water table to well (WWAT) component of the SWAT values. The SWAT values were processed to assign vulnerability indices (High, Medium, and Low) to each model cell. The vulnerability indices were increased in the areas within the WHPA with land use classes of “developed” or “transportation” to account for excavations and ditching that could compromise the confining layer and for the presence of older water wells. Finally, vulnerability scores were calculated by combining the WHPAs with the vulnerability indices (High, Medium, and Low) from the SWAT analysis, as per the Technical Rules for Assessment Reports (MECP, 2017).

8 Limitations

Services performed by Earth*fx* Incorporated were conducted in a manner consistent with a level of care and skill ordinarily exercised by members of the environmental engineering and consulting profession. This report presents the results of data compilation and computer simulations of a complex hydrogeologic setting. Data errors and data gaps are likely present in the information supplied to Earth*fx*, and it was beyond the scope of this project to review each data measurement and infill all gaps. Models constructed from these data are limited by the quality and completeness of the information available at the time the work was performed. Computer models represent a simplification of the actual hydrologic and hydrogeologic conditions. The applicability of the simplifying assumptions may or may not be suitable to a variety of end uses.

This report does not exhaustively cover an investigation of all possible environmental conditions or circumstances that may exist in the study area. If a service is not expressly indicated, it should not be assumed that it was provided. It should be recognized that the passage of time affects the information provided in this report. Environmental conditions and the amount of data available can change. Any discussion relating to the conditions are based upon information that existed at the time the conclusions were formulated.

This report was prepared by Earth*fx* Incorporated for the sole benefit of the City of Hamilton. Any use which a third party makes of this report, any reliance thereon, or decisions made based on it, are the responsibility of such third parties. Earth*fx* Incorporated accepts no responsibility for damages, if any, suffered by any third party as a result of decisions made or actions taken based on this report.

Report prepared by:

E.J. Wexler, P.Eng., M.Sc., M.S.E.
Vice President, Senior Hydrogeologist

9 References

AECOM Canada Limited (AECOM), 2009, Volume 1 – Hydrogeological Level 2 Report St Marys Flamborough Quarry: February 2009.

Bajc, A.F., F.R. Brunton, E.H Priebe, K.E. MacCormack, M. Bingham, 2009, An Evaluation of Deeply Buried Aquifers along the Dundas Buried Valley at Lynden and Copetown, Southern Ontario.

Brunton, F.R., Belanger, D., DiBase, S., Yungwirth, G., and Boonstra, G., 2007, Caprock carbonate stratigraphy and bedrock aquifer character of the Niagara Escarpment-City of Guelph region, southern Ontario: OttawaGeo2007 conference proceedings, p.371-377.

Brunton, F.R., 2009, Update of revisions to the Early Silurian Stratigraphy of the Niagara Escarpment: integration of sequence stratigraphy, sedimentology and hydrogeology to delineate hydrogeologic units: in Summary of Field Work and Other Activities - 2009, Ontario Geological Survey, Open File Report 6240, p.25-1 to 25-20.

Chapman, L.J. and Putnam, D.F., 1984, The physiography of southern Ontario: Ontario Geological Survey, Special Volume 2, 270p.

Charlesworth & Associates and SNC Lavalin, 2006, Hamilton Groundwater Resources Characterization and Wellhead Protection Partnership Study: April 2006.

Costello, W.R. and Walker, R.G., 1972, Pleistocene sedimentology, Credit River, Southern Ontario – a new component of the braided river model: Journal of Sedimentary Petrology, v.42, no. 2, p.389-400.

Dickinson, W.T., Whiteley, H.Q., 1970, Watershed areas contributing to runoff: International Association of Hydrologic Sciences Publication 96, p. 1.12-1.28.

Dillon Consulting, 2008, Hydrogeological Study of the New Freelton Well: March 2008.

Earthfx Incorporated, 2010, Vulnerability Assessment and Scoring of Wellhead Protection Areas: prepared for the City of Hamilton Public Works Department, April 2010, 162 p.

Earthfx Incorporated, 2010b, Water Balance Analysis of the Lake Simcoe Basin using the Precipitation-Runoff Modelling System (PRMS): prepared for the South Georgian Bay - Lake Simcoe Source Protection Region, October 2010, 106 p.

Earthfx Incorporated, 2014, Tier 3 Water Budget and Local Area Risk Assessment for the Kelso and Campbellville Groundwater Municipal Systems - Phase 2 Risk Assessment Report: prepared for the Halton Region Conservation Authority, February 2014.

Gartner Lee Limited, 2005, Proposed Dolostone Quarry, Hamilton Volume 1: Hydrogeological Level 2 Report: June 2005.

Harbaugh, A.W., 2005, MODFLOW-2005, the U.S. Geological Survey modular ground-water model—the Ground-Water Flow Process: U.S. Geological Survey Techniques and Methods 6-A16.

Hargreaves, G. H., and Samani, Z. A., 1982, Estimating potential evapotranspiration: Journal of the Irrigation and Drainage Division, 108(3), 225-230.

Jagger Hims Limited, 2003, Freelton FDF01 (formerly 3A) Permit to Take Water: prepared for City of Hamilton, March 2003.

Karrow, P.F., 1987, Quaternary geology of the Hamilton-Cambridge area, southern Ontario: Ontario Geological Survey Geoscience Report 255, 94p.

Karrow, P.F., 2005, Quaternary geology of the Brampton area, southern Ontario: Ontario Geological Survey Geoscience Report 257, 59p.

Kassenaar, J.D.C. and Wexler, E.J., 2006, Groundwater modelling of the Oak Ridges Moraine area: YPDT-CAMC Technical Report #01-06: Available at http://www.ypdt-camc.ca.

Kassenaar, J.D.C., 2013, VIEWLOG (version 4) - Microsoft Windows, v.3.1 through 8.1: VIEWLOG Systems Inc., Toronto, ON

Leavesley, G.H., Litchty, R.W., Troutman, B.M., and Saindon, L.G., 1986, Precipitation-Runoff Modeling System - User's Manual: USGS Water Resources Investigations Report 83-4283, Denver Colorado.

Liberty, B.A., Bond, I.J., and Telford, P.G., 1976, Paleozoic geology of the Hamilton area, southern Ontario: Ontario Geological Survey. Map 2336, scale 1:50 000.

Markstrom, S.L., Niswonger, R.G., Regan, R.S., Prudic, D.E., and Barlow, P.M., 2008, GSFLOW: Coupled ground-water and surface-water flow model based on the integration of the Precipitation-Runoff Modeling System (PRMS) and the Modular Ground-Water Flow Model (MODFLOW-2005): U.S. Geological Survey Techniques and Methods 6-D1, 240 p.

Nash, J.E. and J.V. Sutcliffe, 1970, River flow forecasting through conceptual models, Part I - A discussion of principles: Journal of Hydrology 10, p. 282-290.

Niswonger, R.G., and Prudic, D.E., 2005, Documentation of the Streamflow-Routing (SFR2) Package to include unsaturated flow beneath streams — A modification to SFR1: U.S. Geological Survey Techniques and Methods 6-A13.

Niswonger, R.G., Prudic, D.E., and Regan, R.S., 2006, Documentation of the Unsaturated-Zone Flow (UZF1) Package for modeling unsaturated flow between the land surface and the water table with MODFLOW-2005: U.S. Geological Survey Techniques and Methods, Book 6, Chapter A19, 62 p.

Niswonger, R.G., Panday, S., and Ibaraki, M., 2011, MODFLOW-NWT, A Newton formulation for MODFLOW-2005: U.S. Geological Survey Techniques and Methods 6–A37, 44 p.

Ontario Geological Survey (OGS), 2010, Surficial geology of southern Ontario: Ontario Geological Survey, Miscellaneous Release—Data 128–Revised, attributed digital compilation map.

Ontario Ministry of the Environment and Climate Change (MOECC), 2001, Terms of Reference: Hydrogeological Study to Examine Groundwater Sources Potentially Under Direct Influence of Surface Water, October, 2001.

Ontario Ministry of the Environment and Climate Change (MOECC), 2006, Technical Support Document for Ontario Drinking Water Standards, Objectives and Guidelines, PIBS 4449e01:

Ontario Ministry of Environment, Conservation, and Parks (MECP), 2017, Technical Rules for Assessment Reports https://www.ontario.ca/page/2017-technical-rules-under-clean-water-act#section-3).

Pollock, D.W., 2012, User Guide for MODPATH Version 6—A Particle-Tracking Model for MODFLOW: U.S. Geological Survey Techniques and Methods 6–A41, 58 p.

Telford, P.G. 1976, Paleozoic geology of the Guelph area, southern Ontario: Ontario Geological Survey, Map 2342, scale 1:50,000.

Todd, D.K., 1980, Groundwater Hydrology: John Wiley and Sons, New York, 535 p.

Wood Environment & Infrastructure Solutions (Wood), 2018a, Freelton Well FDF01 Increased Water Taking Assessment – Phase 3 Community of Freelton, Ontario: September 2018

Wood Environment & Infrastructure Solutions (Wood), 2018b, Freelton Well FDF01 GUDI Assessment for Operation at an Increased Pumping Rate Community of Freelton, Ontario: November 2018

WSP, 2016, Freelton Well and Water Storage System Capacity Study: February 2016.